

Full supplementary materials for: Slow, fast, and  
abrupt vegetation change during a period of  
climate stability

Alyssa M. Willson, Pierluigi R. Guaita, Hannah O'Grady,  
Paola Crippa, Ian Shuman, Jason S. McLachlan

January 30, 2025



## Appendix A

# Data sources and figures

Here, we provide figures of all data sources used in this analysis. Figures A.1-A.11 show the median estimates of relative abundances of each taxon over space and time. These show the full extent of observations used to both fit and evaluate the model. The relative abundances within grid cells used to fit the model are shown in Appendix B. Figures A.12- A.17 show the estimates of our downscaled climate drivers (1) across our entire spatiotemporal domain, and (2) over time. The first set of figures (Figures A.12- A.15) shows how climate evolves over space and time, while the final climate figure in this Appendix highlights the relative stability of climate over time in the Upper Midwest, USA (UMW) region (Figure A.16). Finally, Figure A.17 shows the spatial distribution of the climate texture covariates, soil % sand and soil% silt used to fit our models. The soil variables are only shown over space because the same values are used over time, owing to the lack of data on soil texture in the past and the fact that soil texture is unlikely to evolve on the time scale of hundreds of years.

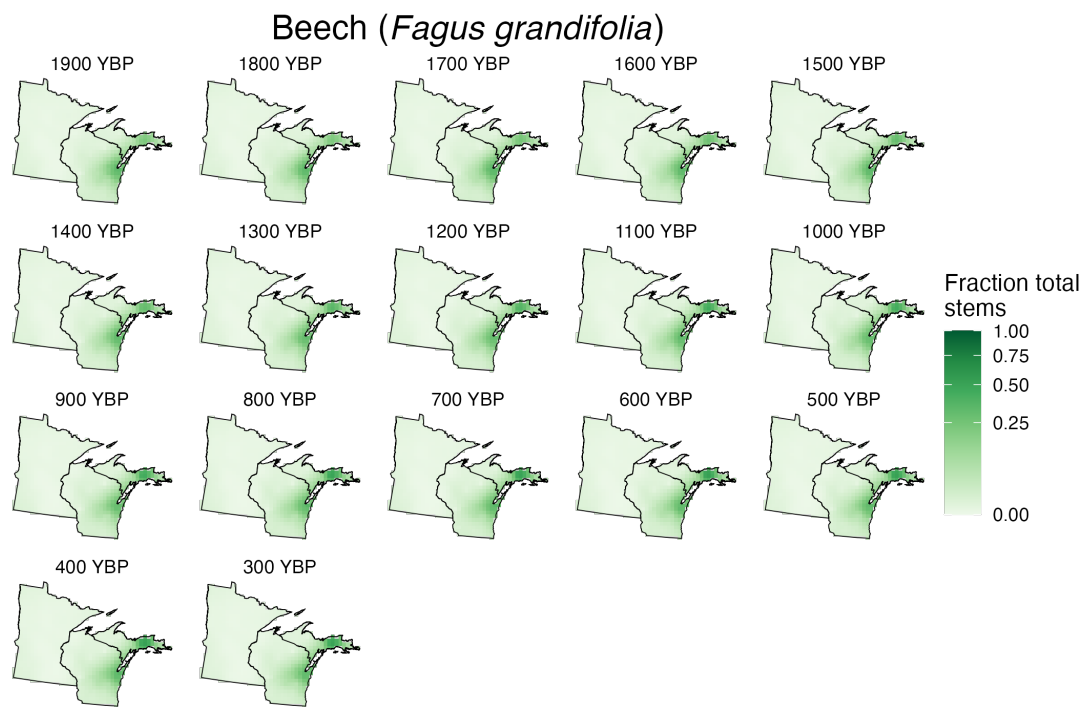


Figure A.1: Estimated median relative abundance of beech (*Fagus grandifolia*) over space and time. Each facet shows the relative abundance of beech over space. Facets represent different time periods, moving from 1900 years before 1950 (YBP) in the top left to 300 YBP in the bottom right. Color scale shows the relative abundance of beech. Note that the color scale has been square root transformed to emphasize smaller relative abundances.

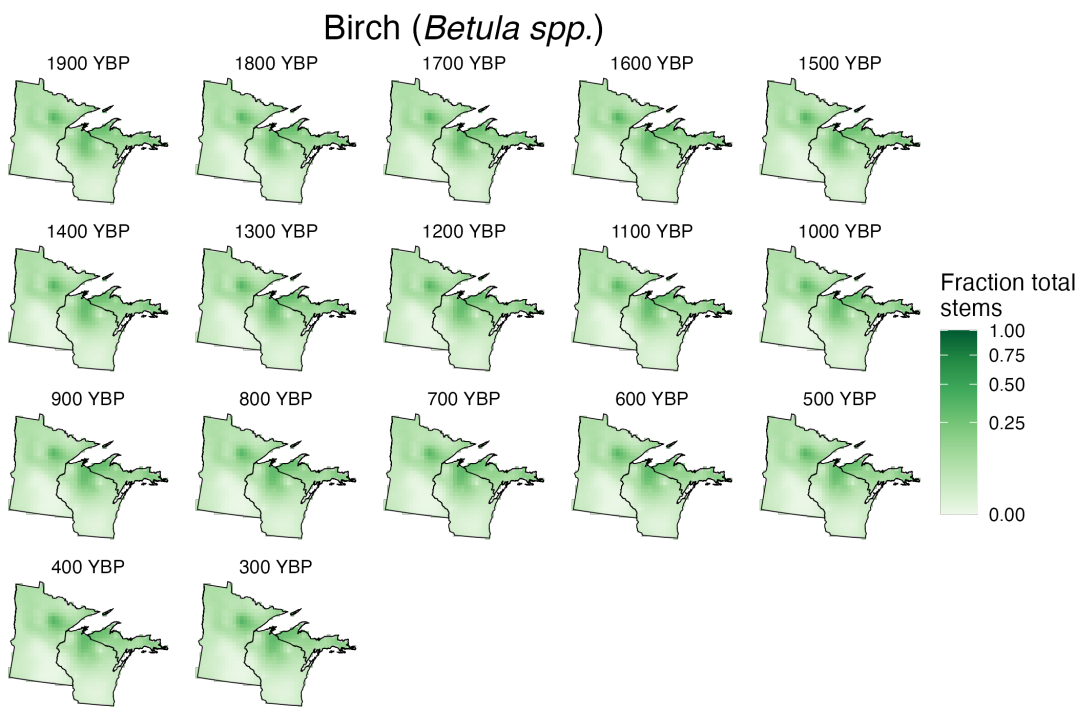


Figure A.2: Estimated median relative abundance of birch (*Betula spp.*) over space and time. Each facet shows the relative abundance of birch over space. Facets represent different time periods, moving from 1900 years before 1950 (YBP) in the top left to 300 YBP in the bottom right. Color scale shows the relative abundance of birch. Note that the color scale has been square root transformed to emphasize smaller relative abundances.

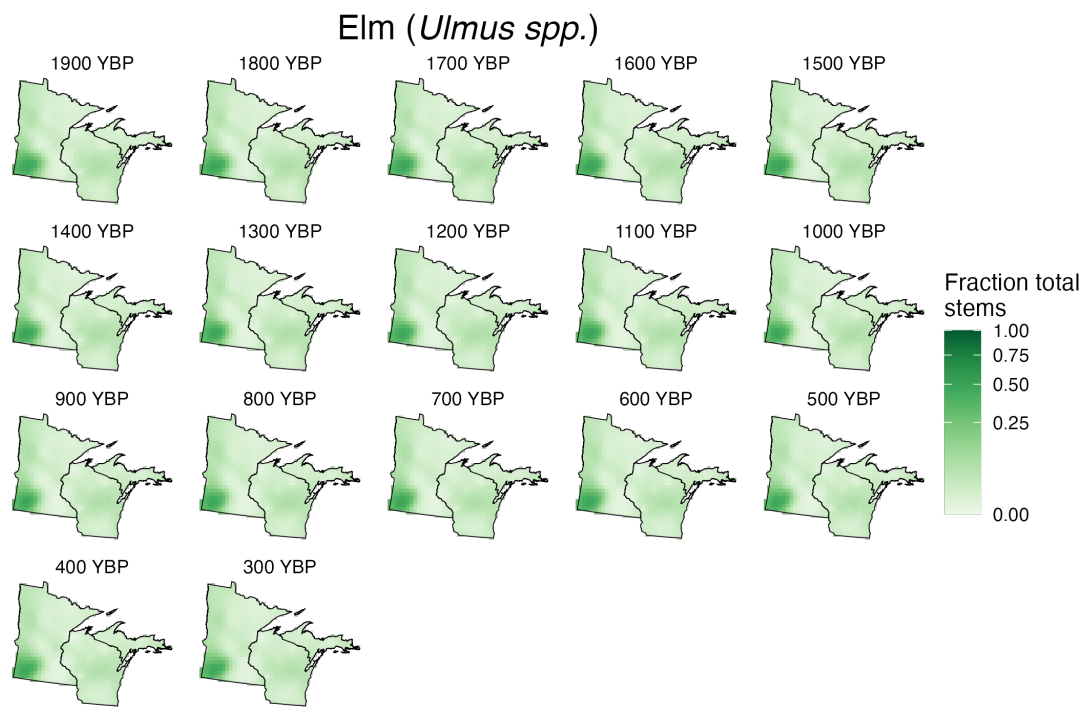


Figure A.3: Estimated median relative abundance of elm (*Ulmus spp.*) over space and time. Each facet shows the relative abundance of elm over space. Facets represent different time periods, moving from 1900 years before 1950 (YBP) in the top left to 300 YBP in the bottom right. Color scale shows the relative abundance of elm. Note that the color scale has been square root transformed to emphasize smaller relative abundances.

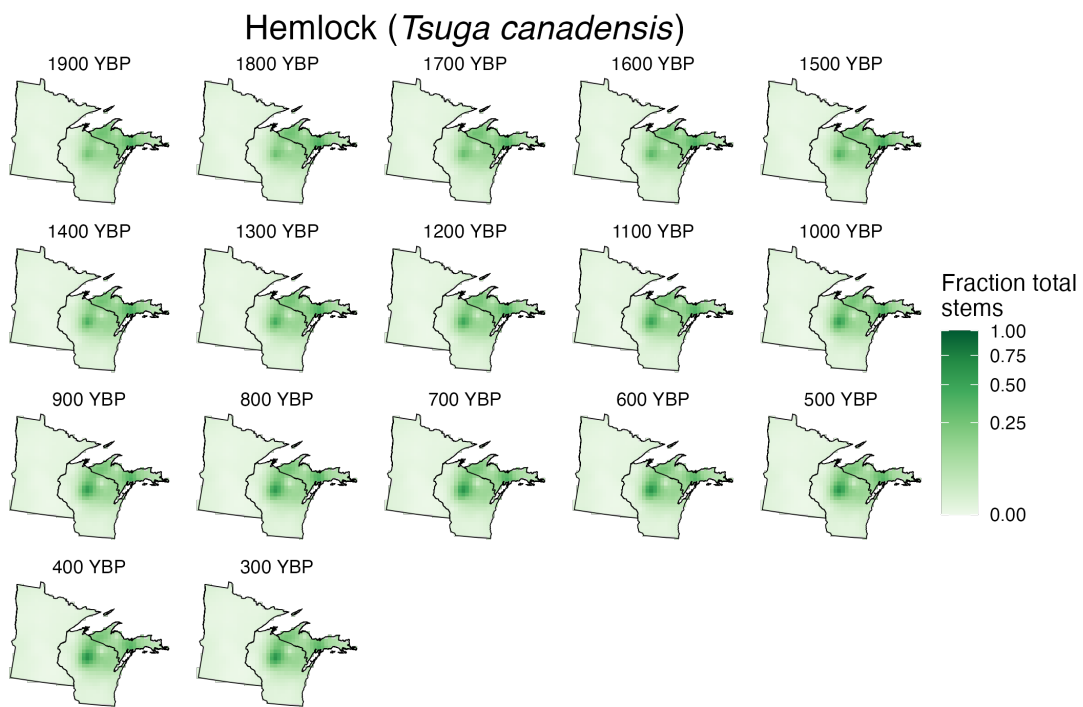


Figure A.4: Estimated median relative abundance of hemlock (*Tsuga canadensis*) over space and time. Each facet shows the relative abundance of hemlock over space. Facets represent different time periods, moving from 1900 years before 1950 (YBP) in the top left to 300 YBP in the bottom right. Color scale shows the relative abundance of hemlock. Note that the color scale has been square root transformed to emphasize smaller relative abundances.

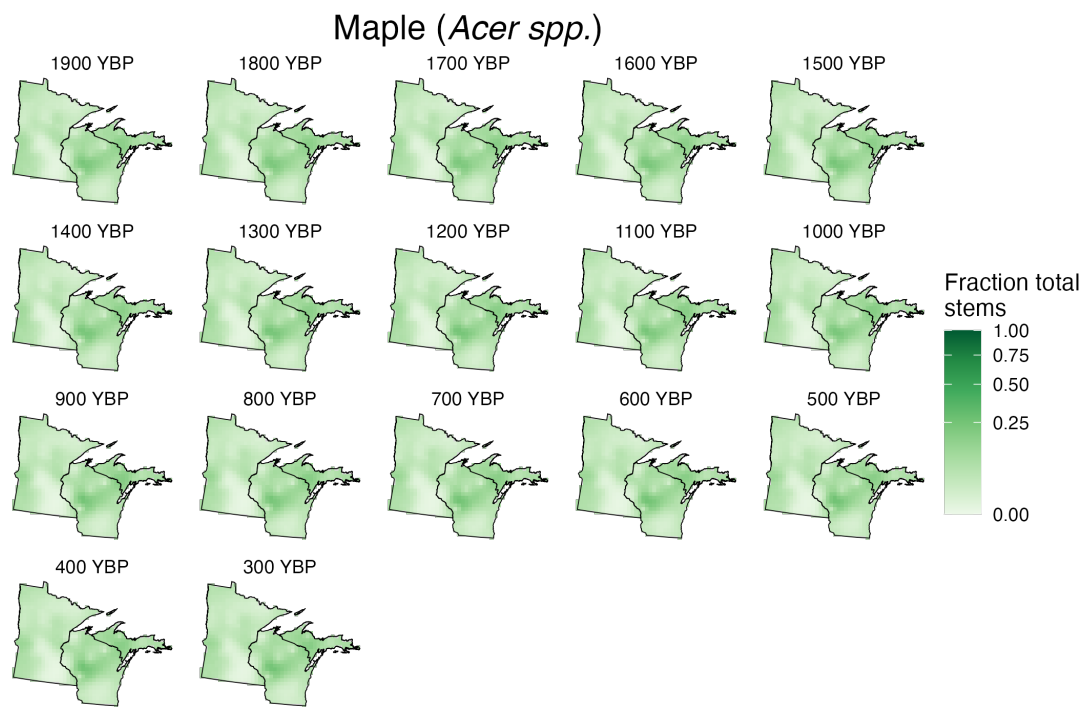


Figure A.5: Estimated median relative abundance of maple (*Acer spp.*) over space and time. Each facet shows the relative abundance of maple over space. Facets represent different time periods, moving from 1900 years before 1950 (YBP) in the top left to 300 YBP in the bottom right. Color scale shows the relative abundance of maple. Note that the color scale has been square root transformed to emphasize smaller relative abundances.

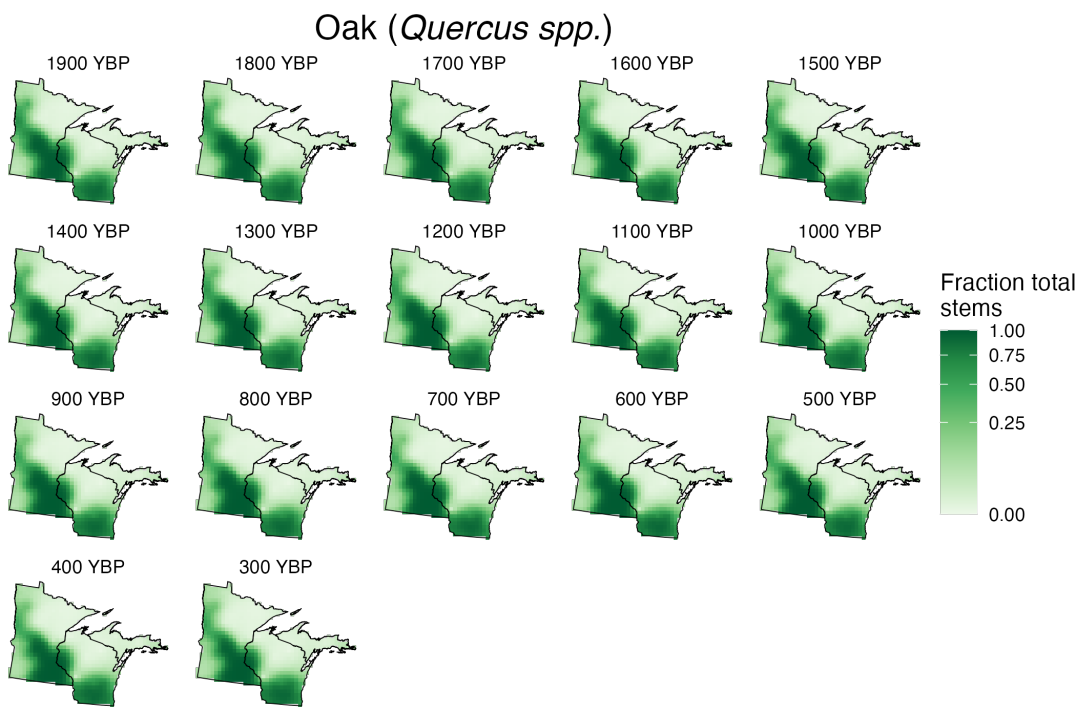


Figure A.6: Estimated median relative abundance of oak (*Quercus spp.*) over space and time. Each facet shows the relative abundance of oak over space. Facets represent different time periods, moving from 1900 years before 1950 (YBP) in the top left to 300 YBP in the bottom right. Color scale shows the relative abundance of oak. Note that the color scale has been square root transformed to emphasize smaller relative abundances.

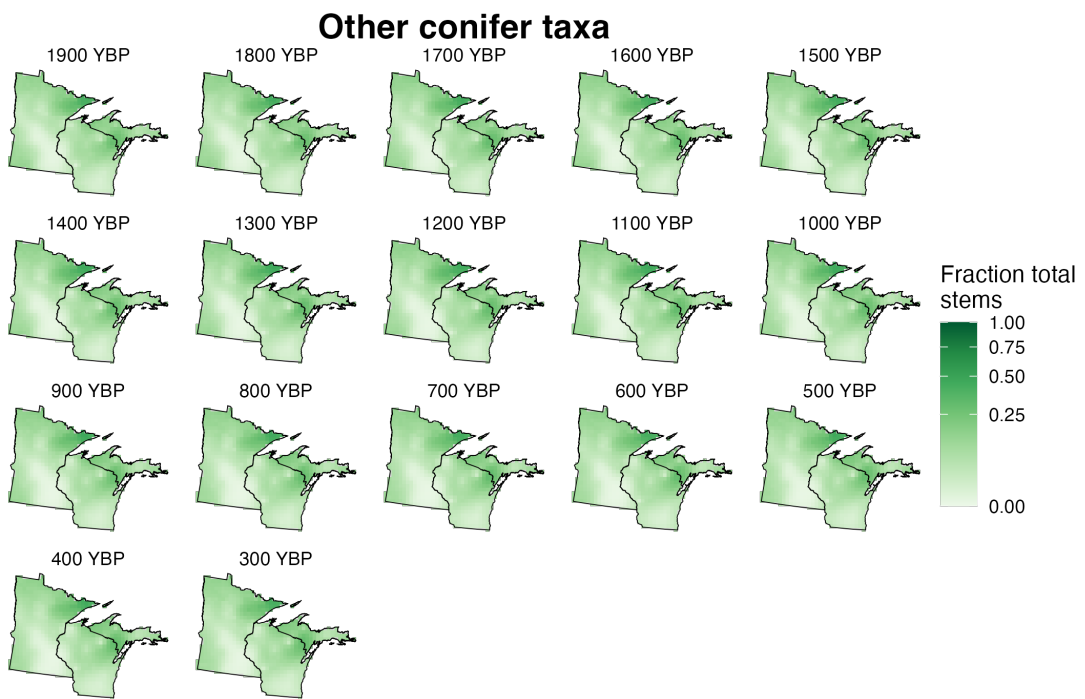


Figure A.7: Estimated median relative abundance of other conifer taxa over space and time. Each facet shows the relative abundance of other conifer taxa over space. Facets represent different time periods, moving from 1900 years before 1950 (YBP) in the top left to 300 YBP in the bottom right. Color scale shows the relative abundance of other conifer taxa. Note that the color scale has been square root transformed to emphasize smaller relative abundances.

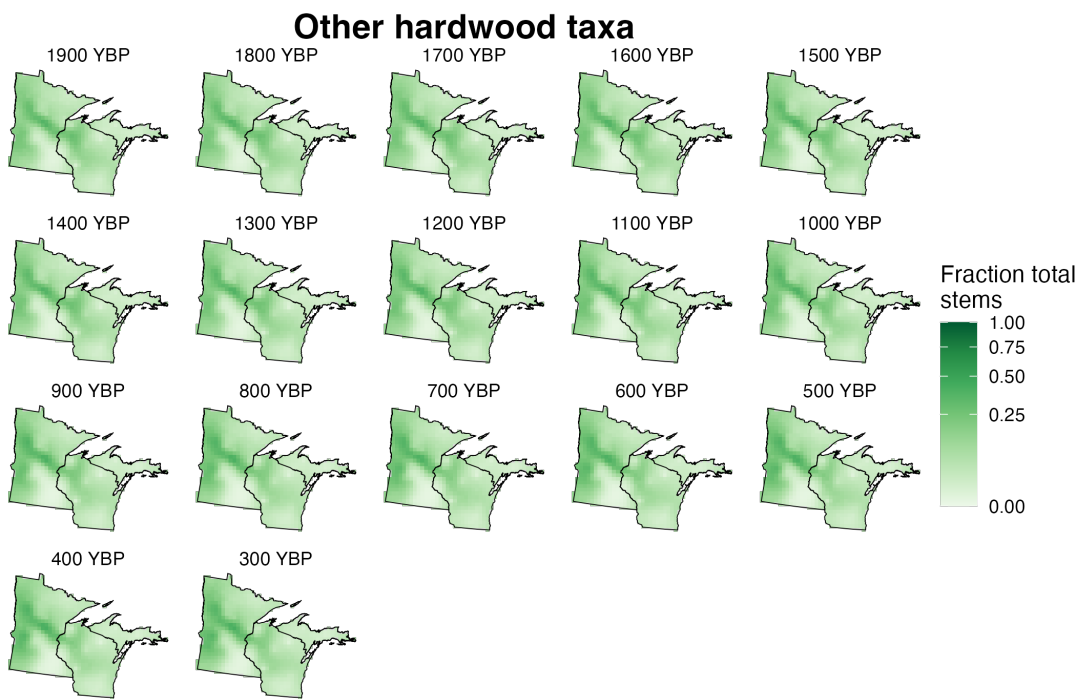


Figure A.8: Estimated median relative abundance of other hardwood taxa over space and time. Each facet shows the relative abundance of other hardwood taxa over space. Facets represent different time periods, moving from 1900 years before 1950 (YBP) in the top left to 300 YBP in the bottom right. Color scale shows the relative abundance of other hardwood taxa. Note that the color scale has been square root transformed to emphasize smaller relative abundances.

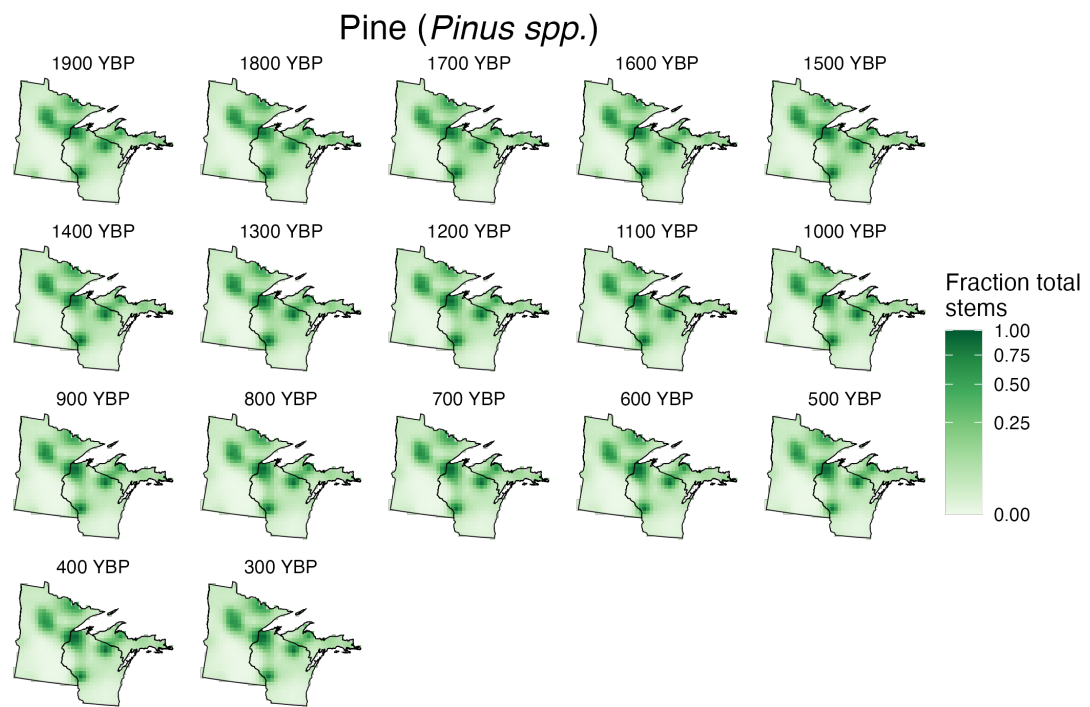


Figure A.9: Estimated median relative abundance of pine (*Pinus spp.*) over space and time. Each facet shows the relative abundance of pine over space. Facets represent different time periods, moving from 1900 years before 1950 (YBP) in the top left to 300 YBP in the bottom right. Color scale shows the relative abundance of pine. Note that the color scale has been square root transformed to emphasize smaller relative abundances.

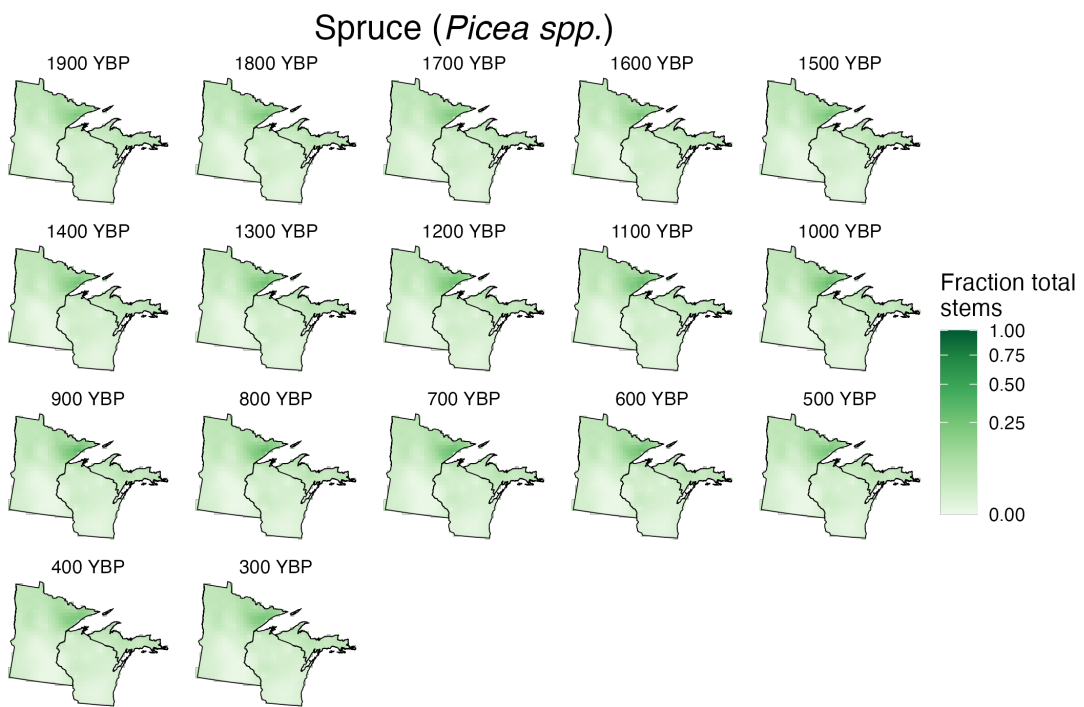


Figure A.10: Estimated median relative abundance of spruce (*Picea spp.*) over space and time. Each facet shows the relative abundance of spruce over space. Facets represent different time periods, moving from 1900 years before 1950 (YBP) in the top left to 300 YBP in the bottom right. Color scale shows the relative abundance of spruce. Note that the color scale has been square root transformed to emphasize smaller relative abundances.

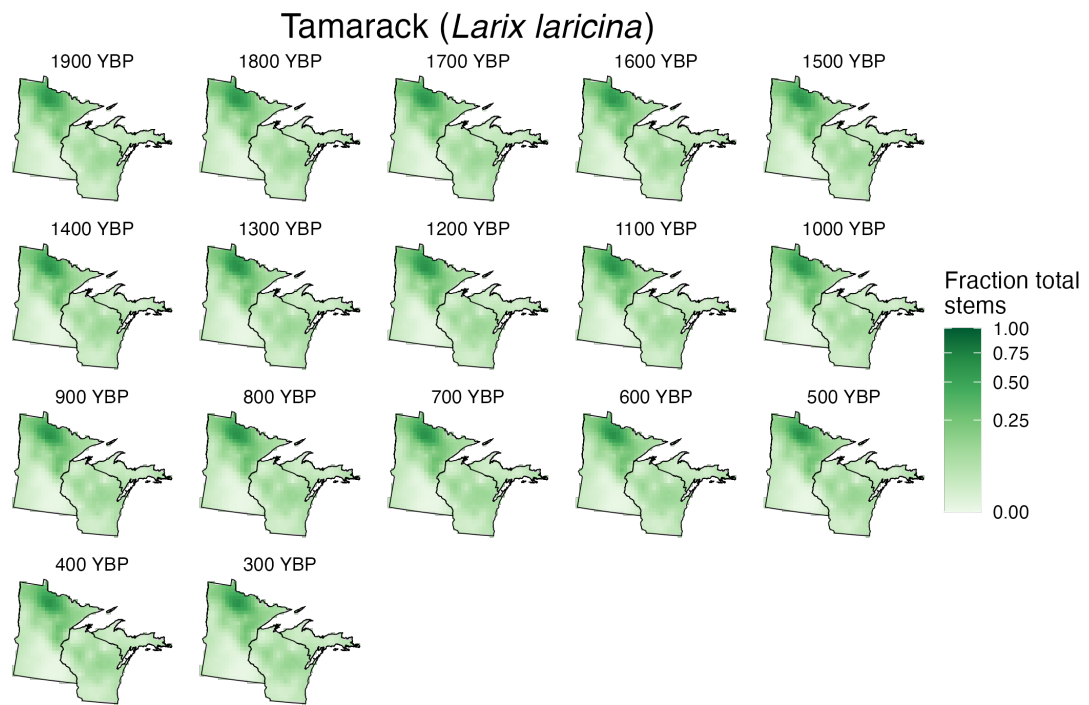


Figure A.11: Estimated median relative abundance of tamarack (*Larix laricina*) over space and time. Each facet shows the relative abundance of tamarack over space. Facets represent different time periods, moving from 1900 years before 1950 (YBP) in the top left to 300 YBP in the bottom right. Color scale shows the relative abundance of tamarack. Note that the color scale has been square root transformed to emphasize smaller relative abundances.

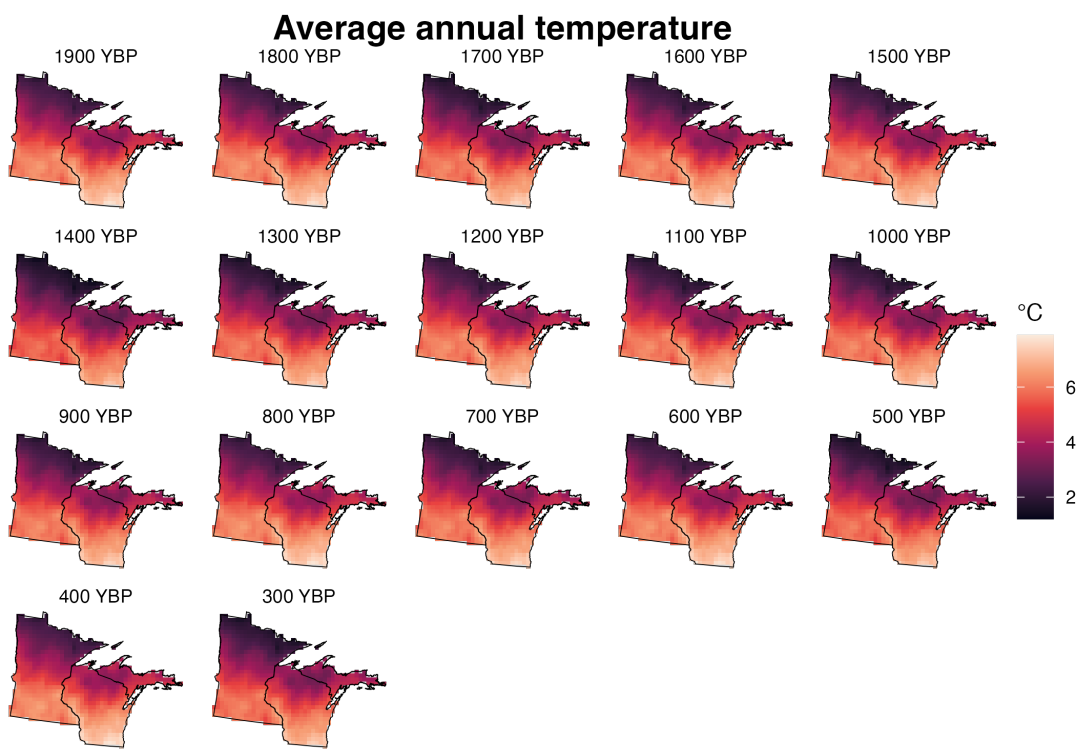


Figure A.12: Estimated average annual temperature ( $^{\circ}\text{C}$ ) over space and time. Each facet shows average annual temperature over space. Facets represent different time periods, moving from 1900 years before 1950 (YBP) in the top left to 300 YBP in the bottom right. Color scale shows average annual temperature.

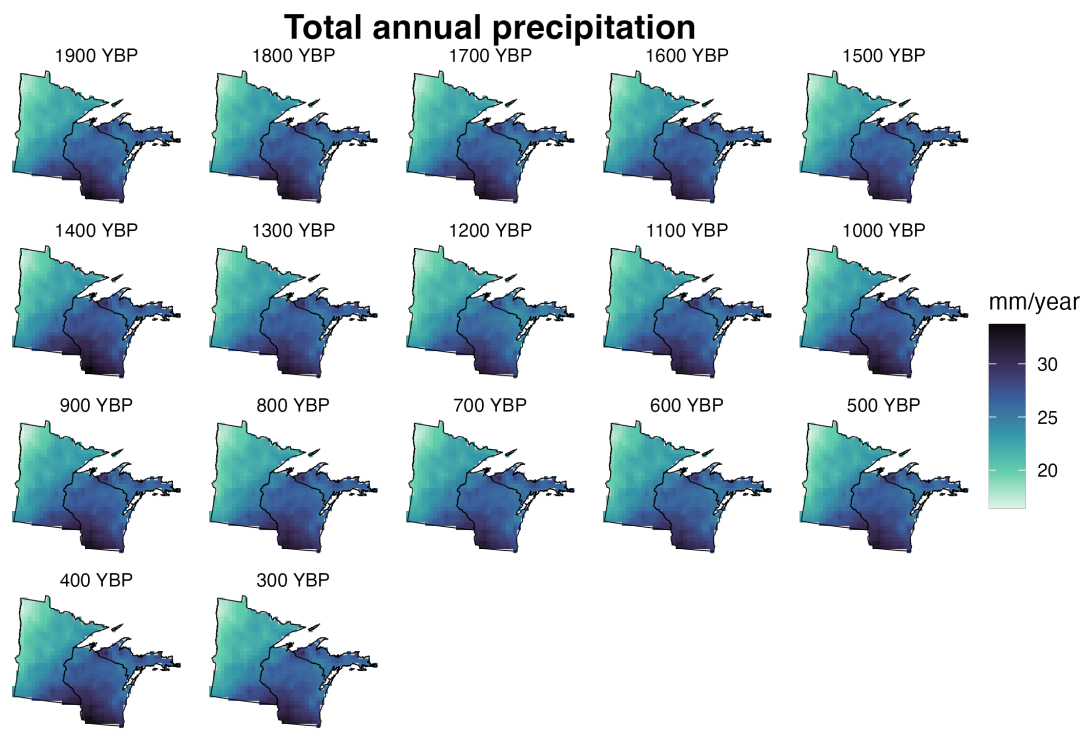


Figure A.13: Estimated total annual precipitation (mm/year) over space and time. Each facet shows total annual precipitation over space. Facets represent different time periods, moving from 1900 years before 1950 (YBP) in the top left to 300 YBP in the bottom right. Color scale shows total annual precipitation.

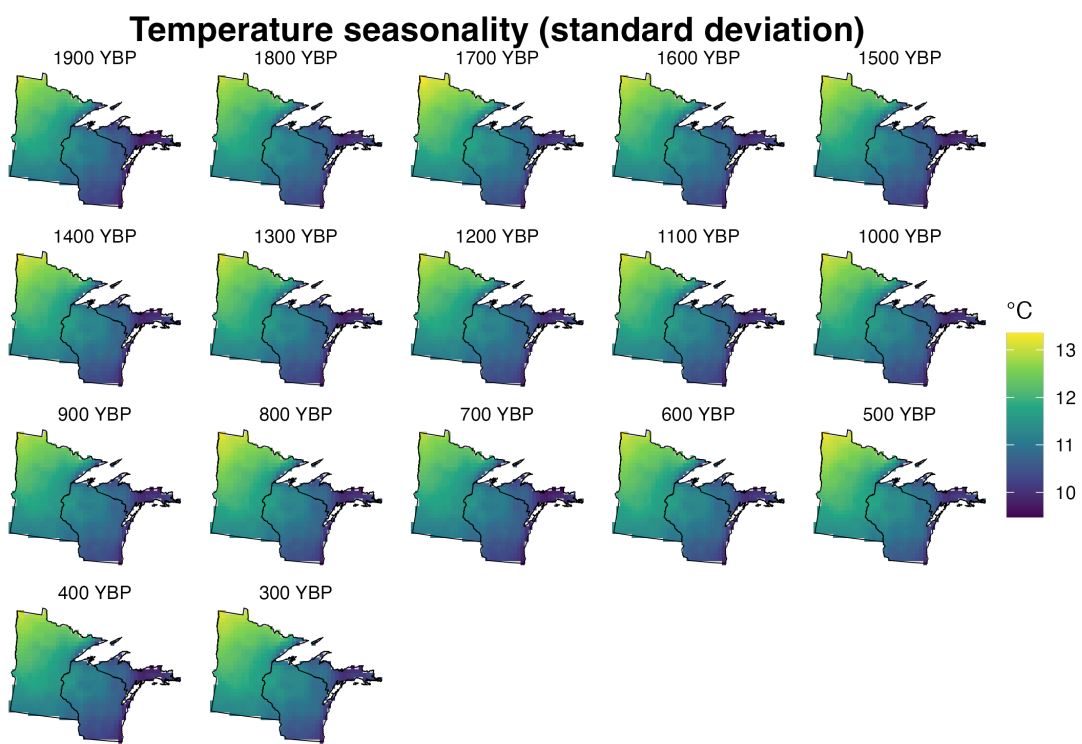


Figure A.14: Estimated temperature seasonality ( $^{\circ}\text{C}$ ) over space and time. Each facet shows temperature seasonality over space. Facets represent different time periods, moving from 1900 years before 1950 (YBP) in the top left to 300 YBP in the bottom right. Color scale shows temperature seasonality.

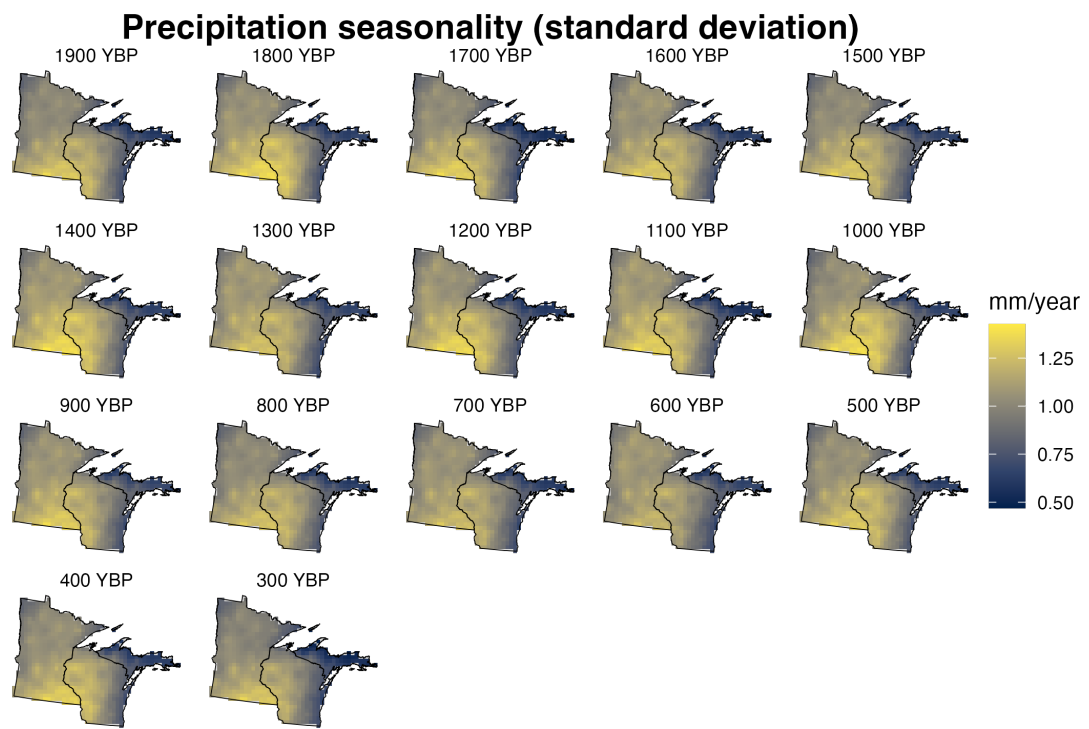


Figure A.15: Estimated precipitation seasonality (mm/year) over space and time. Each facet shows precipitation seasonality over space. Facets represent different time periods, moving from 1900 years before 1950 (YBP) in the top left to 300 YBP in the bottom right. Color scale shows precipitation seasonality.

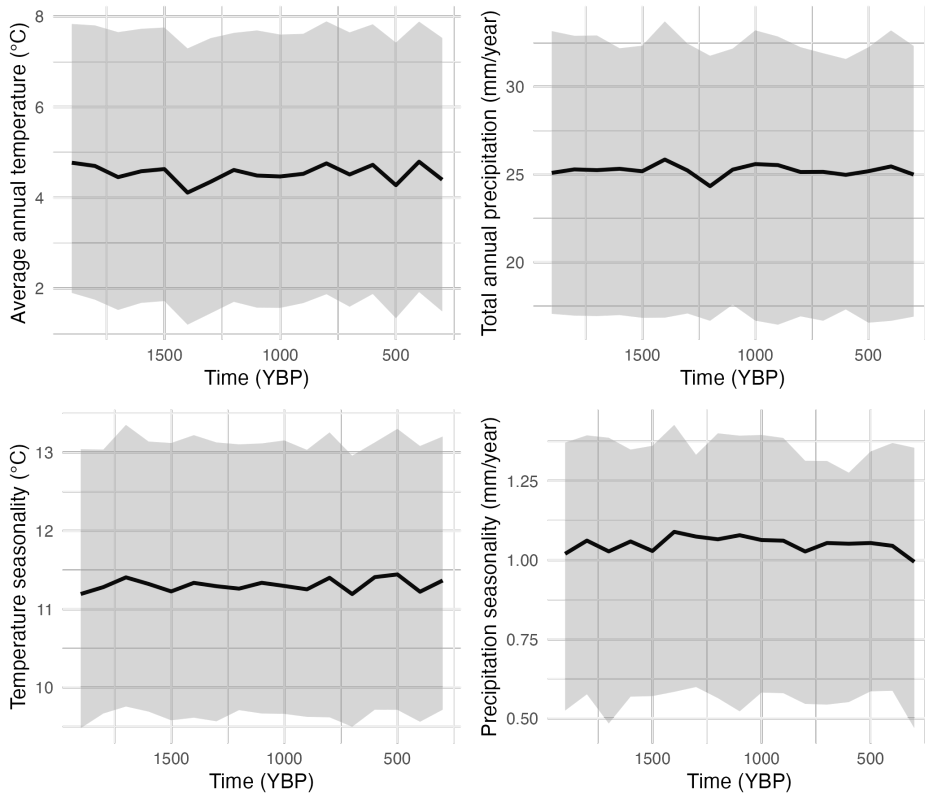


Figure A.16: Variability in climate variables over time. Each facet shows the temporal variability of one climate variable. Top left: average annual temperature, top right: total annual precipitation, bottom left: temperature seasonality, bottom right: precipitation seasonality. The thick black line shows the median value of the climate variable over space at the given time point. The light gray shading shows the maximum extent of the climate variable over space at the given time point. These plots highlight the relative stability of the climate variables in the Upper Midwest, USA over the last 2000 years of the pre-Industrial Holocene.

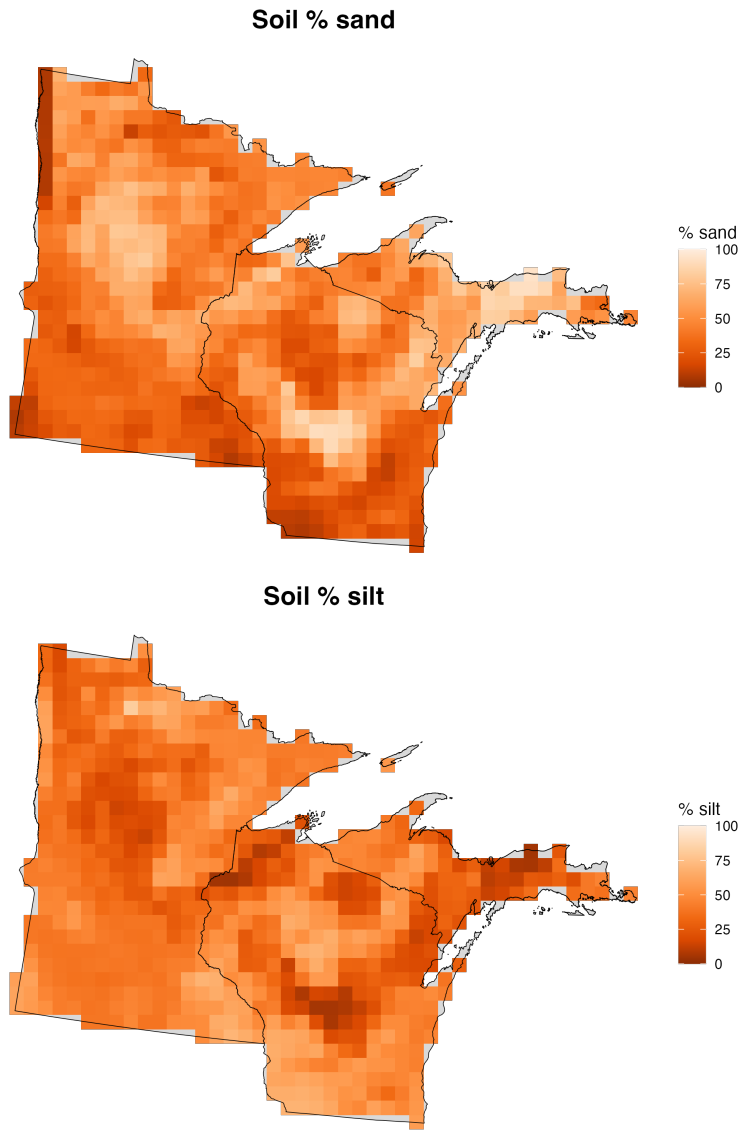


Figure A.17: Estimated soil texture over space. Top: soil % sand, bottom: soil% silt. The color scale shows the % of soil with sand (top) or silt (bottom) particle size. Variables are not shown over time because soil texture is assumed to be constant over time.

## Appendix B

# Relative abundance subsampling

The relative abundance estimates from STEPPS are smoothed over space and time for several reasons. First, STEPPS borrows strength over space and time to improve estimates of relative abundance, especially in locations and time periods with limited fossil pollen data (Dawson 2016). Second, additional temporal smoothness occurs as a result of the natural mixing of lake sediments, from which fossil pollen data are collected (Dawson 2016). Third, additional spatial smoothness occurs as a result of the natural process of pollen dispersal from the source location to the lake in which it eventually settles (Dawson 2016). Collectively, these processes improve the accuracy of estimates of relative abundance at any spatiotemporal locale, but also make it so that adjacent reconstructions in space and time are correlated with one another. Our hierarchical model of the vegetation-environment relationship does not account for the correlations between relative abundances in space and time. To account for this, we sub-sampled the relative abundance estimates in space and time.

The optimal sampling density in space was determined in two ways. First, we assessed the rate at which correlations in relative abundance over space decayed for estimates with known sampling artifacts. For example, peaks in the relative abundance of pine are known to occur in locations of high fossil pollen sampling density near sand plains; we therefore visually estimated the number of grid cells around peaks in pine relative abundance that were affected by the intentional sampling of pine-dominated sand plains. Next, we fit Gaussian variograms to the relative abundances of each taxon individually at each time period across space. Using the fitted Gaussian variograms, we estimated the range parameter, which quantifies the distance after which estimates of relative abundance are independent. On average, the range parameter for a given taxon indicated that relative abundance estimates approximately five grid cells apart are independent. We chose to sample more densely than every five grid cells, choosing to sample every third grid cell, because some dependence in space is

expected as a result of the ecological processes we are interested in investigating (dependence on spatially varying environmental conditions and dependence between taxa). This decision was supported by our visual assessment of the peaks in relative abundances, with relative abundance returning to the background rate by three grid cells away.

The sampling density in time was determined using multivariate autocorrelation functions across all spatial locations for each taxon individually. Using the autocorrelation functions, we plotted the spatial distribution of the maximum lag considered significant at the 95% significance level. On average, the maximum lag for a given taxon was 5 time steps. However, the longest significant time lags were often spatially distributed in regions with little ecological significance (e.g., time lag of 12 for spruce in northwest Minnesota, where spruce is not abundant). Therefore, a sampling density of every four time steps was chosen to maximize the amount of data retained in our analysis.

In total, we sampled every third grid cell in space across all time steps and sampled every fourth time step. This sampling protocol left us with 80 unique grid cells across all time steps and five unique time steps (1,900, 1,500, 1,100, 700, and 300 YBP) (Supplementary Figures B.1- B.11). More information on the analyses leading to our final sub-sampled grid cells can be found in our Github repository (<https://github.com/amwillson/GJAM-STEPPS>).

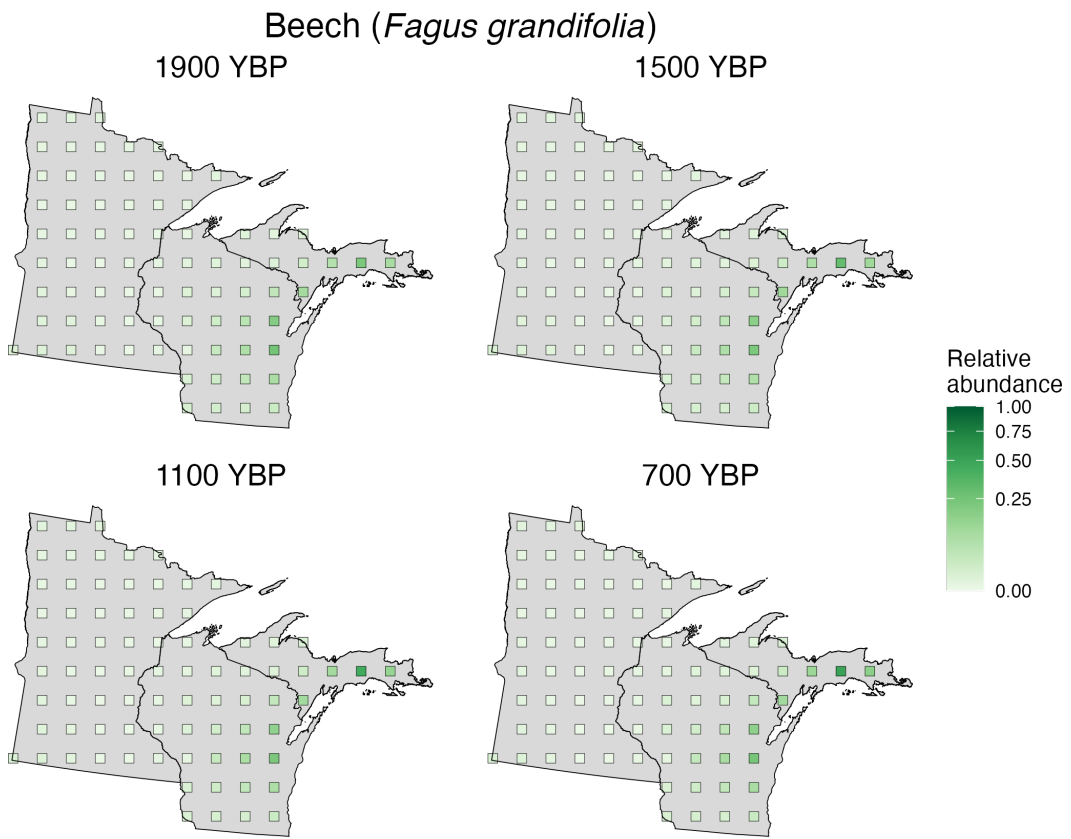


Figure B.1: Median beech (*Fagus grandifolia*) relative abundance over space and time for sub-sampled grid cells used to fit the model (GJAM). Each facet shows relative abundance of beech over space. Facets show the four time periods used for fitting the model. The color scale shows relative abundance of beech. Sub-sampled grid cells are outlined in black to differentiate them from the gray background color. Note that the color scale has been square root-transformed to emphasize lower relative abundances.

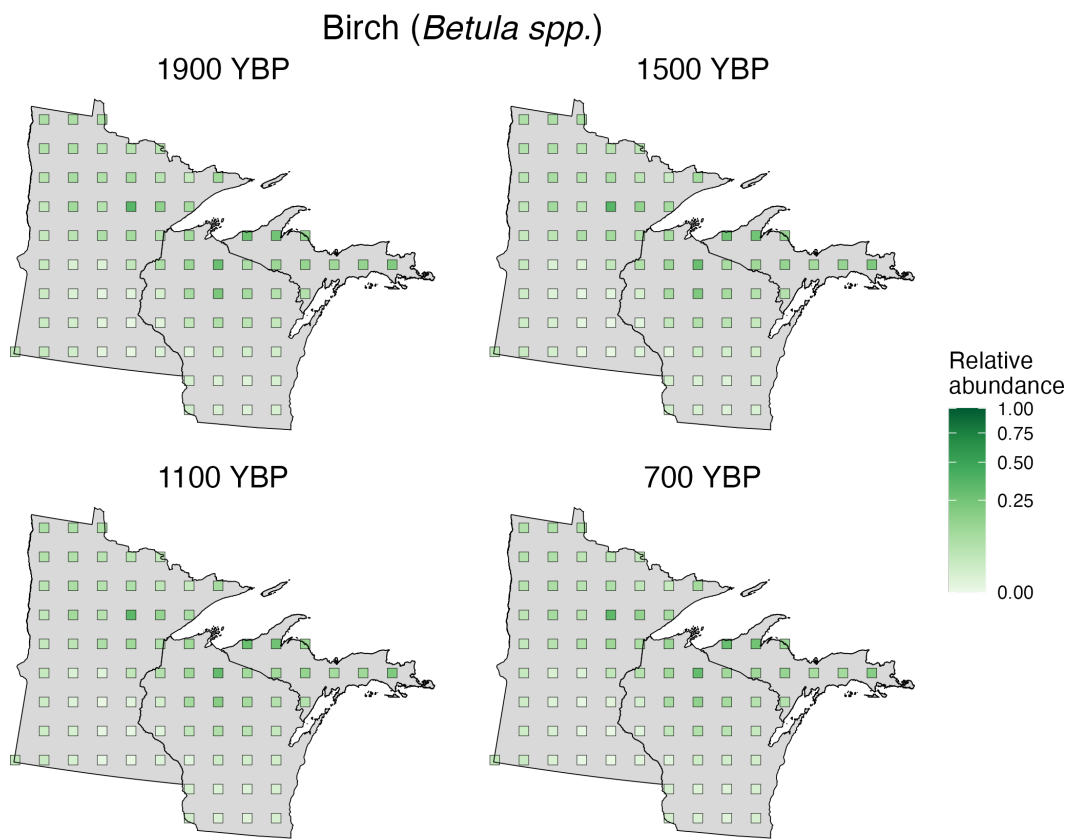


Figure B.2: Median birch (*Betula spp.*) relative abundance over space and time for sub-sampled grid cells used to fit the model (GJAM). Each facet shows relative abundance of birch over space. Facets show the four time periods used for fitting the model. The color scale shows relative abundance of birch. Sub-sampled grid cells are outlined in black to differentiate them from the gray background color. Note that the color scale has been square root-transformed to emphasize lower relative abundances.

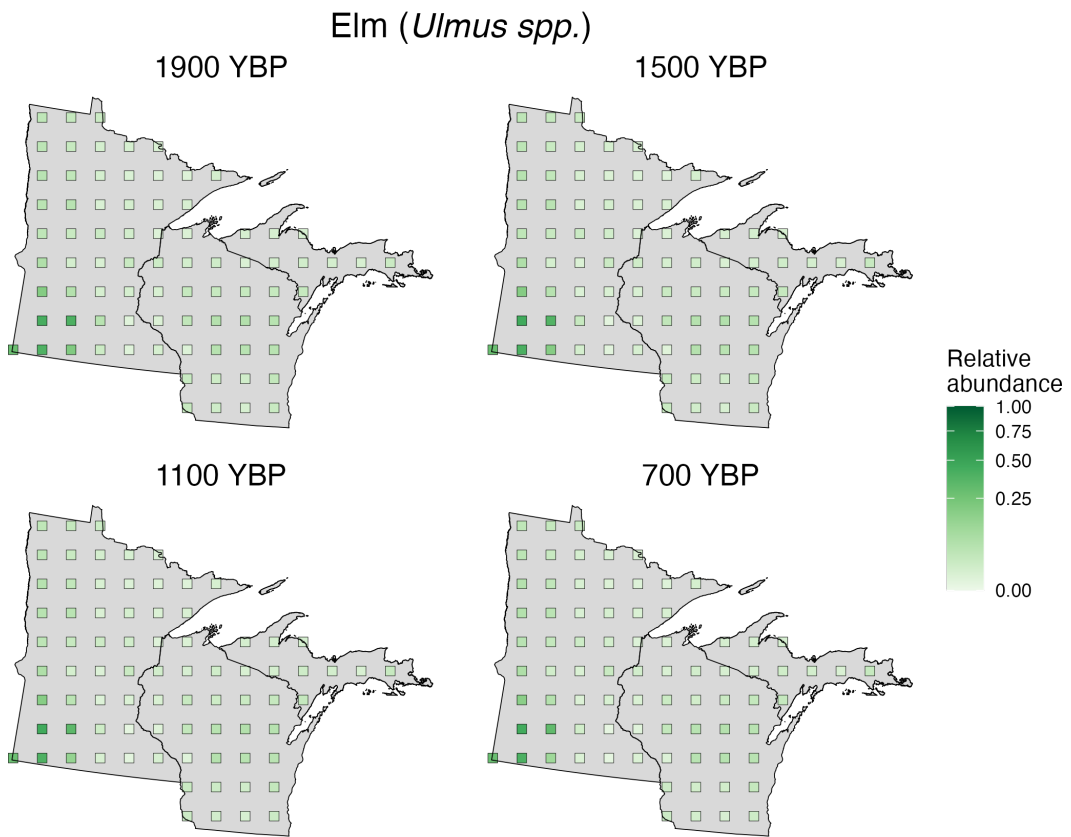


Figure B.3: Median elm (*Ulmus spp.*) relative abundance over space and time for sub-sampled grid cells used to fit the model (GJAM). Each facet shows relative abundance of elm over space. Facets show the four time periods used for fitting the model. The color scale shows relative abundance of elm. Sub-sampled grid cells are outlined in black to differentiate them from the gray background color. Note that the color scale has been square root-transformed to emphasize lower relative abundances.

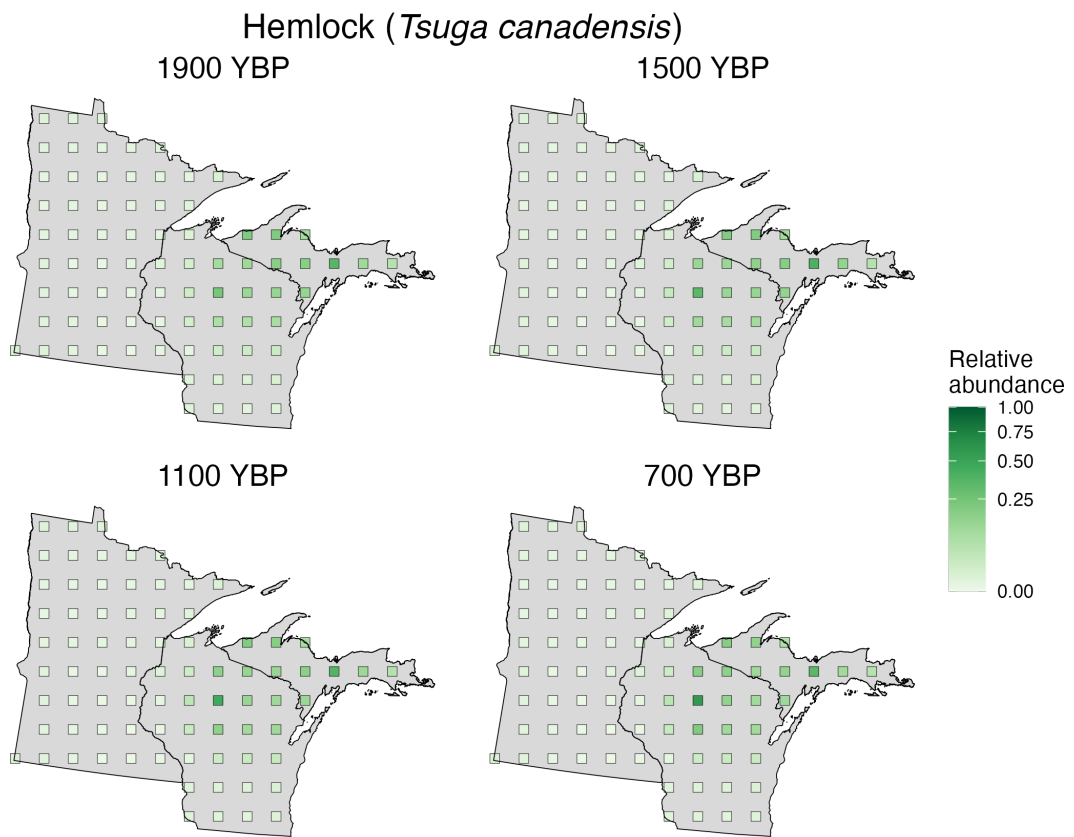


Figure B.4: Median hemlock (*Tsuga canadensis*) relative abundance over space and time for sub-sampled grid cells used to fit the model (GJAM). Each facet shows relative abundance of hemlock over space. Facets show the four time periods used for fitting the model. The color scale shows relative abundance of hemlock. Sub-sampled grid cells are outlined in black to differentiate them from the gray background color. Note that the color scale has been square root-transformed to emphasize lower relative abundances.

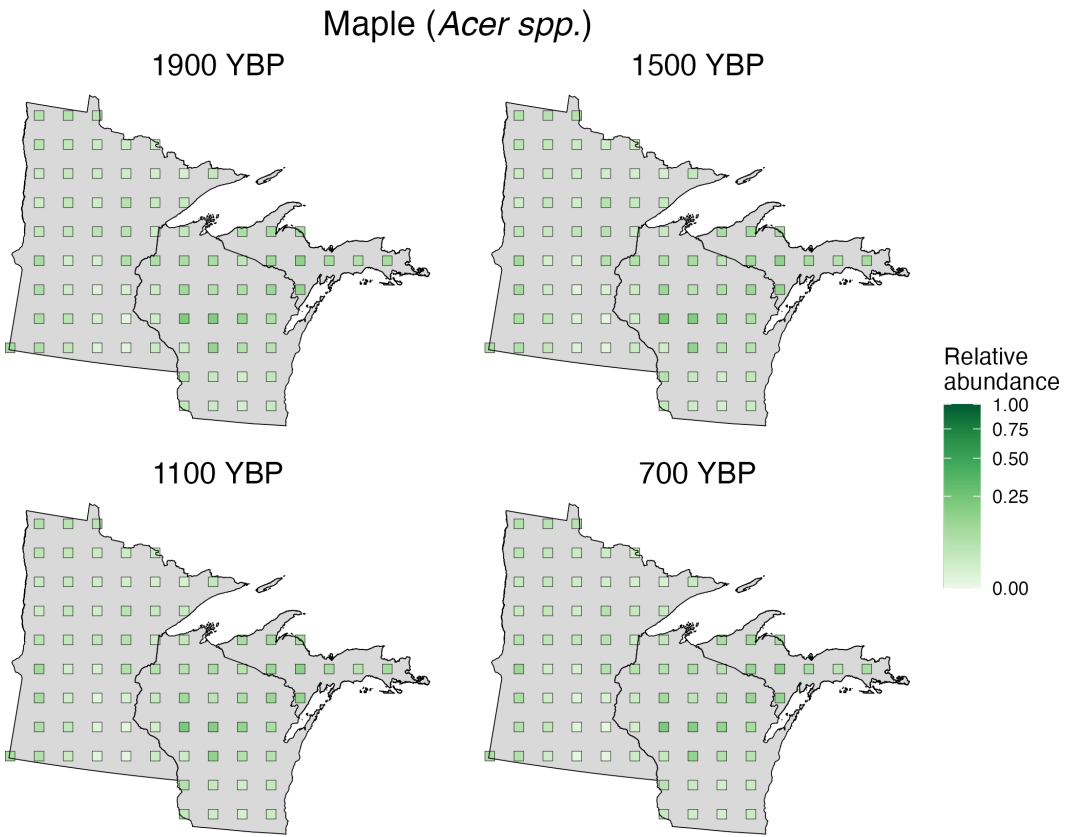


Figure B.5: Median maple (*Acer spp.*) relative abundance over space and time for sub-sampled grid cells used to fit the model (GJAM). Each facet shows relative abundance of maple over space. Facets show the four time periods used for fitting the model. The color scale shows relative abundance of maple. Sub-sampled grid cells are outlined in black to differentiate them from the gray background color. Note that the color scale has been square root-transformed to emphasize lower relative abundances.

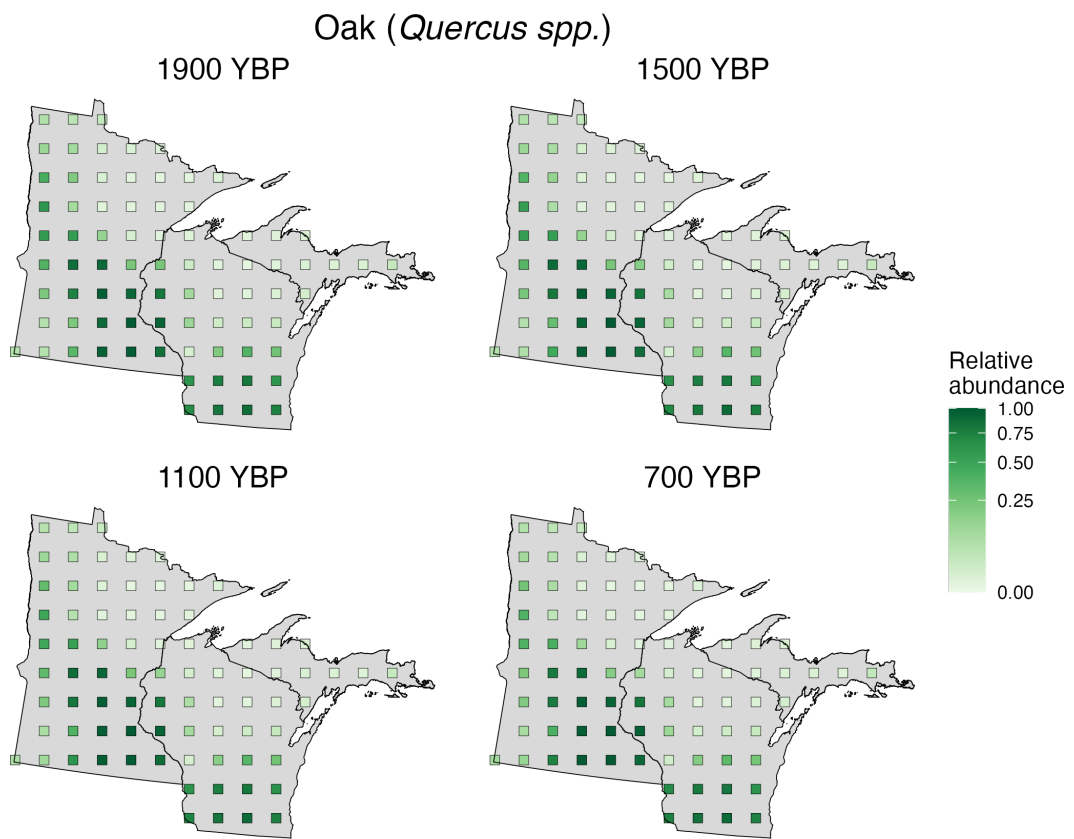


Figure B.6: Median oak (*Quercus spp.*) relative abundance over space and time for sub-sampled grid cells used to fit the model (GJAM). Each facet shows relative abundance of oak over space. Facets show the four time periods used for fitting the model. The color scale shows relative abundance of oak. Sub-sampled grid cells are outlined in black to differentiate them from the gray background color. Note that the color scale has been square root-transformed to emphasize lower relative abundances.

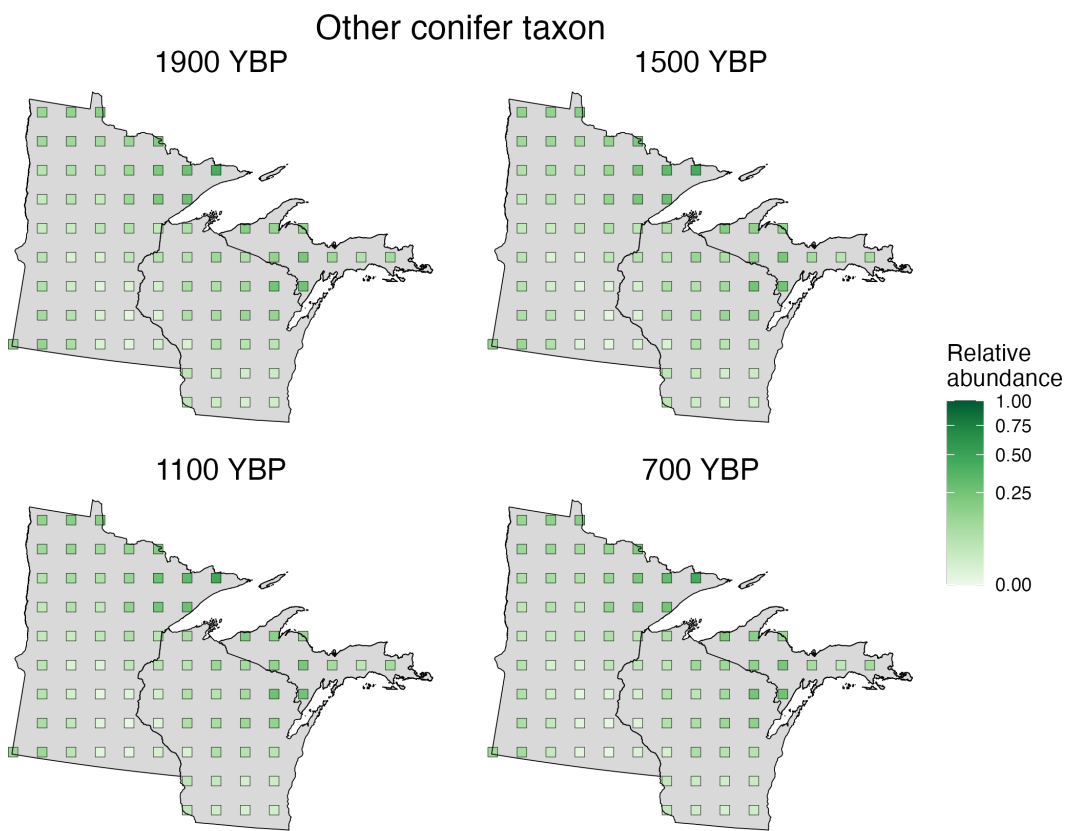


Figure B.7: Median other conifer taxa relative abundance over space and time for sub-sampled grid cells used to fit the model (GJAM). Each facet shows relative abundance of other conifer taxa over space. Facets show the four time periods used for fitting the model. The color scale shows relative abundance of other conifer taxa. Sub-sampled grid cells are outlined in black to differentiate them from the gray background color. Note that the color scale has been square root-transformed to emphasize lower relative abundances.

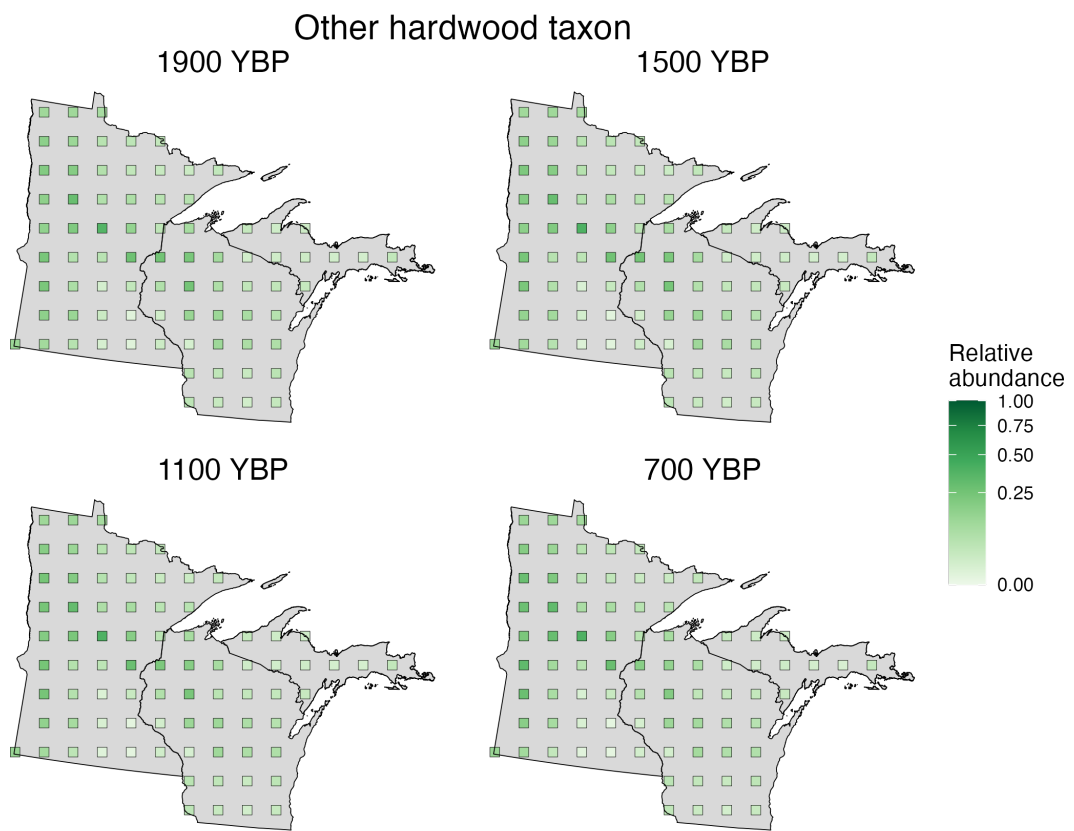


Figure B.8: Median other hardwood taxa relative abundance over space and time for sub-sampled grid cells used to fit the model (GJAM). Each facet shows relative abundance of other hardwood taxa over space. Facets show the four time periods used for fitting the model. The color scale shows relative abundance of other hardwood taxa. Sub-sampled grid cells are outlined in black to differentiate them from the gray background color. Note that the color scale has been square root-transformed to emphasize lower relative abundances.

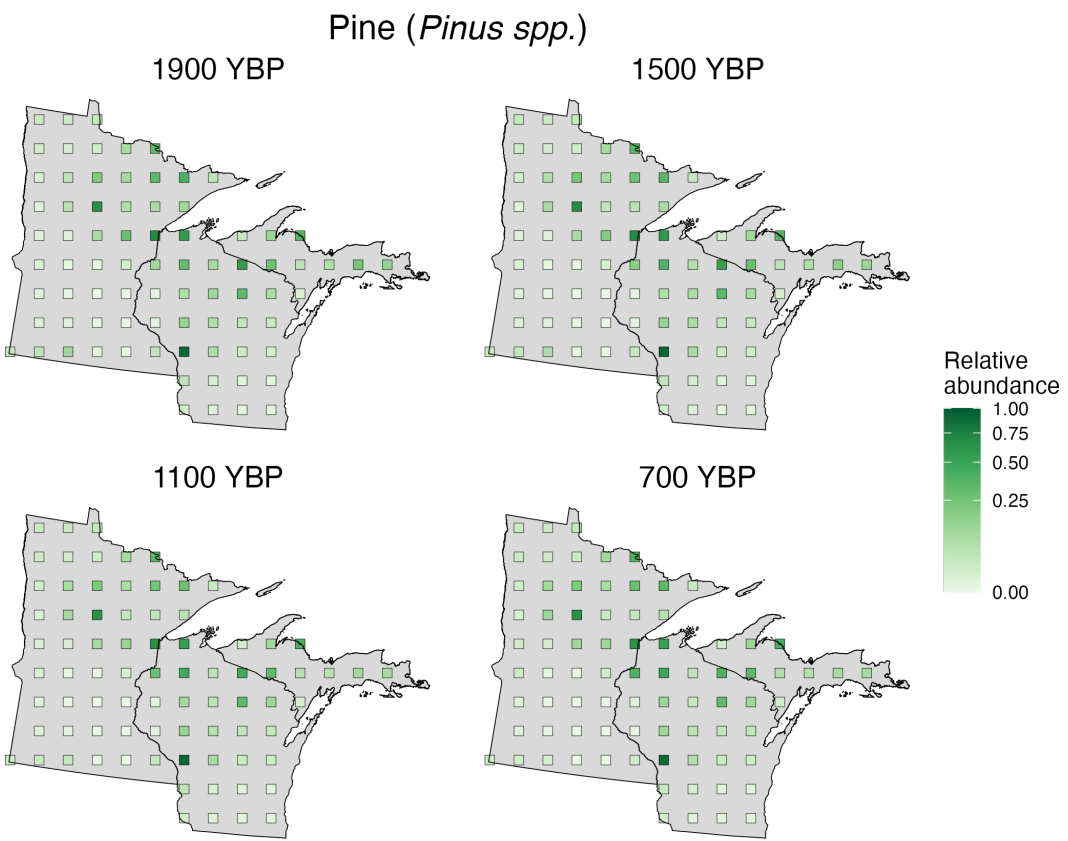


Figure B.9: Median pine (*Pinus spp.*) relative abundance over space and time for sub-sampled grid cells used to fit the model (GJAM). Each facet shows relative abundance of pine over space. Facets show the four time periods used for fitting the model. The color scale shows relative abundance of pine. Sub-sampled grid cells are outlined in black to differentiate them from the gray background color. Note that the color scale has been square root-transformed to emphasize lower relative abundances.

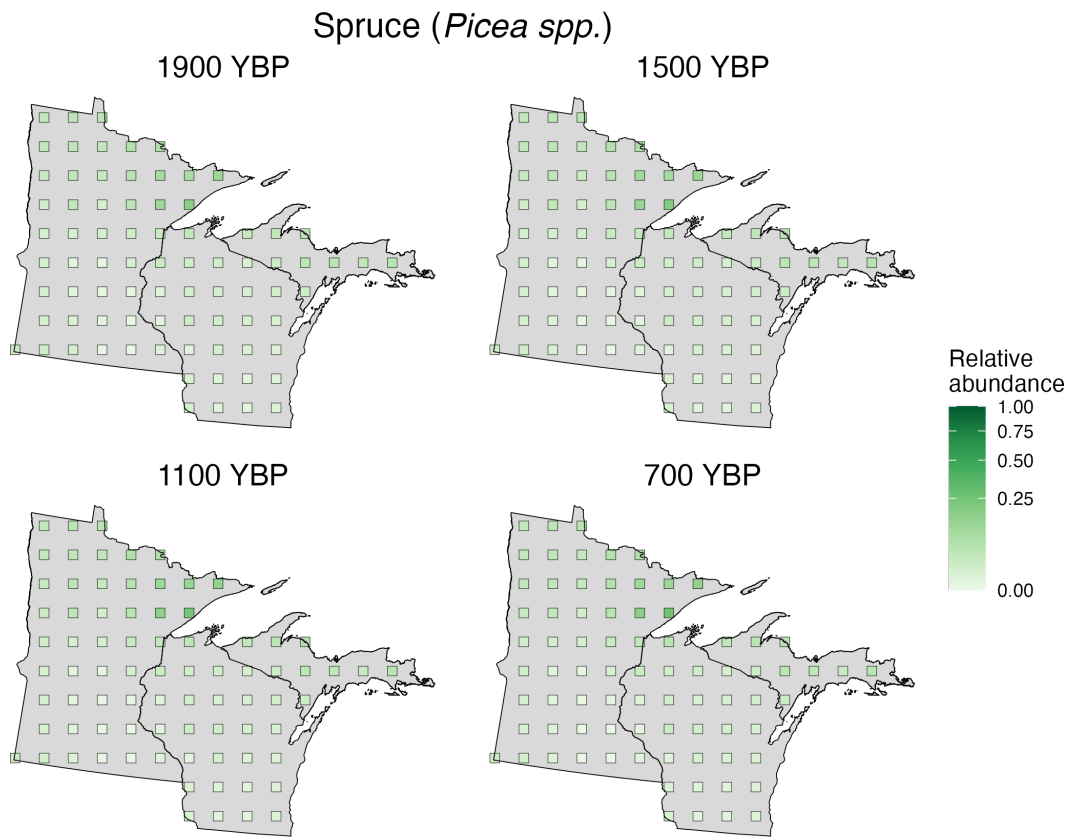


Figure B.10: Median spruce (*Picea spp.*) relative abundance over space and time for sub-sampled grid cells used to fit the model (GJAM). Each facet shows relative abundance of spruce over space. Facets show the four time periods used for fitting the model. The color scale shows relative abundance of spruce. Sub-sampled grid cells are outlined in black to differentiate them from the gray background color. Note that the color scale has been square root-transformed to emphasize lower relative abundances.

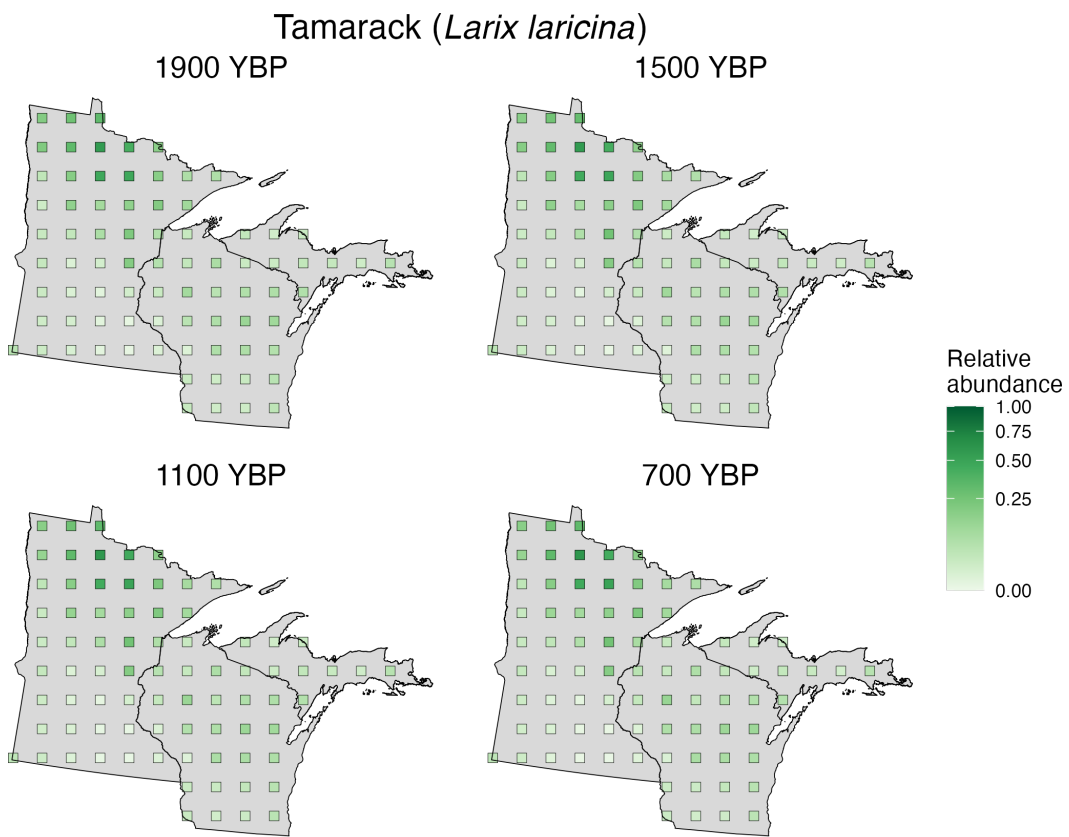


Figure B.11: Median tamarack (*Larix laricina*) relative abundance over space and time for sub-sampled grid cells used to fit the model (GJAM). Each facet shows relative abundance of tamarack over space. Facets show the four time periods used for fitting the model. The color scale shows relative abundance of tamarack. Sub-sampled grid cells are outlined in black to differentiate them from the gray background color. Note that the color scale has been square root-transformed to emphasize lower relative abundances.



## Appendix C

# Fitting GJAM with mean relative abundances

### C.1 Fitting models

#### C.1.1 Methods

We began our analysis by fitting GJAM to the mean relative abundance data product from STEPPS. When using the mean relative abundance, it is only necessary to fit GJAM once, rather than 100 times, for each of the 100 posterior samples of STEPPS. This step was therefore used to perform initial model selection and to evaluate average trends in the environment-vegetation and residual correlation parameters before proceeding with the analysis using the posterior samples of GJAM.

We used the mean relative abundances to fit five models, which differed in their covariates and whether or not interactions were included. We fit separate models with different covariate combinations instead of including all covariates in one model because of strong collinearity among covariates. Specifically, our two metrics of soil texture, soil % sand and soil % silt were strongly correlated. Additionally, temperature seasonality was correlated with total annual precipitation. Our four formulas each included only one of each set of correlated covariates (Table C.1). We fit GJAM with four formulas differing in the covariates included, with no interaction terms.

It might be expected physiologically that there could be a significant interaction between soil texture and total annual precipitation because soil texture defines the bioavailability of water in the soil. We therefore fit another model including an interaction between soil % sand and total annual precipitation in formula 1 (Table C.1).

Each model was fit using the `textscgjam` function from the `GJAM` R package using R version 4.4.2. Each model was run with a total of 10,000 iterations in one chain, with 2,000 iterations removed for burn-in. We visually assessed for con-

36 APPENDIX C. FITTING GJAM WITH MEAN RELATIVE ABUNDANCES

vergence using trace plots. All parameters appeared converged after the burn-in period. We confirmed that each set of four covariates were minimally correlated by calculating Variance Inflation Factors (all VIFs < 2.8). All code to reproduce trace plots and VIFs is available from <https://github.com/amwillson/GJAM-STEPPS>.

We evaluated differences in the coefficient estimates between models to determine which model best captured spatiotemporal trends in mean relative abundances estimates. We additionally assessed the extent to which estimates of residual correlations between taxa differed between fitted models to understand the extent to which patterns in residual correlations were sensitive to the covariates included in the model.

Table C.1: Covariates included in each of four independent formulas for fitting the GJAM model.

Formula	Sand	Silt	Average annual temperature	Total annual precipitation	Temperature seasonality	Precipitation seasonality
1	Yes	No	Yes	Yes	No	Yes
2	No	Yes	Yes	Yes	No	Yes
3	Yes	No	Yes	No	Yes	Yes
4	No	Yes	Yes	No	Yes	Yes

### C.1.2 Results

We report the coefficient estimates for the models fit with each of our four model formulas (Figures C.1- C.4). We found that patterns in the coefficients between each taxon-level relative abundance and temperature seasonality were better explained by tree physiological responses to total annual precipitation (with which temperature seasonality was strongly correlated; Figures C.3 & C.4), so we chose to focus on the two formulas including total annual precipitation instead of temperature seasonality (Formulas 1 and 2) in our analysis presented in the main text. Coefficient estimates for the soil % sand and soil % silt covariates in formulas 1 and 2, respectively, were nearly the inverse of each other (Figures C.1 & C.3 versus Figures C.2 & C.4), highlighting the strong correlation between these two soil texture covariates. Soil % sand is a more ecologically interpretable variable in our domain, owing to the strong physiological relationship between soil % sand and bioavailable water, so we chose to focus on the soil % sand covariate (Formula 1) in our main analysis with the posterior draws from STEPPS presented in the main text.

Next, we evaluated the importance of the soil texture x total annual precipitation interaction term. We used the covariate sensitivity calculated by GJAM, which measures the joint sensitivity of all taxon relative abundances to each covariate. We found that, jointly, taxon relative abundances were minimally sensitive to the interaction term (Figure C.5). Additionally, coefficients relating taxon relative abundances to the interaction overlapped zero for most taxa (Figure C.6). The taxa with significant coefficients for the interaction term showed patterns following the relationship between the taxa's relative abundances and the main soil % sand and total annual precipitation terms (Figure C.6). For instance, the negative coefficients relating oak and other hardwood taxa relative abundances and the interaction term reflected the negative relationships between oak and other hardwood taxa relative abundances and total annual precipitation. The same was true for the positive coefficients between maple and hemlock and the interaction term, which were positively related to total annual precipitation. The relative unimportance of the interaction suggested that spatiotemporal patterns in soil texture and total annual precipitation themselves sufficiently characterized patterns of soil water availability, so the interaction term was not used in the final model. In summary, our final model that we used to make inference in the main text included four covariates with no interactions: average annual temperature, total annual precipitation, precipitation seasonality, and soil % sand (Formula 1).

Finally, we compared the residual correlations between taxa from each model, which represent patterns between taxa that cannot be explained by the environmental covariates in the model. We found that each of our models (including the model with the interaction term) had similar patterns in residual correlations (Figures C.7- C.11). Specifically, we identified negative residual correlations between oak and nearly every other tree taxon (Figures C.1- C.11). Weaker positive and negative correlations occurred, but were less consistent between models and therefore less likely to represent ecological phenomena. Therefore,

we concluded that our inference on residual correlations, that environmental conditions alone cannot explain the difference between communities dominated by oak and other tree taxa, was not sensitive to the specific set of uncorrelated covariates we chose.

## C.2 Model validation

### C.2.1 Methods

After selecting the formula four our final model (above), we used our fitted model to make joint predictions of taxon relative abundances at our final time step, 300 YBP. Doing so with the model fit to the mean relative abundance estimates from STEPPS allowed us to perform several out-of-sample validation experiments. First, we used our model to make predictions based only on the environmental conditions from each grid cell at 300 YBP using the `GJAMPREDICT` function in the `GJAM` R package. We term this experiment “non-conditional prediction;” it is equivalent to the out-of-sample validation we performed with the models fit to the STEPPS posterior draws (see below). From this experiment, we found that GJAM systematically underpredicted the relative abundances of all taxa at their highest observed abundance (see below).

Second, to investigate the source of this systematic bias, we additionally used our fitted models to make predictions of each taxon’s relative abundance in each grid cell at 300 YBP, conditional on both the environmental covariates (soil % sand, average annual temperature, total annual precipitation, precipitation seasonality) and the observed mean relative abundance of each other taxon. For example, to predict the relative abundance of beech in each of our out-of-sample grid cells at 300 YBP, we used our estimates of each environmental covariate used to fit the model as well as the relative abundances of birch, elm, hemlock, maple, oak, other conifer taxa, other hardwood taxa, pine, spruce, and tamarack. Because we specified in our model formula that the relative abundances should sum to one by using the “fractional composition” data type in GJAM, the model’s predictions of the one taxon’s relative abundance that was not provided should be such that the relative abundances approximately sum to one. Failure for the relative abundances to sum to one would be indicative of limitations of our model to predict high relative abundances. This out-of-sample experiment was only possible with the model fit to mean relative abundance because the model was fit separately for each taxon, including the relative abundances of all other taxa as predictors ( $n = 11$  model runs). When we used the posterior draws of relative abundance, we bootstrapped over each posterior draw, meaning that to calculate conditional predictions, we would have to run the model 100 times for each predictor, for a total of 1,100 prediction runs. This was prohibitively computationally expensive.

### C.2.2 Results

We found that in general, our model had reasonably high prediction accuracy in our non-conditional prediction experiment (Figure C.12), with most taxa predicted well at low relative abundances. The median correlation coefficient between observed and predicted relative abundance across all taxa was  $r = 0.65$ . The best predicted taxon was oak ( $r = 0.78$ ) and the worst predicted taxon was maple ( $r = 0.39$ ). However, at high observed relative abundances all taxa were underpredicted. Additionally, oak was overpredicted at intermediate relative abundances, with these locations corresponding to forest and prairie grid cells adjacent to the savanna (not shown).

We investigated whether our model was capable of predicting high relative abundances with our conditional prediction experiment. As expected, predicted relative abundances were highly accurate with conditional prediction, mainly falling along the observed vs. predicted one-to-one line (Figure C.13). This is expected because the relative abundances must approximately sum to one and all relative abundances except the one being predicted were known. However, at high abundances, the model was still unable to predict the observed relative abundance of all taxa (Figure C.13). This demonstrates that our GJAM was structurally unable to make accurate predictions of relative abundances when the observed relative abundance was very high.

As described in the main text, patterns in relative abundance were consistent with observed trends, with predicted relative abundances higher at higher observed relative abundance. However, the failure to predict high relative abundances represents a systematic bias of our modeling approach, which limits the inference that can be made from the model. Because our out-of-sample validation showed this limitation, we focus on describing trends between environmental conditions and relative abundances (trends in coefficient estimates) and trends in residual correlations, rather than focusing on specific parameter estimates or predicted relative abundances from our model, because the model is accurately capturing trends in relative abundances (strong positive correlation coefficients). By focusing our inference on trends captured by the model, we reduce the impact that this systematic bias has on our inference.

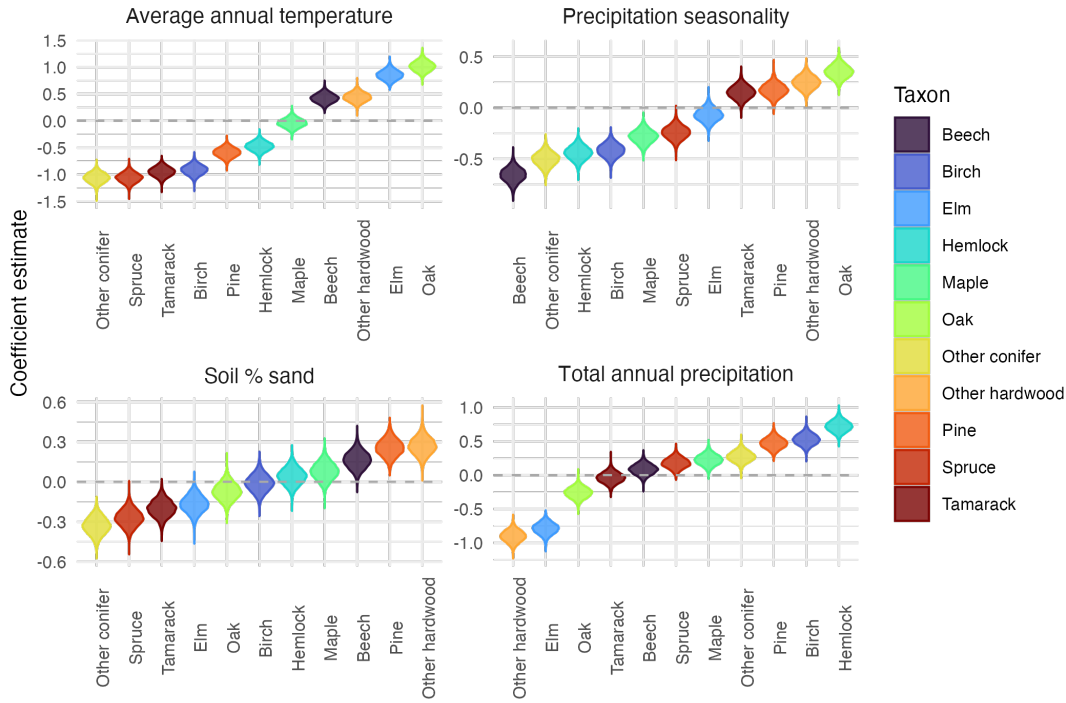


Figure C.1: Coefficient estimates quantifying the relationship between each taxon and each covariate in the model fit with Formula 1. Each facet contains the coefficient estimates relating each taxon and one environmental covariate. Top left: average annual temperature, top right: precipitation seasonality, bottom left: soil % sand, bottom right: total annual precipitation. The taxa are ordered from lowest to highest coefficient estimate on the x-axis of each facet. Note that the order of taxa differs in each facet, but the taxa are the same color across facets to facilitate intercomparison. The y-axis is the estimated model coefficient, standardized by the covariate and the taxon covariance matrix. The violins represent the distribution of coefficient estimates across Gibbs posterior samples from the model after removing burn-in. The dashed line gray line highlights 0, with violins overlapping zero suggesting a negligible influence of the covariate on a given taxon. Note that the y-axis differs between facets to highlight patterns in the coefficients.

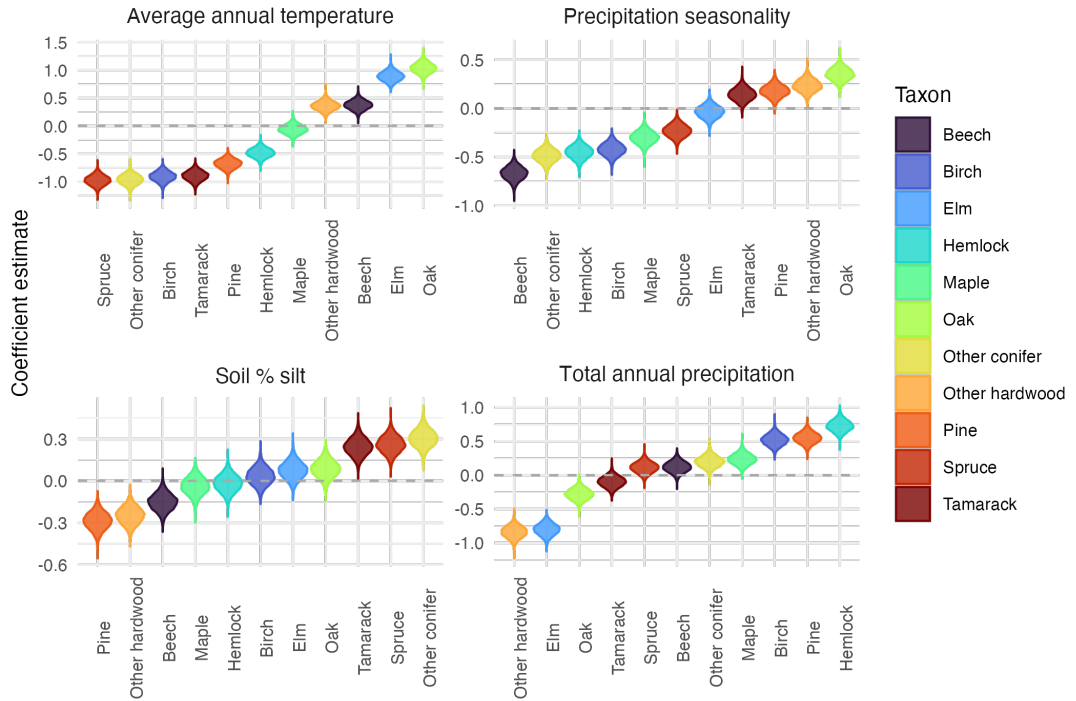


Figure C.2: Coefficient estimates quantifying the relationship between each taxon and each covariate in the model fit with Formula 2. Each facet contains the coefficient estimates relating each taxon and one environmental covariate. Top left: average annual temperature, top right: precipitation seasonality, bottom left: soil % silt, bottom right: total annual precipitation. The taxa are ordered from lowest to highest coefficient estimate on the x-axis of each facet. Note that the order of taxa differs in each facet, but the taxa are the same color across facets to facilitate intercomparison. The y-axis is the estimated model coefficient, standardized by the covariate and the taxon covariance matrix. The violins represent the distribution of coefficient estimates across Gibbs posterior samples from the model after removing burn-in. The dashed line gray line highlights 0, with violins overlapping zero suggesting a negligible influence of the covariate on a given taxon. Note that the y-axis differs between facets to highlight patterns in the coefficients.

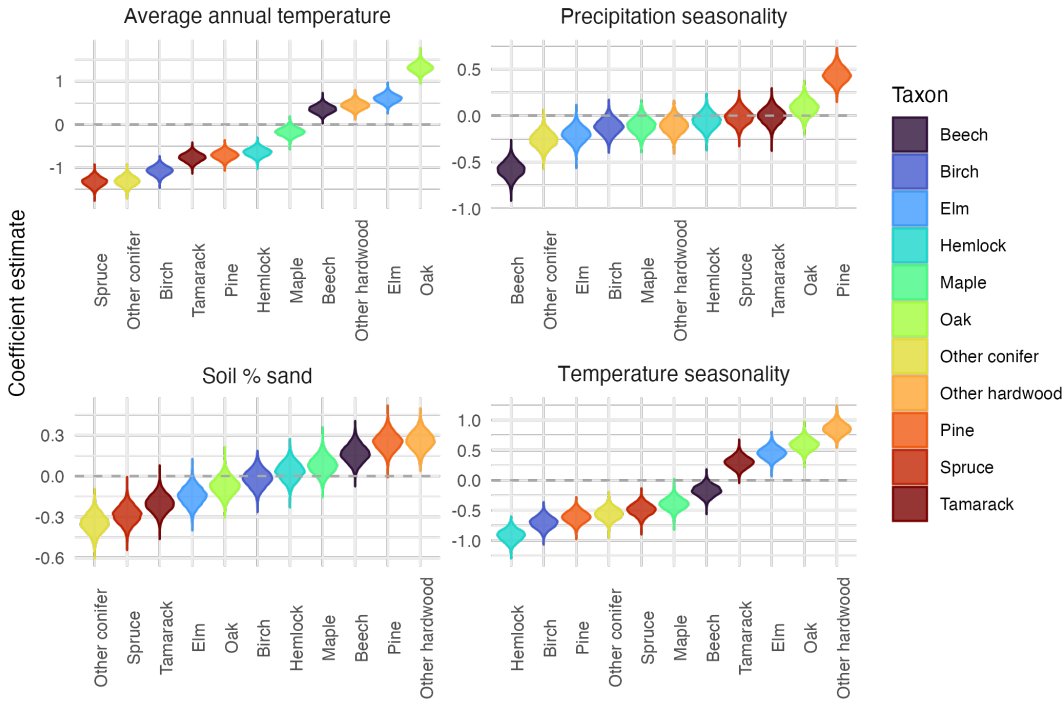


Figure C.3: Coefficient estimates quantifying the relationship between each taxon and each covariate in the model fit with Formula 3. Each facet contains the coefficient estimates relating each taxon and one environmental covariate. Top left: average annual temperature, top right: precipitation seasonality, bottom left: soil % sand, bottom right: temperature seasonality. The taxa are ordered from lowest to highest coefficient estimate on the x-axis of each facet. Note that the order of taxa differs in each facet, but the taxa are the same color across facets to facilitate intercomparison. The y-axis is the estimated model coefficient, standardized by the covariate and the taxon covariance matrix. The violins represent the distribution of coefficient estimates across Gibbs posterior samples from the model after removing burn-in. The dashed line gray line highlights 0, with violins overlapping zero suggesting a negligible influence of the covariate on a given taxon. Note that the y-axis differs between facets to highlight patterns in the coefficients.

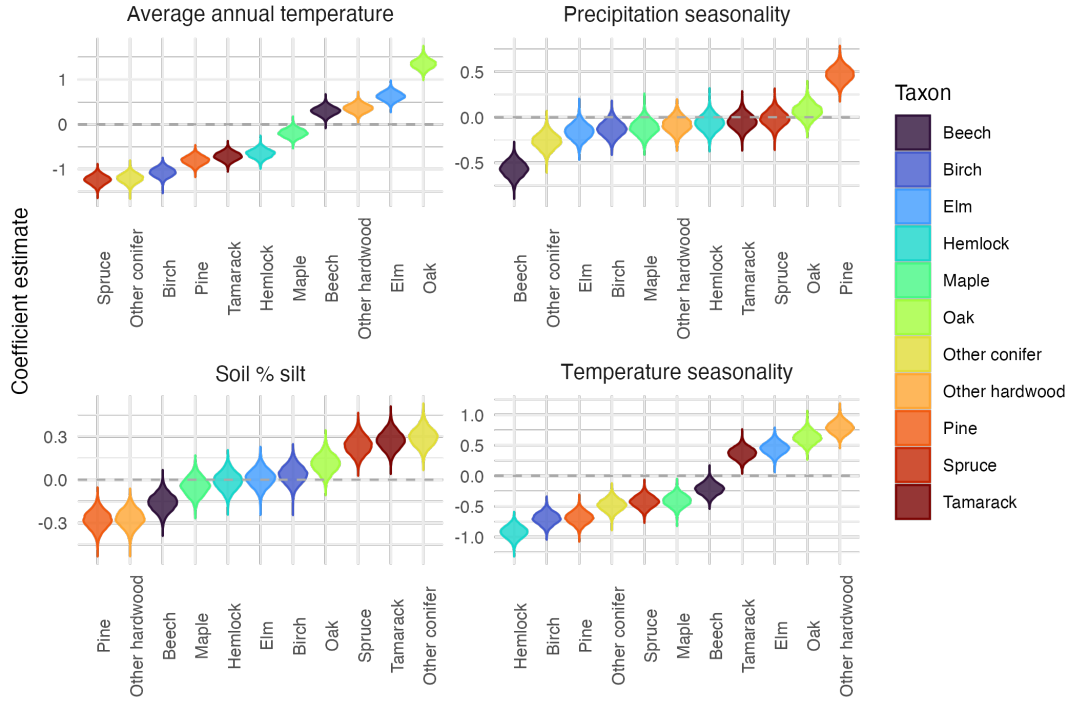


Figure C.4: Coefficient estimates quantifying the relationship between each taxon and each covariate in the model fit with Formula 4. Each facet contains the coefficient estimates relating each taxon and one environmental covariate. Top left: average annual temperature, top right: precipitation seasonality, bottom left: soil % silt, bottom right: temperature seasonality. The taxa are ordered from lowest to highest coefficient estimate on the x-axis of each facet. Note that the order of taxa differs in each facet, but the taxa are the same color across facets to facilitate intercomparison. The y-axis is the estimated model coefficient, standardized by the covariate and the taxon covariance matrix. The violins represent the distribution of coefficient estimates across Gibbs posterior samples from the model after removing burn-in. The dashed line gray line highlights 0, with violins overlapping zero suggesting a negligible influence of the covariate on a given taxon. Note that the y-axis differs between facets to highlight patterns in the coefficients.

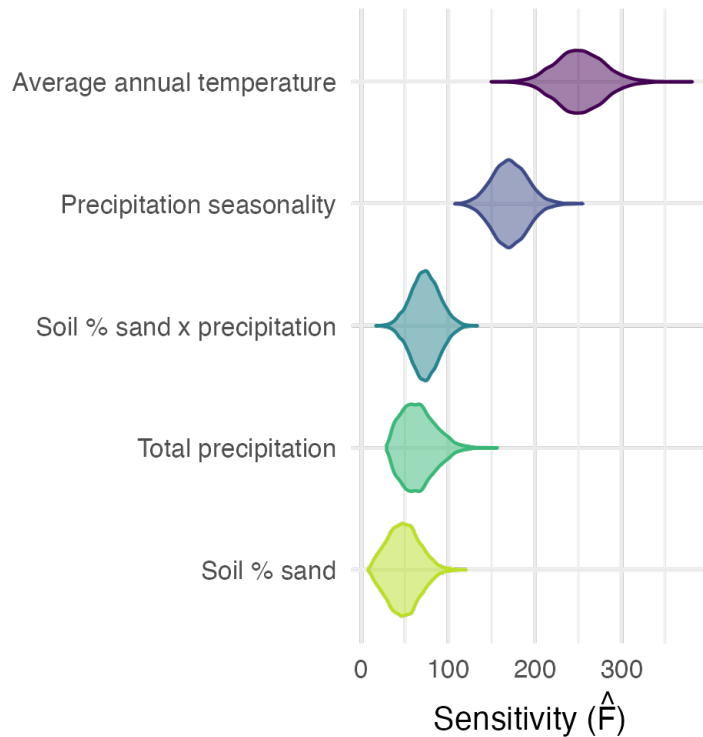


Figure C.5: Model estimated joint sensitive of taxon relative abundances to each environmental covariate for the model fit with formula 1, plus an interaction term of soil % sand x total annual precipitation. The x-axis shows the joint sensitivity of taxon relative abundances. Larger values mean that jointly, taxa are more sensitive to the environmental condition relative to the other environmental variables. The y-axis shows the environmental covariates included in the model, including the interaction term. The violins show the distribution of estimated sensitivities across the posterior Gibbs samples, after removing burn-in. Jointly, taxon relative abundances are most sensitive to average annual temperature and precipitation seasonality, with lower sensitivity to the interaction term, total annual precipitation, and soil % sand.

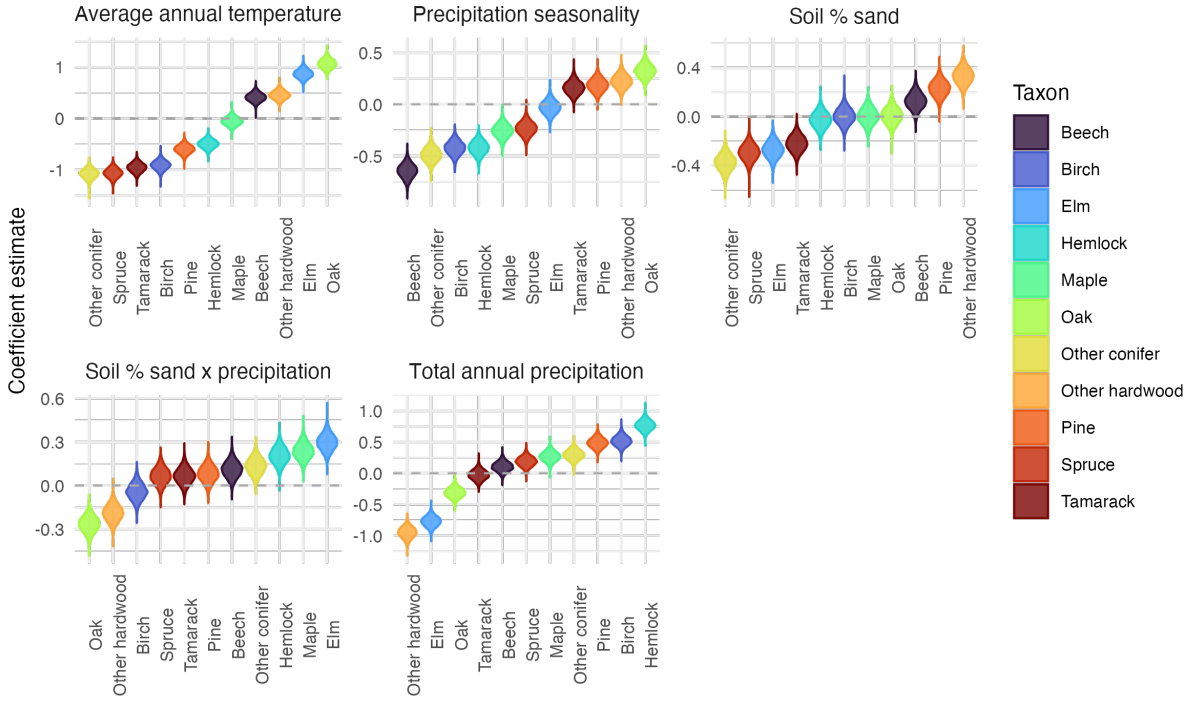


Figure C.6: Coefficient estimates quantifying the relationship between each taxon and each covariate in the model fit with Formula 1, including the interaction term between soil % sand and total annual precipitation. Each facet contains the coefficient estimates relating each taxon and one environmental covariate. Top left: average annual temperature, top middle: precipitation seasonality, top right: soil % sand, bottom left: soil % sand x total annual precipitation interaction, bottom right: total annual precipitation. The taxa are ordered from lowest to highest coefficient estimate on the x-axis of each facet. Note that the order of taxa differs in each facet, but the taxa are the same color across facets to facilitate intercomparison. The y-axis is the estimated model coefficient, standardized by the covariate and the taxon covariance matrix. The violins represent the distribution of coefficient estimates across Gibbs posterior samples from the model after removing burn-in. The dashed line gray line highlights 0, with violins overlapping zero suggesting a negligible influence of the covariate on a given taxon. Note that the y-axis differs between facets to highlight patterns in the coefficients.

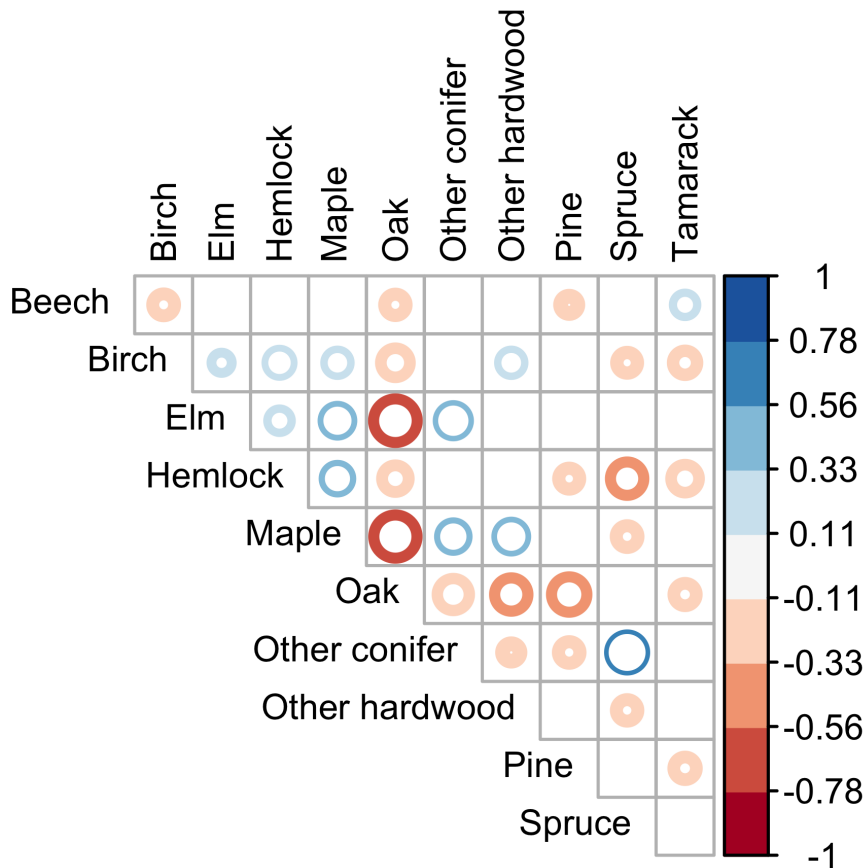


Figure C.7: Model estimated residual correlations between each taxon pair for the model fit with formula 1. Environmental covariates in this model were soil % sand, average annual temperature, total annual precipitation, and precipitation seasonality. Residual correlations quantify the relationship between taxon relative abundances after accounting for their joint dependence on the environmental covariates in the model. The size of the ring shows the magnitude of the residual correlation between the taxon pair shown to the left and top of the plot, with larger circles denoting larger residual correlations. The color of the ring shows the magnitude and direction of the correlation, with blue denoting positive correlations (taxa are more abundant together than explained by the environmental conditions) and red denoting negative correlations (taxa are less abundant together than explained by the environmental conditions). The inner and outer limits of the ring indicate the 95% credible intervals of the residual correlations from the Gibbs samples after removing burn-in. Blank cells (with no ring) have correlations overlapping 0 at the 95% credibility level.

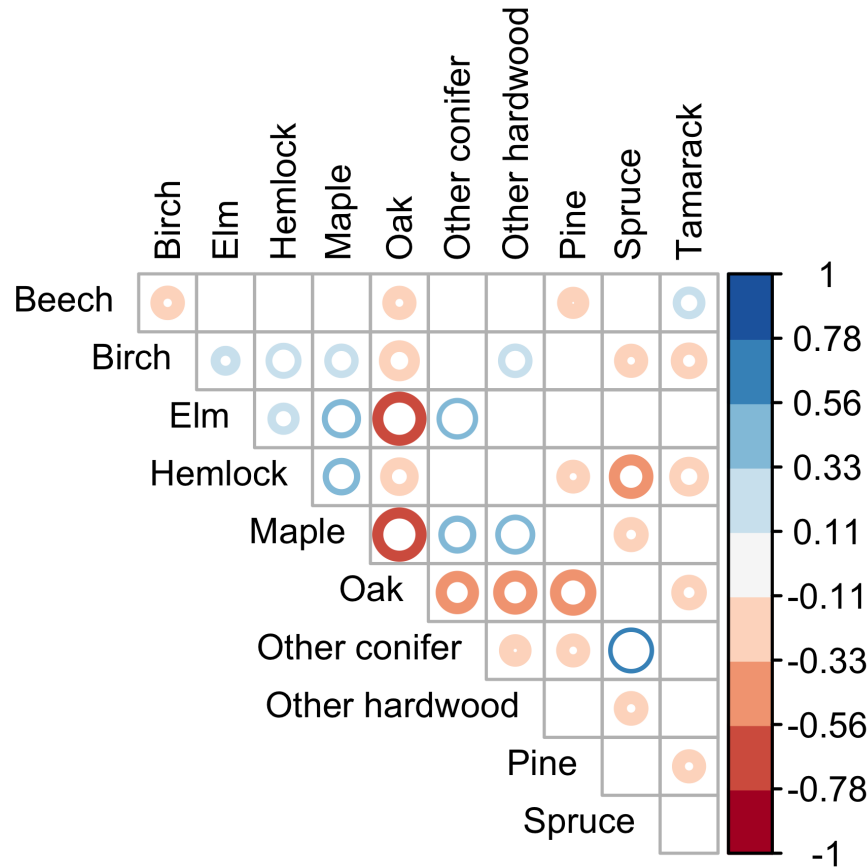


Figure C.8: Model estimated residual correlations between each taxon pair for the model fit with formula 2. Environmental covariates in this model were soil % silt, average annual temperature, total annual precipitation, and precipitation seasonality. Residual correlations quantify the relationship between taxon relative abundances after accounting for their joint dependence on the environmental covariates in the model. The size of the ring shows the magnitude of the residual correlation between the taxon pair shown to the left and top of the plot, with larger circles denoting larger residual correlations. The color of the ring shows the magnitude and direction of the correlation, with blue denoting positive correlations (taxa are more abundant together than explained by the environmental conditions) and red denoting negative correlations (taxa are less abundant together than explained by the environmental conditions). The inner and outer limits of the ring indicate the 95% credible intervals of the residual correlations from the Gibbs samples after removing burn-in. Blank cells (with no ring) have correlations overlapping 0 at the 95% credibility level.

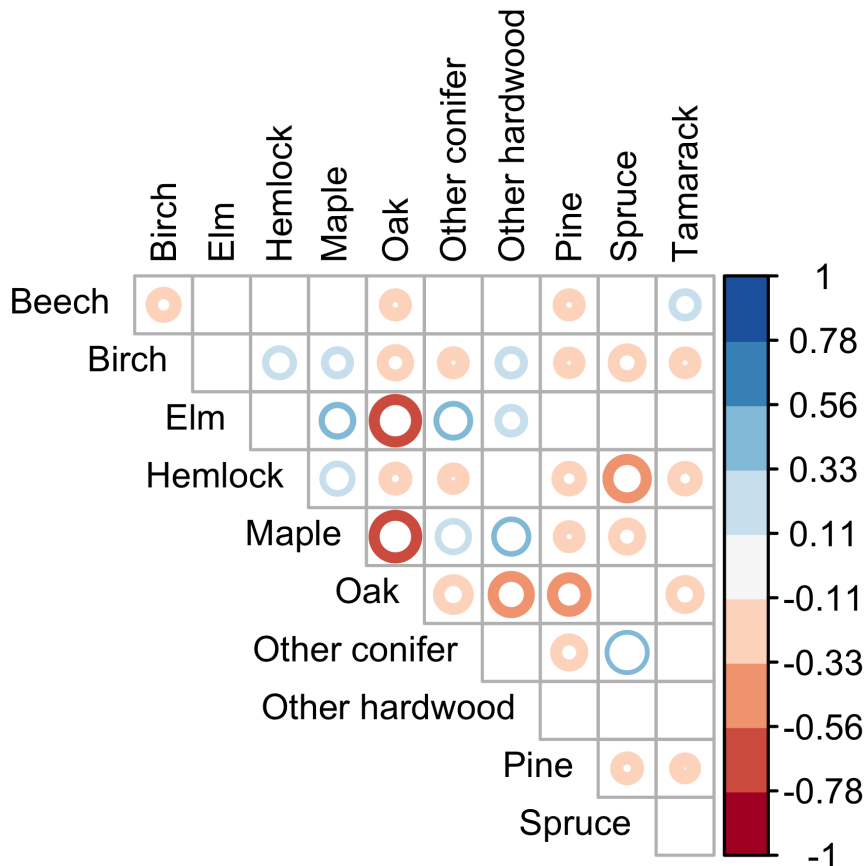


Figure C.9: Model estimated residual correlations between each taxon pair for the model fit with formula 3. Environmental covariates in this model were soil % sand, average annual temperature, temperature seasonality, and precipitation seasonality. Residual correlations quantify the relationship between taxon relative abundances after accounting for their joint dependence on the environmental covariates in the model. The size of the ring shows the magnitude of the residual correlation between the taxon pair shown to the left and top of the plot, with larger circles denoting larger residual correlations. The color of the ring shows the magnitude and direction of the correlation, with blue denoting positive correlations (taxa are more abundant together than explained by the environmental conditions) and red denoting negative correlations (taxa are less abundant together than explained by the environmental conditions). The inner and outer limits of the ring indicate the 95% credible intervals of the residual correlations from the Gibbs samples after removing burn-in. Blank cells (with no ring) have correlations overlapping 0 at the 95% credibility level.

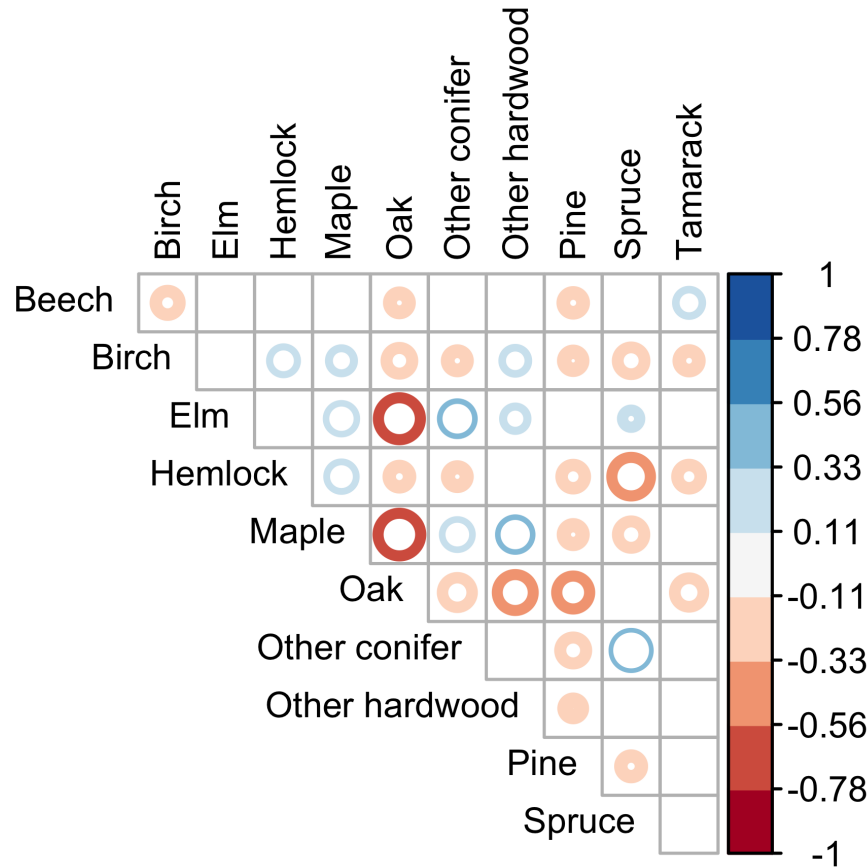


Figure C.10: Model estimated residual correlations between each taxon pair for the model fit with formula 4. Environmental covariates in this model were soil % silt, average annual temperature, temperature seasonality, and precipitation seasonality. Residual correlations quantify the relationship between taxon relative abundances after accounting for their joint dependence on the environmental covariates in the model. The size of the ring shows the magnitude of the residual correlation between the taxon pair shown to the left and top of the plot, with larger circles denoting larger residual correlations. The color of the ring shows the magnitude and direction of the correlation, with blue denoting positive correlations (taxa are more abundant together than explained by the environmental conditions) and red denoting negative correlations (taxa are less abundant together than explained by the environmental conditions). The inner and outer limits of the ring indicate the 95% credible intervals of the residual correlations from the Gibbs samples after removing burn-in. Blank cells (with no ring) have correlations overlapping 0 at the 95% credibility level.

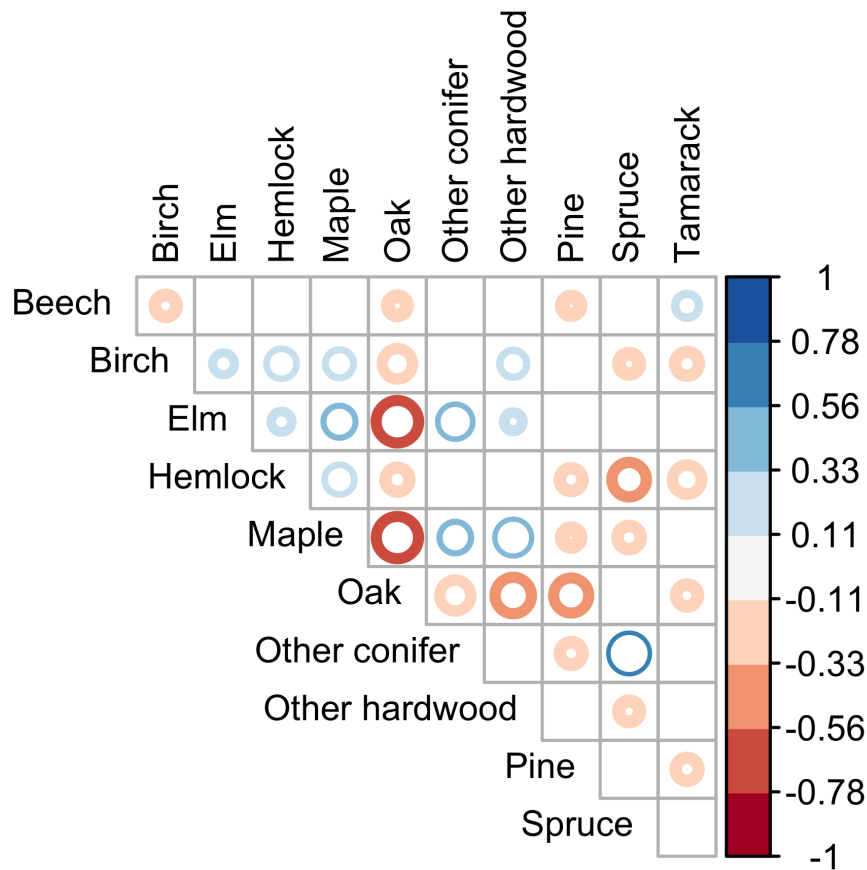


Figure C.11: Model estimated residual correlations between each taxon pair for the model fit with formula 1, plus an interaction term of soil % sand x total annual precipitation. Environmental covariates in this model were soil % sand, average annual temperature, total annual precipitation, and precipitation seasonality, and the soil % sand x total annual precipitation interaction. Residual correlations quantify the relationship between taxon relative abundances after accounting for their joint dependence on the environmental covariates. The size of the ring shows the magnitude of the residual correlation between the taxon pair shown to the left and top of the plot, with larger circles denoting larger residual correlations. The color of the ring shows the magnitude and direction of the correlation, with blue denoting positive correlations (taxa are more abundant together than explained by the environmental conditions) and red denoting negative correlations (taxa are less abundant together than explained by the environmental conditions). The inner and outer limits of the ring indicate the 95% credible intervals of the residual correlations from the Gibbs samples after removing burn-in. Blank cells (with no ring) have correlations overlapping 0 at the 95% credibility level.

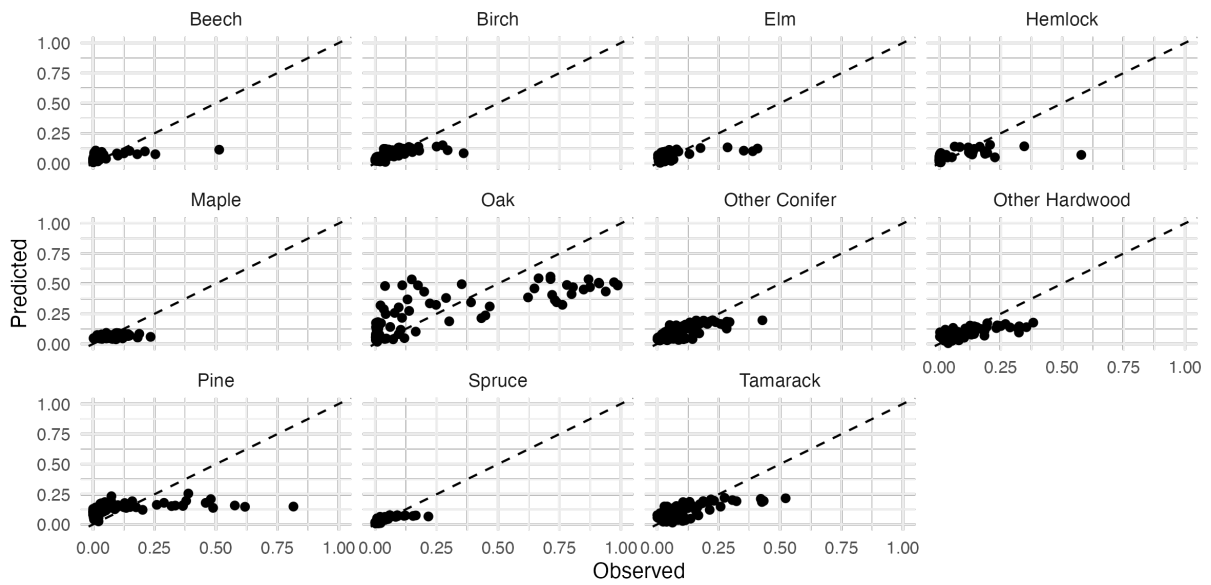


Figure C.12: Observed vs predicted relative abundance of each taxon from each grid cell for the 300 years before present (YBP) time step. Observed relative abundance (fraction of all stems) is on the x-axis; predicted relative abundance (fraction of all stems) from our GJAM conditional on environmental conditions (soil % sand, average annual temperature, total annual precipitation, precipitation seasonality). The dashed black line shows the 1:1 line indicating perfect predictions. Each facet shows the observed vs predicted relative abundance of one of eleven taxa. Overall, relative abundances are reasonable at low observed relative abundance and poor for all taxa at the highest observed relative abundance. Oak relative abundance is additionally poorly predicted at intermediate abundances.

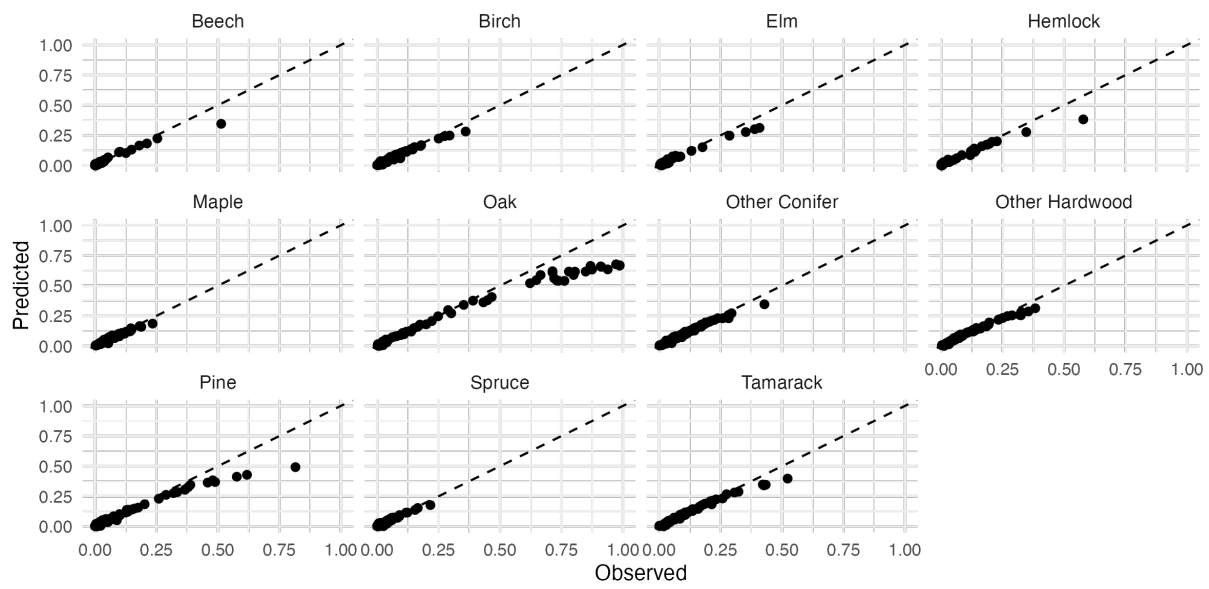


Figure C.13: Observed vs predicted relative abundance of each taxon from each grid cell for the 300 years before present (YBP) time step. Observed relative abundance (fraction of all stems) is on the x-axis; predicted relative abundance (fraction of all stems) from our GJAM conditional on environmental conditions (soil % sand, average annual temperature, total annual precipitation, precipitation seasonality) and on the relative abundances of all other taxa at that grid cell. The dashed black line shows the 1:1 line indicating perfect predictions. Each facet shows the observed vs predicted relative abundance of one of eleven taxa. Overall, relative abundances are predicted very well, but predictions are low for the highest observed relative abundances.



## Appendix D

# Fitting GJAM with posterior draws

After fitting GJAM using the mean estimates of taxon relative abundances, we chose the model formula with average annual temperature, total annual precipitation, precipitation seasonality, and soil % sand covariates. However, it could still be the case that the parameters estimated when fitting the model to posterior relative abundances could be sensitive to the set of covariates included. Therefore, we additionally fit GJAM to each of our four model formulas in Appendix C to the posterior draws of GJAM to ensure that our interpretation was not biased by the covariates we chose to include.

Here, we report the results fitting GJAM to each of the four model formulas from Appendix C, but with uncertainty accounting from fitting the model to posterior draws of STEPPS. The first section compares models fit with four time steps (1900, 1500, 1100, and 700 YBP) with the same covariate combinations as in Appendix C. In the next section, we report the results of out-of-sample prediction of the 300 YBP time step for each of the models fit with different covariate combinations. This corresponds to Validation Phase 1 in the main text. We then refit our final model (including average annual temperature, total annual precipitation, precipitation seasonality, and soil % sand covariates) with five time steps (1900, 1500, 1100, 700, and 300 YBP), including the data that was originally withheld for validation in Validation Phase 1. Figures of the parameter estimates from this model are shown in the main text; we additionally include tables of the parameter estimates from our final model in this appendix. Finally, we show the full out-of-sample validation of our final model.

## D.1 Fitting models with alternate covariate combinations

### D.1.1 Methods

To ensure that our ecological interpretations of the model were not specific to the environmental covariates used to fit the models with the posterior draws from GJAM, we fit models with the other three environmental covariate combinations from Appendix C. This also allowed us to investigate environment-vegetation relationships from environmental covariates not in our main model with the fully specified uncertainty in the relative abundance reconstructions.

We fit GJAM 100 times to each of the following four environmental covariate combinations (Formulas 1-4 in Table C.1): soil % silt, average annual temperature, total annual precipitation, precipitation seasonality (Formula 2); soil % sand, average annual temperature, temperature seasonality, precipitation seasonality (Formula 3); and soil % silt, average annual temperature, temperature seasonality, precipitation seasonality (Formula 4). We fit the model with the following time steps, withholding the 300 YBP time step as initial model validation: 1900, 1500, 1100, and 700 YBP. For each model formula fit with each posterior draw, the model was run with a total of 10,000 iterations in one chain, with 2,000 iterations removed for burn-in. We assessed for convergence of each of the model formulas fit to the 100 posterior draws of STEPPS using trace plots. All parameters appeared to be converged after removing the burn-in period. All code to reproduce trace plots is available from <https://github.com/amwillson/GJAM-STEPS>.

Here, we report the coefficient estimates, joint sensitivity, and residual correlations for the four models fit with different combinations of environmental covariates (Formulas 1-4). Before fitting our final model with the 300 YBP time step, we ensured that the conclusions we drew regarding model selection using the mean relative abundances (Appendix C) were consistent when using the posterior draws from the STEPPS model.

### D.1.2 Results

#### Vegetation-environment coefficient estimates

The estimates of the coefficients describing the relationship between the environmental covariates to the taxon relative abundances were similar between models sharing the environmental covariate (Figures D.1- D.4, Table D.1). Between formulas that used the soil % sand covariate (Formulas 1 & 3), coefficient estimates were approximately equal; the same was true for formulas using the soil % silt covariate. The only exception was the estimates of the relationship between soil % silt and spruce relative abundance, which was negative in Formula 2 and overlapped zero in Formula 4. For most taxa, the coefficient estimates for soil % sand and soil % silt were approximately the reciprocal of each other: when a taxon relative abundance was positively related to soil % sand,

it was correspondingly negatively related to soil % silt. This was especially true when accounting for the uncertainty in the coefficient estimates. These observations indicated that the soil % sand and soil % silt covariates contained approximately the same information about taxon relative abundances and were relatively independent of the climate covariates. We chose to use the soil % sand covariate in our main model (Formula 1) because soil % sand is more ecologically interpretable, given the known relationship between soil sand content and taxa like pine; this decision is consistent with that made with the mean relative abundances in Appendix C.

Similarly, taxon-specific coefficient estimates for average annual temperature remained relatively consistent across model formulas: the sign of the coefficient estimates was consistent for all taxa, although the magnitude of coefficient estimates varied slightly. Between formulas with the total annual precipitation covariate (Formulas 1 & 2), coefficient estimates were similar, except in the case of spruce, where spruce was positively related to total annual precipitation only when using Formula 2. The difference in coefficient estimates for spruce relative abundance may represent a correlation between soil texture and climate only in the northern portion of our study region, where spruce was most abundant.

The taxon-specific temperature seasonality coefficients remained consistent between Formulas 3 & 4. On the other hand, precipitation seasonality coefficients were different between Formulas 1 & 2 and Formulas 3 & 4. The coefficient estimates were always similar between Formulas 1 & 2 and between Formulas 3 & 4, but differed between the first two and last two formulas. This likely represented a trade-off between precipitation seasonality and total annual precipitation or precipitation seasonality and temperature seasonality. We chose to focus on the formula with total annual precipitation because this variable was more ecologically interpretable than temperature seasonality, and many of the patterns in coefficient estimates for temperature seasonality were similar to the patterns in coefficient estimates for total annual precipitation. Nevertheless, the sign of precipitation seasonality coefficients generally remained consistent across Formulas. The difference in coefficient estimates between Formulas 1 & 2 and Formulas 3 & 4 highlights that interpretations of the precipitation seasonality coefficients, and especially their magnitude, may be dependent on the specific covariates included in the model.

### **Joint sensitivity to environmental covariates**

Similar to the environment-vegetation coefficient estimates, we found consistency in the joint sensitivity of all taxa's relative abundance to each environmental covariate across model formulas (Figures D.5- D.8, Table D.2). The sensitivity of taxa to soil % sand and soil % silt remained consistent between Formulas 1 & 3 and Formulas 2 & 4, respectively. Similarly, sensitivity of taxa to total annual precipitation and temperature seasonality remained consistent between formulas that contained these terms. The sensitivity of average annual temperature differed between Formulas 1 & 2 and Formulas 3 & 4, but in all cases, taxa were jointly most sensitive to average annual temperature. In the

case of precipitation seasonality, the joint sensitivity differed between Formulas 1 & 2 and Formulas 3 & 4, with taxa jointly more sensitive to precipitation seasonality than total annual precipitation (Formulas 1 & 2), but less sensitive to precipitation seasonality than temperature seasonality (Formulas 3 & 4). We conclude that across formulas, taxa were jointly most sensitive to average annual temperature and least sensitive to soil texture. The relative sensitivity of our taxon relative abundances to total annual precipitation, temperature seasonality, and precipitation seasonality should be interpreted with caution, with the sensitivity differing depending on the specific formula used. However, jointly, taxa were clearly sensitive to total annual precipitation and climate seasonality, supporting our inclusion of these variables in our models.

#### **Residual correlations among taxon relative abundances**

Residual correlations represent the correlations that remained between taxa after accounting for their relationship with the environmental covariates in the model. Negative residual correlations indicate that in the same environmental conditions, the taxa did not associate with one another, while positive residual correlations indicate that in the same environmental conditions, the taxa favored associating with one another (Table D.3). The values of the residual correlations remained stable across the four formulas we tested (Table D.3, Figures D.9- D.12). Overall, most residual correlations were small in magnitude with large error, such that most residual correlations overlapped zero at the 95% credibility level, indicating that the environmental conditions sufficiently explained differences in relative abundances between taxa. In contrast, across all formulas, oak was negatively correlated with nearly all taxa, indicating that oak existed in a different community from forest and prairie tree taxa, even in the same environmental conditions. Similarly, hemlock was negatively correlated with other northern forest tree taxa, highlighting the role of lagged community dynamics in perpetuating high hemlock abundance. Overall, the lack of sensitivity of our residual correlations to the formula used demonstrates that the residual correlations are robust to different sets of environmental covariates.

## **D.2 Out-of-sample validation**

Similar to our out-of-sample validation with the mean relative abundance estimates, we used our main model using Formula 1 (soil % sand, average annual temperature, total annual precipitation, and precipitation seasonality covariates) to predict relative abundances at the 300 YBP time step. Unlike with the model fit to mean relative abundances, we only performed non-conditional prediction, where all taxon relative abundances were jointly predicted based only on the environmental conditions of each grid cell. As explained above, doing conditional prediction with the posterior draws was prohibitively computationally expensive.

The predictions of the 300 YBP time step using the model fit to posterior

draws generally mirrors the predictions using the model fit to mean relative abundances (Figure D.13). The median correlation coefficient between observed and predicted relative abundance across taxa is 0.63 [0.48, 0.72] (median [95% CrI]). As with the predictions from the mean relative abundances, oak is the best predicted taxon ( $r = 0.75$  [0.68, 0.81]) and maple is the worst predicted taxon ( $r = 0.31$  [0.12, 0.53]). As before, relative abundance is underpredicted for all taxa at the highest observed relative abundance and this trend remains significant when accounting for the uncertainty in the prediction arising from the uncertainty in relative abundance estimates (Figure D.13). Additionally, oak is again overpredicted at intermediate relative abundances, which reflects the inability of the model to capture trends in oak relative abundance at the savanna-forest and prairie-savanna ecotones (not shown).

These results reinforce our interpretation of our previous validation, showing that our GJAM is not suitable for making point predictions or quantifying the magnitude of specific environment-vegetation relationships. However, because the model again captures the appropriate trends in taxon relative abundances, we conclude that the model is suitable for understanding patterns in environment-vegetation relationships and patterns in residual correlations.

Table D.1: Coefficient estimates of environment-taxon relative abundance relationships from models fit with each of four formulas.

Taxon	Covariate	Formula 1	Formula 2	Formula 3	Formula 4
Beech	Soil % sand	0.14 [-0.035, 0.35]		0.14 [-0.036, 0.35]	
	Soil % silt		-0.13 [-0.31, 0.036]		-0.13 [-0.32, 0.030]
	Average annual temperature	0.36 [0.15, 0.57]	0.31 [0.11, 0.53]	0.29 [0.061, 0.54]	0.25 [0.011, 0.50]
	Total annual precipitation	0.078 [-0.11, 0.27]	0.11 [-0.087, 0.31]		
	Temperature seasonality			-0.16 [-0.40, 0.073]	-0.19 [-0.44, 0.043]
	Precipitation seasonality	-0.56 [-0.76, -0.37]	-0.57 [-0.77, -0.38]	-0.49 [-0.72, -0.27]	-0.48 [-0.71, -0.26]

Table D.1: (Continued)

Taxon	Covariate	Formula 1	Formula 2	Formula 3	Formula 4
Birch	Soil % sand	-0.021 [-0.19, 0.16]		-0.025 [-0.19, 0.15]	
	Soil % silt		0.039 [-0.13, 0.21]		0.043 [-0.13, 0.21]
	Average annual temperature	-0.81 [-1.1, -0.58]	-0.80 [-1.1, -0.58]	-0.95 [-1.3, -0.65]	-0.94 [-1.3, -0.64]
	Total annual precipitation	0.46 [0.25, 0.67]	0.45 [0.24, 0.67]		
	Temperature seasonality			-0.62 [-0.91, -0.30]	-0.61 [-0.91, -0.29]
	Precipitation seasonality	-0.38 [-0.58, -0.19]	-0.39 [-0.59, -0.20]	-0.12 [-0.36, 0.11]	-0.13 [-0.38, 0.11]
Elm	Soil % sand	-0.15 [-0.31, 0.051]		-0.13 [-0.29, 0.057]	
	Soil % silt		0.066 [-0.11, 0.22]		0.0075 [-0.15, 0.15]
	Average annual temperature	0.77 [0.54, 1.0]	0.80 [0.56, 1.0]	0.55 [0.33, 0.79]	0.58 [0.36, 0.82]
	Total annual precipitation	-0.71 [-0.98, -0.47]	-0.72 [-0.99, -0.47]		
	Temperature seasonality			0.42 [0.20, 0.69]	0.42 [0.19, 0.69]
	Precipitation seasonality	-0.063 [-0.22, 0.12]	-0.032 [-0.18, 0.14]	-0.19 [-0.39, 0.022]	-0.14 [-0.35, 0.066]

Table D.1: (Continued)

Taxon	Covariate	Formula 1	Formula 2	Formula 3	Formula 4
Hemlock	Soil % sand	0.035 [-0.11, 0.18]		0.030 [-0.12, 0.18]	
	Soil % silt		-0.015 [-0.16, 0.13]		-0.0059 [-0.15, 0.14]
	Average annual temperature	-0.43 [-0.62, -0.24]	-0.44 [-0.62, -0.26]	-0.58 [-0.80, -0.38]	-0.59 [-0.80, -0.39]
	Total annual precipitation	0.65 [0.46, 0.85]	0.66 [0.46, 0.86]		
	Temperature seasonality			-0.83 [-1.1, -0.61]	-0.83 [-1.1, -0.61]
	Precipitation seasonality	-0.41 [-0.58, -0.23]	-0.42 [-0.59, -0.24]	-0.059 [-0.26, 0.14]	-0.067 [-0.27, 0.14]
Maple	Soil % sand	0.081 [-0.13, 0.28]		0.080 [-0.14, 0.28]	
	Soil % silt		-0.047 [-0.23, 0.16]		-0.055 [-0.23, 0.16]
	Average annual temperature	-0.027 [-0.32, 0.27]	-0.050 [-0.35, 0.27]	-0.12 [-0.45, 0.16]	-0.14 [-0.48, 0.15]
	Total annual precipitation	0.18 [-0.15, 0.50]	0.19 [-0.15, 0.52]		
	Temperature seasonality			-0.31 [-0.66, 0.067]	-0.32 [-0.67, 0.062]
	Precipitation seasonality	-0.20 [-0.45, 0.010]	-0.22 [-0.46, 0.0086]	-0.072 [-0.38, 0.23]	-0.078 [-0.39, 0.22]

Table D.1: (Continued)

Taxon	Covariate	Formula 1	Formula 2	Formula 3	Formula 4
Oak	Soil % sand	-0.072 [-0.23, 0.086]		-0.072 [-0.23, 0.088]	
	Soil % silt		0.083 [-0.066, 0.23]		0.11 [-0.047, 0.25]
	Average annual temperature	0.95 [0.73, 1.2]	0.97 [0.75, 1.2]	1.2 [0.97, 1.5]	1.3 [0.99, 1.5]
	Total annual precipitation	-0.24 [-0.49, -0.024]	-0.26 [-0.51, -0.044]		
	Temperature seasonality			0.56 [0.31, 0.84]	0.58 [0.34, 0.87]
	Precipitation seasonality	0.33 [0.17, 0.48]	0.33 [0.18, 0.47]	0.077 [-0.14, 0.28]	0.056 [-0.16, 0.25]
Other conifer taxa	Soil % sand	-0.24 [-0.43, -0.057]		-0.25 [-0.44, -0.062]	
	Soil % silt		0.22 [0.046, 0.42]		0.21 [0.036, 0.42]
	Average annual temperature	-0.80 [-1.1, -0.44]	-0.73 [-1.0, -0.37]	-0.96 [-1.4, -0.61]	-0.88 [-1.3, -0.53]
	Total annual precipitation	0.22 [-0.076, 0.54]	0.17 [-0.13, 0.48]		
	Temperature seasonality			-0.43 [-0.83, 0.0079]	-0.38 [-0.78, 0.065]
	Precipitation seasonality	-0.35 [-0.57, -0.15]	-0.34 [-0.56, -0.14]	-0.16 [-0.47, 0.13]	-0.16 [-0.47, 0.13]

Table D.1: (Continued)

Taxon	Covariate	Formula 1	Formula 2	Formula 3	Formula 4
Other hardwood taxa	Soil % sand	0.21 [0.012, 0.43]		0.21 [0.013, 0.43]	
	Soil % silt		-0.20 [-0.38, -0.021]		-0.22 [-0.40, -0.046]
	Average annual temperature	0.36 [0.024, 0.65]	0.29 [-0.038, 0.60]	0.36 [0.040, 0.67]	0.29 [-0.025, 0.61]
	Total annual precipitation	-0.73 [-1.0, -0.44]	-0.68 [-1.0, -0.38]		
	Temperature seasonality			0.69 [0.37, 1.1]	0.64 [0.31, 1.0]
	Precipitation seasonality	0.20 [0.018, 0.39]	0.19 [0.020, 0.36]	-0.083 [-0.34, 0.18]	-0.062 [-0.32, 0.19]
Pine	Soil % sand	0.23 [0.083, 0.39]		0.23 [0.081, 0.38]	
	Soil % silt		-0.26 [-0.41, -0.12]		-0.25 [-0.40, -0.11]
	Average annual temperature	-0.54 [-0.74, -0.34]	-0.62 [-0.82, -0.42]	-0.65 [-0.87, -0.43]	-0.73 [-0.95, -0.51]
	Total annual precipitation	0.43 [0.26, 0.61]	0.50 [0.31, 0.68]		
	Temperature seasonality			-0.55 [-0.78, -0.33]	-0.62 [-0.86, -0.40]
	Precipitation seasonality	0.16 [0.013, 0.30]	0.16 [0.019, 0.30]	0.40 [0.22, 0.58]	0.43 [0.24, 0.61]

Table D.1: (Continued)

Taxon	Covariate	Formula 1	Formula 2	Formula 3	Formula 4
Spruce	Soil % sand	-0.19 [-0.37, -0.018]		-0.19 [-0.38, -0.022]	
	Soil % silt		0.18 [-0.0019, 0.36]		0.16 [-0.017, 0.35]
	Average annual temperature	-0.72 [-1.1, -0.43]	-0.62 [-0.82, -0.42]	-0.98 [-1.3, -0.67]	-0.92 [-1.2, -0.62]
	Total annual precipitation	0.15 [-0.075, 0.35]	0.10 [-0.12, 0.31]		
	Temperature seasonality			-0.39 [-0.68, 0.069]	-0.35 [-0.64, 0.11]
	Precipitation seasonality	-0.18 [-0.37, 0.0035]	-0.17 [-0.37, 0.015]	0.00023 [-0.28, 0.23]	-0.00048 [-0.29, 0.23]
Tamarack	Soil % sand	-0.16 [-0.37, 0.052]		-0.16 [-0.37, 0.053]	
	Soil % silt		0.19 [-0.026, 0.41]		0.21 [-0.010, 0.43]
	Average annual temperature	-0.74 [-1.0, -0.45]	-0.70 [-0.95, -0.43]	-0.60 [-0.91, -0.30]	-0.56 [-0.85, -0.26]
	Total annual precipitation	-0.020 [-0.32, 0.21]	-0.066 [-0.37, 0.17]		
	Temperature seasonality			0.22 [-0.17, 0.61]	0.28 [-0.14, 0.67]
	Precipitation seasonality	0.12 [-0.066, 0.29]	0.11 [-0.066, 0.28]	0.0066 [-0.30, 0.28]	-0.029 [-0.34, 0.26]

Columns titled “Formula 1”-“Formula 4” report the median and 95% credible interval in brackets.

Taxon scientific names are as follows: beech (*Fagus grandifolia*), birch (*Betula spp.*), elm (*Ulmus spp.*), hemlock (*Tsuga canadensis*), maple (*Acer spp.*), oak (*Quercus spp.*), pine (*Pinus spp.*), spruce (*Picea spp.*), and tamarack (*Larix laricina*).

Formula 1 includes the following covariates: soil % sand, average annual temperature, total annual precipitation, and precipitation seasonality. Formula 2 includes the following covariates: soil % silt, average annual temperature, total annual precipitation, and precipitation seasonality. Formula 3 includes the following covariates: soil % sand, average annual temperature, temperature seasonality, and precipitation seasonality. Formula 4 includes the following covariates: soil % silt, average annual temperature, temperature seasonality, and precipitation seasonality.

Table D.2: Joint sensitivity of all taxon relative abundances to each environmental covariate

Covariate	Formula 1	Formula 2	Formula 3	Formula 4
Soil % sand	12.8 [6.53, 33.1]		13.1 [6.62, 33.5]	
Soil % silt		12.5 [6.19, 34.2]		12.2 [6.23, 31.8]
Average annual temperature	104 [60.1, 165]	103 [60.3, 164]	148 [94.9, 218]	147 [93.9, 217]
Total annual precipitation	35.7 [22.0, 70.4]	34.9 [21.4, 69.2]		
Temperature seasonality			83.2 [41.0, 137]	82.2 [40.3, 136]
Precipitation seasonality	78.7 [48.7, 119]	79.0 [48.8, 119]	44.1 [15.7, 82.8]	43.2 [15.2, 81.9]

Columns titled “Formula 1” - “Formula 4” report the median and 95% credible intervals (in brackets) of the joint sensitivity of all taxa to each environmental covariate for the model fit with that formula. Larger values indicate that taxa are jointly more sensitive to the given environmental covariate.

Formula 1 includes the following covariates: soil % sand, average annual temperature, total annual precipitation, and precipitation seasonality. Formula 2 includes the following covariates: soil % silt, average annual temperature, total annual precipitation, and precipitation seasonality. Formula 3 includes the following covariates: soil % sand, average annual temperature, temperature seasonality, and precipitation seasonality. Formula 4 includes the following covariates: soil % silt, average annual temperature, temperature seasonality, and precipitation seasonality.

Table D.3: Coefficient estimates of environment-taxon relative abundance relationships from models fit with each of four formulas.

Taxon 1	Taxon 2	Formula 1	Formula 2	Formula 3	Formula 4
Beech	Beech	1.0 [1.0,1.0]	1.0 [1.0,1.0]	1.0 [1.0,1.0]	1.0 [1.0,1.0]
	Birch	-0.12 [-1.0,0.0094]	-0.12 [-1.0,0.010]	-0.14 [-1.0,0.0030]	-0.14 [-1.0,0.0040]
	Elm	-0.0023 [-0.53,0.061]	-0.0099 [-0.57,0.055]	-0.0038 [-0.57,0.057]	-0.015 [-0.63,0.049]
	Hemlock	0.0039 [-0.64,0.074]	-0.0057 [-0.63,0.075]	-0.016 [-0.74,0.065]	-0.014 [-0.72,0.067]
	Maple	-0.0080 [-0.79,0.092]	-0.0043 [-0.77,0.094]	-0.017 [-0.83,0.086]	-0.014 [-0.81,0.087]
	Oak	-0.14 [-0.90,-0.0078]	-0.14 [-0.89,-0.0071]	-0.13 [-0.86,0.0026]	-0.13 [-0.84,0.0049]
	Other conifer taxa	-0.036 [-0.90,0.062]	-0.037 [-0.90,0.062]	-0.050 [-1.0,0.054]	-0.051 [-1.0,0.054]
	Other hardwood taxa	-0.043 [-0.60,0.042]	-0.041 [-0.59,0.042]	-0.029 [-0.54,0.047]	-0.031 [-0.55,0.046]
	Pine	-0.094 [-0.76,0.014]	-0.098 [-0.77,0.012]	-0.11 [-0.82,0.0060]	-0.11 [-0.84,0.0038]
	Spruce	-0.022 [-0.92,0.047]	-0.023 [-0.92,0.047]	-0.037 [-1.0,0.041]	-0.039 [-1.0,0.040]
	Tamarack	0.12 [-0.027,0.18]	0.12 [-0.021,0.18]	0.13 [0.011,0.19]	0.14 [0.026,0.20]

Table D.3: (Continued)

Taxon 1	Taxon 2	Formula 1	Formula 2	Formula 3	Formula 4
Birch	Beech	-0.12 [-1.0,0.0094]	-0.12 [-1.0,0.010]	-0.14 [-1.0,0.0030]	-0.14 [-1.0,0.0040]
	Birch	1.0 [1.0,1.0]	1.0 [1.0,1.0]	1.0 [1.0,1.0]	1.0 [1.0,1.0]
	Elm	0.14 [0.025,0.17]	0.13 [0.024,0.17]	0.065 [-0.13,0.11]	0.066 [-0.13,0.11]
	Hemlock	0.22 [0.079,0.22]	0.22 [0.081,0.22]	0.20 [0.0045,0.21]	0.20 [0.0064,0.21]
	Maple	0.16 [-0.031,0.22]	0.16 [-0.034,0.22]	0.14 [-0.081,0.21]	0.14 [-0.081,0.21]
	Oak	-0.24 [-0.56,-0.078]	-0.24 [-0.56,-0.079]	-0.19 [-0.47,-0.045]	-0.19 [-0.47,-0.047]
	Other conifer taxa	-0.031 [-0.61,0.11]	-0.035 [-0.62,0.11]	-0.078 [-0.65,0.089]	-0.082 [-0.67,0.086]
	Other hardwood taxa	0.21 [0.065,0.24]	0.21 [0.074,0.24]	0.19 [0.047,0.23]	0.20 [0.056,0.23]
	Pine	-0.12 [-0.48,0.020]	-0.12 [-0.47,0.022]	-0.14 [-0.53,0.0032]	-0.14 [-0.52,0.0051]
	Spruce	-0.070 [-0.95,0.079]	-0.073 [-0.95,0.076]	-0.12 [-1.0,0.050]	-0.12 [-1.0,0.048]
Elm	Tamarack	-0.17 [-0.78,0.024]	-0.17 [-0.79,0.022]	-0.13 [-0.65,0.042]	-0.13 [-0.66,0.040]
	Beech	-0.0023 [-0.53,0.061]	-0.0099 [-0.57,0.055]	-0.0038 [-0.57,0.057]	-0.015 [-0.63,0.049]
	Birch	0.14 [0.025,0.17]	0.13 [0.024,0.17]	0.065 [-0.13,0.11]	0.066 [-0.13,0.11]
	Elm	1.0 [1.0,1.0]	1.0 [1.0,1.0]	1.0 [1.0,1.0]	1.0 [1.0,1.0]
	Hemlock	0.16 [0.10,0.17]	0.16 [0.096,0.16]	0.060 [-0.16,0.094]	0.057 [-0.17,0.091]
	Maple	0.23 [0.15,0.29]	0.22 [0.12,0.28]	0.20 [-0.024,0.28]	0.19 [-0.047,0.27]
	Oak	-0.58 [-1.0,-0.15]	-0.57 [-1.0,-0.15]	-0.55 [-1.0,-0.15]	-0.54 [-1.0,-0.14]
	Other conifer taxa	0.25 [0.17,0.25]	0.27 [0.19,0.25]	0.22 [0.096,0.23]	0.24 [0.14,0.25]
	Other hardwood taxa	0.078 [-0.36,0.15]	0.065 [-0.41,0.14]	0.19 [-0.036,0.22]	0.17 [-0.10,0.21]
	Pine	0.014 [-0.22,0.11]	0.0033 [-0.24,0.098]	-0.045 [-0.35,0.050]	-0.065 [-0.40,0.035]
Spruce	Spruce	0.064 [-0.22,0.10]	0.074 [-0.18,0.11]	0.068 [-0.18,0.10]	0.084 [-0.11,0.12]
	Tamarack	-0.031 [-0.50,0.054]	-0.024 [-0.48,0.056]	-0.052 [-0.55,0.042]	-0.039 [-0.50,0.049]

Table D.3: (Continued)

Taxon 1	Taxon 2	Formula 1	Formula 2	Formula 3	Formula 4
Hemlock	Beech	0.0039 [-0.64,0.074]	0.0057 [-0.63,0.075]	-0.016 [-0.74,0.065]	-0.014 [-0.72,0.067]
	Birch	0.22 [0.079,0.22]	0.22 [0.081,0.22]	0.20 [0.0045,0.21]	0.20 [0.0064,0.21]
	Elm	0.16 [0.10,0.17]	0.16 [0.096,0.16]	0.060 [-0.16,0.094]	0.057 [-0.17,0.091]
	Hemlock	1.0 [1.0,1.0]	1.0 [1.0,1.0]	1.0 [1.0,1.0]	1.0 [1.0,1.0]
	Maple	0.21 [0.082,0.23]	0.21 [0.086,0.23]	0.19 [0.016,0.21]	0.19 [0.018,0.21]
	Oak	-0.20 [-0.62,-0.044]	-0.21 [-0.62,-0.044]	-0.13 [-0.47,-0.0021]	-0.13 [-0.47,-0.0028]
	Other conifer taxa	-0.055 [-0.62,0.067]	-0.058 [-0.63,0.066]	-0.11 [-0.77,0.039]	-0.12 [-0.78,0.038]
	Other hardwood taxa	0.028 [-0.21,0.10]	0.031 [-0.20,0.10]	0.0036 [-0.26,0.078]	0.0075 [-0.26,0.079]
	Pine	-0.15 [-0.59,-0.0099]	-0.15 [-0.59,-0.0078]	-0.18 [-0.65,-0.023]	-0.17 [-0.65,-0.020]
	Spruce	-0.23 [-1.0,-0.028]	-0.23 [-1.0,-0.029]	-0.30 [-1.0,-0.042]	-0.30 [-1.0,-0.043]
Maple	Tamarack	-0.18 [-0.79,-0.024]	-0.18 [-0.79,-0.025]	-0.12 [-0.66,0.0059]	-0.13 [-0.66,0.0046]
	Beech	-0.0080 [-0.79,0.092]	-0.0043 [-0.77,0.094]	-0.017 [-0.83,0.086]	-0.014 [-0.81,0.087]
	Birch	0.16 [-0.031,0.22]	0.16 [-0.034,0.22]	0.14 [-0.081,0.21]	0.14 [-0.081,0.21]
	Elm	0.23 [0.15,0.29]	0.22 [0.12,0.28]	0.20 [-0.024,0.28]	0.19 [-0.047,0.27]
	Hemlock	0.21 [0.082,0.23]	0.21 [0.086,0.23]	0.19 [0.016,0.21]	0.19 [0.018,0.21]
	Maple	1.0 [1.0,1.0]	1.0 [1.0,1.0]	1.0 [1.0,1.0]	1.0 [1.0,1.0]
	Oak	-0.46 [-1.0,-0.19]	-0.46 [-1.0,-0.19]	-0.45 [-1.0,-0.18]	-0.44 [-1.0,-0.18]
	Other conifer taxa	0.16 [-0.087,0.23]	0.15 [-0.097,0.23]	0.14 [-0.12,0.23]	0.13 [-0.13,0.23]
	Other hardwood taxa	0.24 [0.078,0.28]	0.25 [0.086,0.28]	0.25 [0.11,0.28]	0.25 [0.12,0.28]
	Pine	-0.11 [-0.52,0.027]	-0.11 [-0.51,0.027]	-0.14 [-0.55,0.0097]	-0.13 [-0.55,0.0087]
	Spruce	-0.074 [-0.87,0.046]	-0.078 [-0.88,0.044]	-0.10 [-1.0,0.033]	-0.11 [-1.0,0.030]
	Tamarack	-0.030 [-0.44,0.097]	-0.033 [-0.45,0.097]	-0.0036 [-0.41,0.11]	-0.0052 [-0.41,0.11]

Table D.3: (Continued)

Taxon 1	Taxon 2	Formula 1	Formula 2	Formula 3	Formula 4
Oak	Beech	-0.14 [-0.90,-0.0078]	-0.14 [-0.89,-0.0071]	-0.13 [-0.86,0.0026]	-0.13 [-0.84,0.0049]
	Birch	-0.24 [-0.56,-0.078]	-0.24 [-0.56,-0.079]	-0.19 [-0.47,-0.045]	-0.19 [-0.47,-0.047]
	Elm	-0.58 [-1.0,-0.15]	-0.57 [-1.0,-0.15]	-0.55 [-1.0,-0.15]	-0.54 [-1.0,-0.14]
	Hemlock	-0.20 [-0.62,-0.044]	-0.21 [-0.62,-0.044]	-0.13 [-0.47,-0.0021]	-0.13 [-0.47,-0.0028]
	Maple	-0.46 [-1.0,-0.19]	-0.46 [-1.0,-0.19]	-0.45 [-1.0,-0.18]	-0.44 [-1.0,-0.18]
	Oak	1.0 [1.0,1.0]	1.0 [1.0,1.0]	1.0 [1.0,1.0]	1.0 [1.0,1.0]
	Other conifer taxa	-0.26 [-0.78,-0.062]	-0.26 [-0.79,-0.063]	-0.22 [-0.70,-0.032]	-0.22 [-0.71,-0.036]
	Other hardwood taxa	-0.37 [-0.83,-0.13]	-0.37 [-0.83,-0.12]	-0.42 [-0.91,-0.16]	-0.42 [-0.90,-0.16]
	Pine	-0.35 [-0.66,-0.18]	-0.35 [-0.66,-0.18]	-0.31 [-0.60,-0.15]	-0.30 [-0.59,-0.14]
	Spruce	-0.035 [-0.40,0.069]	-0.037 [-0.40,0.068]	0.021 [-0.27,0.12]	0.018 [-0.28,0.12]
Other conifer taxa	Tamarack	-0.16 [-0.53,-0.0072]	-0.16 [-0.53,-0.011]	-0.21 [-0.59,-0.052]	-0.22 [-0.61,-0.061]
	Beech	-0.036 [-0.90,0.062]	-0.037 [-0.90,0.062]	-0.050 [-1.0,0.054]	-0.051 [-1.0,0.054]
	Birch	-0.031 [-0.61,0.11]	-0.035 [-0.62,0.11]	-0.078 [-0.65,0.089]	-0.081 [-0.67,0.086]
	Elm	0.25 [0.17,0.25]	0.27 [0.19,0.25]	0.22 [0.096,0.23]	0.24 [0.14,0.25]
	Hemlock	-0.055 [-0.62,0.067]	-0.058 [-0.63,0.066]	-0.11 [-0.77,0.039]	-0.12 [-0.78,0.38]
	Maple	0.16 [-0.087,0.23]	0.15 [-0.097,0.23]	0.14 [-0.12,0.23]	0.13 [-0.13,0.23]
	Oak	-0.26 [-0.78,-0.062]	-0.26 [-0.79,-0.063]	-0.22 [-0.70,-0.032]	-0.22 [-0.71,-0.036]
	Other conifer taxa	1.0 [1.0,1.0]	1.0 [1.0,1.0]	1.0 [1.0,1.0]	1.0 [1.0,1.0]
	Other hardwood taxa	-0.059 [-0.53,0.072]	-0.061 [-0.55,0.071]	-0.025 [-0.53,0.097]	-0.025 [-0.55,0.096]
	Pine	-0.17 [-0.61,0.00055]	-0.16 [-0.61,0.0037]	-0.21 [-0.66,-0.032]	-0.21 [-0.66,-0.032]
Spruce	Spruce	0.22 [-0.13,0.26]	0.22 [-0.12,0.26]	0.19 [-0.22,0.24]	0.20 [-0.20,0.24]
	Tamarack	-0.13 [-0.85,0.065]	-0.14 [-0.86,0.062]	-0.10 [-0.74,0.076]	-0.11 [-0.76,0.072]

Table D.3: (Continued)

Taxon 1	Taxon 2	Formula 1	Formula 2	Formula 3	Formula 4
Other hard-wood taxa	Beech	-0.043 [-0.60,0.042]	-0.041 [-0.59,0.042]	-0.029 [-0.54,0.047]	-0.031 [-0.55,0.046]
	Birch	0.21 [0.065,0.24]	0.21 [0.074,0.24]	0.19 [0.047,0.23]	0.20 [0.056,0.23]
	Elm	0.078 [-0.36,0.15]	0.065 [-0.41,0.14]	0.19 [-0.036,0.22]	0.17 [-0.10,0.21]
	Hemlock	0.028 [-0.21,0.10]	0.031 [-0.20,0.10]	0.0036 [-0.26,0.078]	0.0075 [-0.26,0.079]
	Maple	0.24 [0.078,0.28]	0.25 [0.086,0.28]	0.25 [0.11,0.28]	0.25 [0.12,0.28]
	Oak	-0.37 [-0.83,-0.13]	-0.37 [-0.83,-0.12]	-0.42 [-0.91,-0.16]	-0.42 [-0.90,-0.16]
	Other conifer taxa	-0.059 [-0.53,0.072]	-0.061 [-0.55,0.071]	-0.025 [-0.53,0.097]	-0.025 [-0.55,0.096]
	Other hardwood taxa	1.0 [1.0,1.0]	1.0 [1.0,1.0]	1.0 [1.0,1.0]	1.0 [1.0,1.0]
	Pine	-0.092 [-0.38,0.035]	-0.097 [-0.39,0.031]	-0.10 [-0.38,0.024]	-0.11 [-0.39,0.015]
	Spruce	-0.062 [-0.69,0.055]	-0.063 [-0.70,0.055]	-0.023 [-0.52,0.092]	-0.024 [-0.54,0.091]
Pine	Tamarack	-0.051 [-0.55,0.077]	-0.045 [-0.54,0.081]	-0.095 [-0.66,0.059]	-0.083 [-0.62,0.067]
	Beech	-0.094 [-0.76,0.014]	-0.098 [-0.77,0.012]	-0.11 [-0.82,0.0060]	-0.11 [-0.84,0.0038]
	Birch	-0.12 [-0.48,0.020]	-0.12 [-0.47,0.022]	-0.14 [-0.53,0.0032]	-0.14 [-0.52,0.0051]
	Elm	0.014 [-0.22,0.11]	0.0033 [-0.24,0.098]	-0.045 [-0.35,0.050]	-0.065 [-0.40,0.035]
	Hemlock	-0.15 [-0.59,-0.0099]	-0.15 [-0.59,-0.0078]	-0.18 [-0.65,-0.023]	-0.17 [-0.65,-0.020]
	Maple	-0.11 [-0.52,0.027]	-0.11 [-0.51,0.027]	-0.14 [-0.55,0.0097]	-0.13 [-0.55,0.0087]
	Oak	-0.35 [-0.66,-0.18]	-0.35 [-0.66,-0.18]	-0.31 [-0.60,-0.15]	-0.30 [-0.59,-0.14]
	Other conifer taxa	-0.17 [-0.61,0.00055]	-0.16 [-0.61,0.0037]	-0.21 [-0.66,-0.032]	-0.21 [-0.66,-0.032]
	Other hardwood taxa	-0.092 [-0.38,0.035]	-0.097 [-0.39,0.031]	-0.10 [-0.38,0.024]	-0.11 [-0.39,0.015]
	Pine	1.0 [1.0,1.0]	1.0 [1.0,1.0]	1.0 [1.0,1.0]	1.0 [1.0,1.0]
Spruce	Spruce	-0.085 [-0.74,0.052]	-0.080 [-0.73,0.054]	-0.13 [-0.91,0.042]	-0.13 [-0.92,0.042]
	Tamarack	-0.20 [-0.66,0.0018]	-0.19 [-0.63,0.0056]	-0.17 [-0.57,0.017]	-0.15 [-0.54,0.024]

Table D.3: (Continued)

Taxon 1	Taxon 2	Formula 1	Formula 2	Formula 3	Formula 4
Spruce	Beech	-0.022 [-0.92,0.047]	-0.023 [-0.92,0.047]	-0.037 [-1.0,0.041]	-0.039 [-1.0,0.040]
	Birch	-0.070 [-0.95,0.079]	-0.073 [-0.95,0.076]	-0.12 [-1.0,0.050]	-0.12 [-1.0,0.048]
	Elm	0.064 [-0.22,0.10]	0.074 [-0.18,0.11]	0.068 [-0.18,0.10]	0.084 [-0.11,0.12]
	Hemlock	-0.23 [-1.0,-0.028]	-0.23 [-1.0,-0.029]	-0.30 [-1.0,-0.042]	-0.30 [-1.0,-0.043]
	Maple	-0.074 [-0.87,0.046]	-0.078 [-0.88,0.044]	-0.10 [-1.0,0.033]	-0.11 [-1.0,0.030]
	Oak	-0.035 [-0.40,0.069]	-0.037 [-0.40,0.068]	0.021 [-0.27,0.12]	0.018 [-0.28,0.12]
	Other conifer taxa	0.22 [-0.13,0.26]	0.22 [-0.12,0.26]	0.19 [-0.22,0.24]	0.20 [-0.20,0.24]
	Other hardwood taxa	-0.062 [-0.69,0.055]	-0.063 [-0.70,0.055]	-0.023 [-0.52,0.092]	-0.024 [-0.54,0.091]
	Pine	-0.085 [-0.74,0.052]	-0.080 [-0.73,0.054]	-0.13 [-0.91,0.042]	-0.13 [-0.92,0.042]
	Spruce	1.0 [1.0,1.0]	1.0 [1.0,1.0]	1.0 [1.0,1.0]	1.0 [1.0,1.0]
Tamarack	Tamarack	-0.059 [-1.0,0.074]	-0.064 [-1.0,0.072]	-0.032 [-1.0,0.083]	-0.037 [-1.0,0.082]
	Beech	0.12 [-0.027,0.18]	0.12 [-0.021,0.18]	0.13 [0.011,0.19]	0.14 [0.026,0.20]
	Birch	-0.17 [-0.78,0.024]	-0.17 [-0.79,0.022]	-0.13 [-0.65,0.042]	-0.13 [-0.66,0.040]
	Elm	-0.031 [-0.50,0.054]	-0.024 [-0.48,0.056]	-0.052 [-0.55,0.042]	-0.039 [-0.50,0.049]
	Hemlock	-0.18 [-0.79,-0.024]	-0.18 [-0.79,-0.025]	-0.12 [-0.66,0.0059]	-0.13 [-0.66,0.0046]
	Maple	-0.030 [-0.44,0.097]	-0.033 [-0.45,0.097]	-0.0036 [-0.41,0.11]	-0.0052 [-0.41,0.11]
	Oak	-0.16 [-0.53,-0.0072]	-0.16 [-0.53,-0.011]	-0.21 [-0.59,-0.052]	-0.22 [-0.61,-0.061]
	Other conifer taxa	-0.13 [-0.85,0.065]	-0.14 [-0.86,0.062]	0.10 [-0.74,0.076]	-0.11 [-0.76,0.072]
	Other hardwood taxa	-0.051 [-0.55,0.077]	-0.045 [-0.54,0.081]	-0.095 [-0.66,0.059]	-0.083 [-0.62,0.067]
	Pine	-0.20 [-0.66,0.0018]	-0.19 [-0.63,0.0056]	-0.17 [-0.57,0.017]	-0.15 [-0.54,0.024]
Spruce	Spruce	-0.059 [-1.0,0.074]	-0.064 [-1.0,0.072]	-0.032 [-1.0,0.083]	-0.037 [-1.0,0.082]
	Tamarack	1.0 [1.0,1.0]	1.0 [1.0,1.0]	1.0 [1.0,1.0]	1.0 [1.0,1.0]

Residual correlations quantify the relationship between taxa after accounting for their dependence on the environmental covariates in the model. Note that correlation coefficients are reciprocal: for example, the correlation between beech and birch is the same as the correlation between birch and beech for the same formula.

Columns titled “Formula 1”-“Formula 4” report the median and 95% credible interval of the residual correlations in brackets. Taxon scientific names are as follows: beech (*Fagus grandifolia*), birch (*Betula spp.*), elm (*Ulmus spp.*), hemlock (*Tsuga canadensis*), maple (*Acer spp.*), oak (*Quercus spp.*), pine (*Pinus spp.*), spruce (*Picea spp.*), and tamarack (*Larix laricina*).

Formula 1 includes the following covariates: soil % sand, average annual temperature, total annual precipitation, and precipitation seasonality. Formula 2 includes the following covariates: soil % silt, average annual temperature, total annual precipitation, and precipitation seasonality. Formula 3 includes the following covariates: soil % sand, average annual temperature, temperature seasonality, and precipitation seasonality. Formula 4 includes the following covariates: soil % silt, average annual temperature, temperature seasonality, and precipitation seasonality.

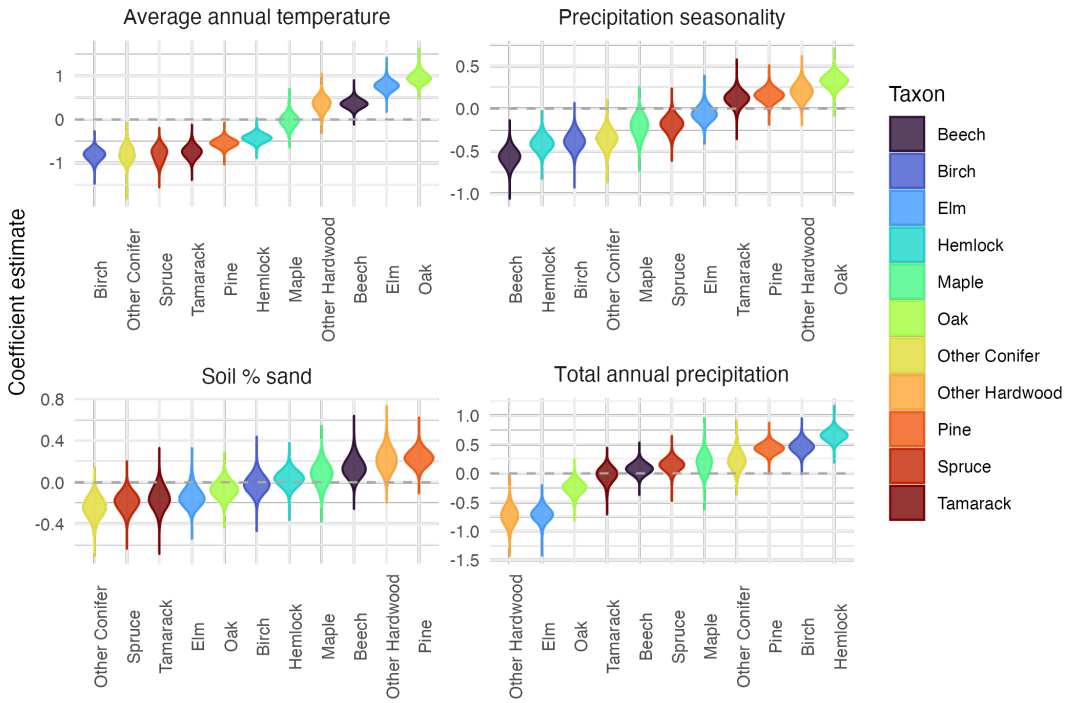


Figure D.1: Coefficient estimates quantifying the relationship between each taxon and each covariate in the model fit with Formula 1 using the posterior draws of taxon relative abundances. Each facet contains the coefficient estimates relating each taxon and one environmental covariate. Top left: average annual temperature, top right: precipitation seasonality, bottom left: soil % sand, bottom right: total annual precipitation. The taxa are ordered from lowest to highest coefficient estimate on the x-axis of each facet. Note that the order of taxa differs in each facet, but the taxa are the same color across facets to facilitate intercomparison. The y-axis is the estimated model coefficient, standardized by the covariate and the taxon covariance matrix. The violins represent the distribution of coefficient estimates across Gibbs posterior samples from the model after removing burn-in and pooled from GJAMs fit to each of 100 posterior draws of taxon relative abundances. The dashed line gray line highlights 0, with violins overlapping zero suggesting a negligible influence of the covariate on a given taxon when accounting for the uncertainty in the vegetation reconstructions. Note that the y-axis differs between facets to highlight patterns in the coefficients. The difference between this figure and Figure C.1 is that this figure accounts for the uncertainty in vegetation reconstructions in the coefficient estimates.

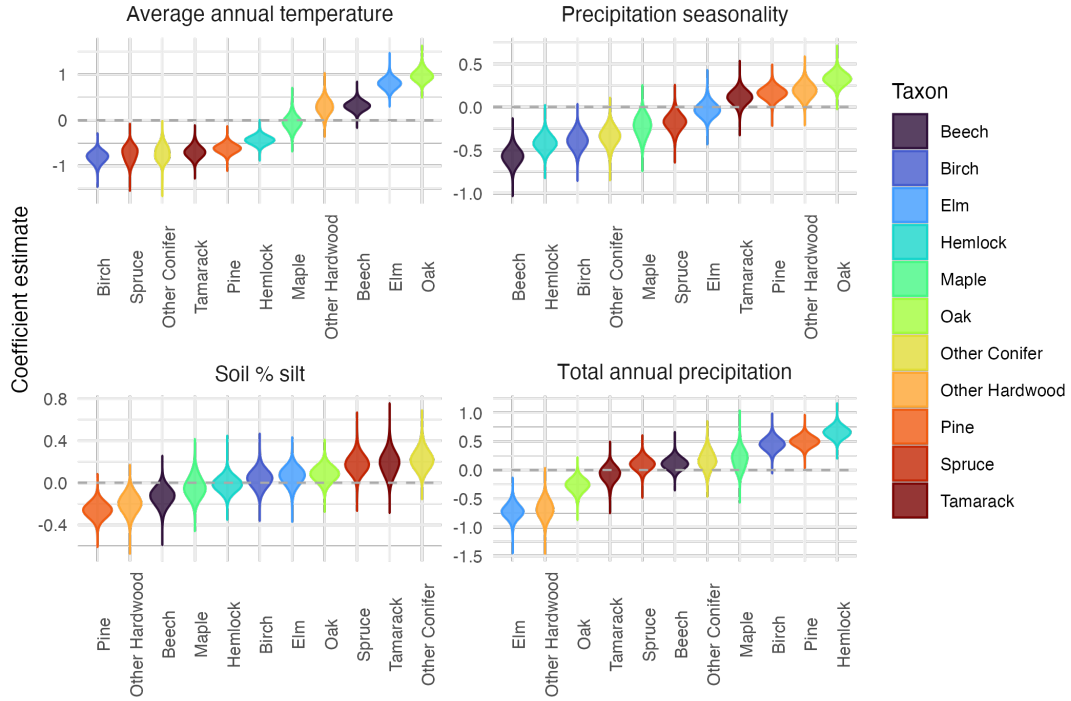


Figure D.2: Coefficient estimates quantifying the relationship between each taxon and each covariate in the model fit with Formula 2. Each facet contains the coefficient estimates relating each taxon and one environmental covariate. Top left: average annual temperature, top right: precipitation seasonality, bottom left: soil % silt, bottom right: total annual precipitation. The taxa are ordered from lowest to highest coefficient estimate on the x-axis of each facet. Note that the order of taxa differs in each facet, but the taxa are the same color across facets to facilitate intercomparison. The y-axis is the estimated model coefficient, standardized by the covariate and the taxon covariance matrix. The violins represent the distribution of coefficient estimates across Gibbs posterior samples from the model after removing burn-in and pooled from GJAMs fit to each of 100 posterior draws of taxon relative abundances. The dashed line gray line highlights 0, with violins overlapping zero suggesting a negligible influence of the covariate on a given taxon. Note that the y-axis differs between facets to highlight patterns in the coefficients. The difference between this figure and Figure C.2 is that this figure accounts for the uncertainty in vegetation reconstructions in the coefficient estimates.

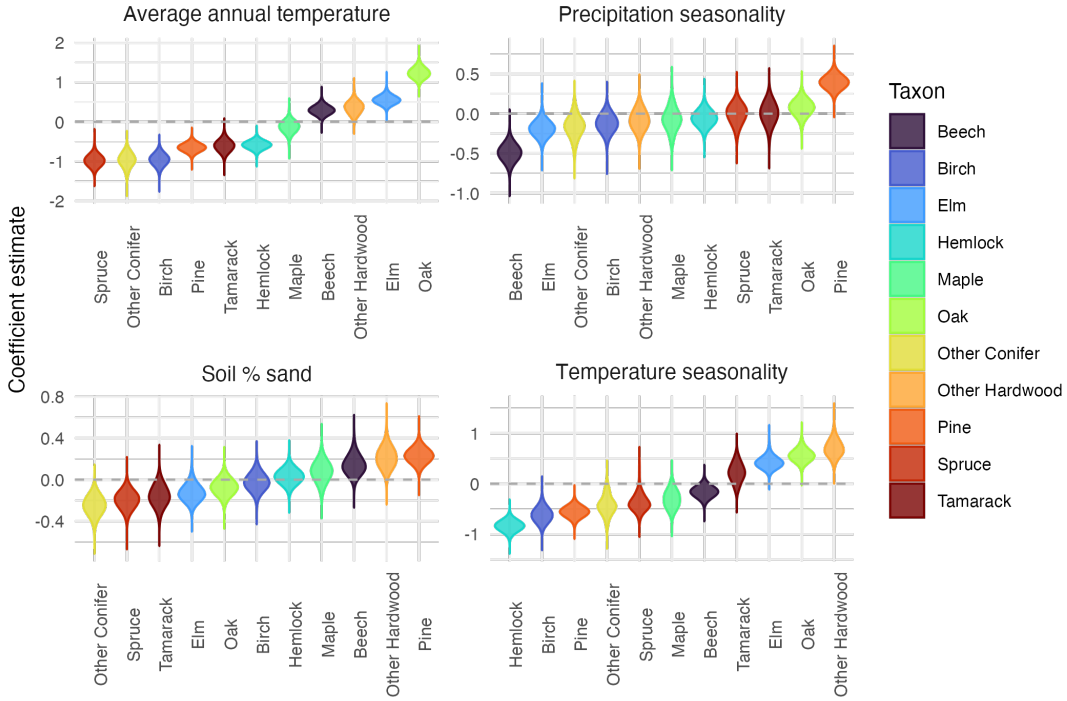


Figure D.3: Coefficient estimates quantifying the relationship between each taxon and each covariate in the model fit with Formula 3. Each facet contains the coefficient estimates relating each taxon and one environmental covariate. Top left: average annual temperature, top right: precipitation seasonality, bottom left: soil % sand, bottom right: temperature seasonality. The taxa are ordered from lowest to highest coefficient estimate on the x-axis of each facet. Note that the order of taxa differs in each facet, but the taxa are the same color across facets to facilitate intercomparison. The y-axis is the estimated model coefficient, standardized by the covariate and the taxon covariance matrix. The violins represent the distribution of coefficient estimates across Gibbs posterior samples from the model after removing burn-in and pooled from GJAMs fit to each of 100 posterior draws of taxon relative abundances. The dashed line gray line highlights 0, with violins overlapping zero suggesting a negligible influence of the covariate on a given taxon. Note that the y-axis differs between facets to highlight patterns in the coefficients. The difference between this figure and Figure C.3 is that this figure accounts for the uncertainty in vegetation reconstructions in the coefficient estimates.

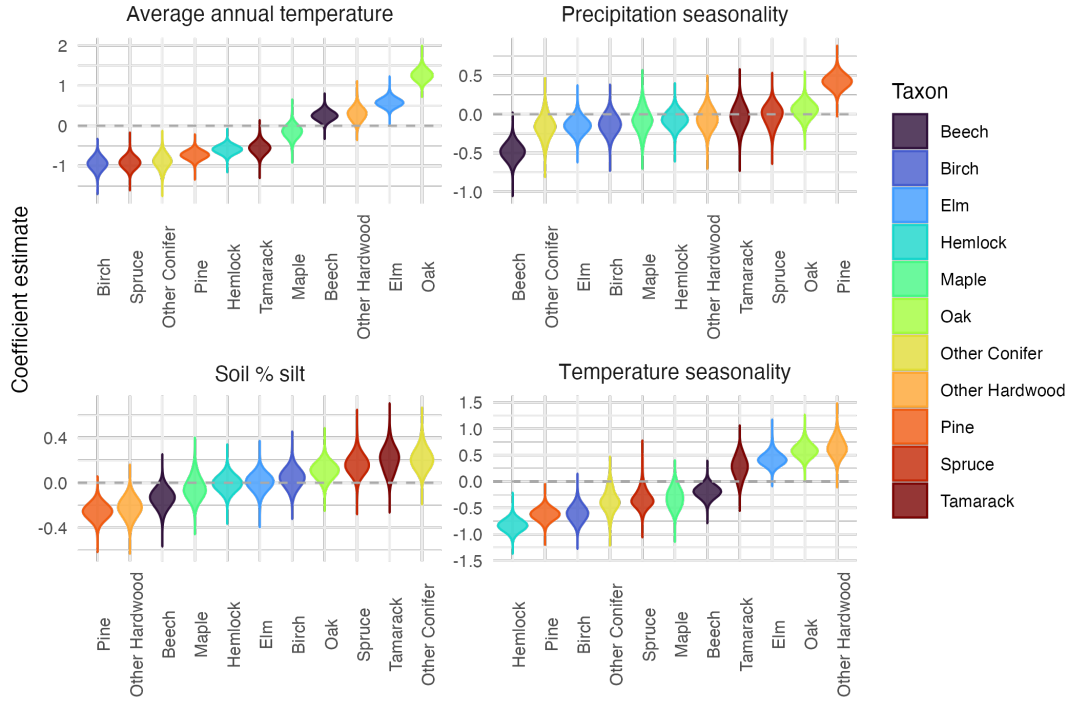


Figure D.4: Coefficient estimates quantifying the relationship between each taxon and each covariate in the model fit with Formula 4. Each facet contains the coefficient estimates relating each taxon and one environmental covariate. Top left: average annual temperature, top right: precipitation seasonality, bottom left: soil % silt, bottom right: temperature seasonality. The taxa are ordered from lowest to highest coefficient estimate on the x-axis of each facet. Note that the order of taxa differs in each facet, but the taxa are the same color across facets to facilitate intercomparison. The y-axis is the estimated model coefficient, standardized by the covariate and the taxon covariance matrix. The violins represent the distribution of coefficient estimates across Gibbs posterior samples from the model after removing burn-in and pooled from GJAMs fit to each of 100 posterior draws of taxon relative abundances. The dashed line gray line highlights 0, with violins overlapping zero suggesting a negligible influence of the covariate on a given taxon. Note that the y-axis differs between facets to highlight patterns in the coefficients. The difference between this figure and Figure C.4 is that this figure accounts for the uncertainty in vegetation reconstructions in the coefficient estimates.

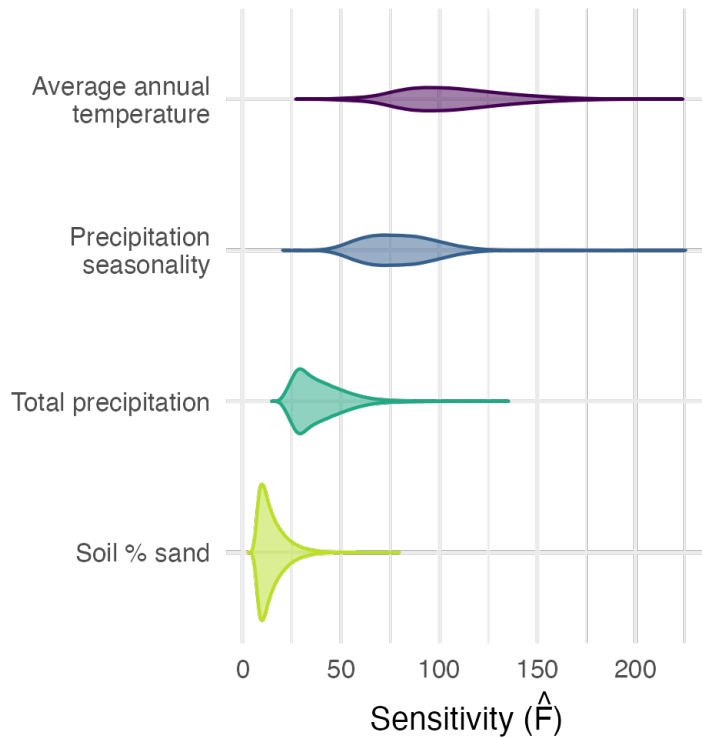


Figure D.5: Model estimated joint sensitivity of all taxon relative abundances to each environmental covariate included in the model fit with Formula 1. The x-axis shows the sensitivity. Higher sensitivity indicates that the covariate has a larger impact on taxon relative abundances jointly, and lower sensitivity indicates that the covariate has a smaller impact. The y-axis shows the four environmental covariates used to fit the model. Jointly, taxon relative abundances were more sensitive to average annual temperature and precipitation seasonality, and less sensitive to total annual precipitation and soil % sand.

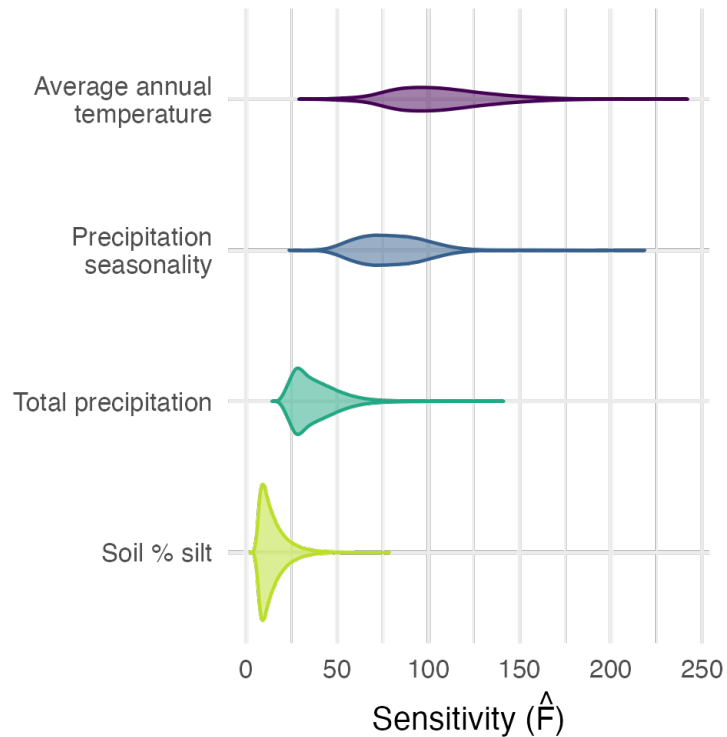


Figure D.6: Model estimated joint sensitivity of all taxon relative abundances to each environmental covariate included in the model fit with Formula 2. The x-axis shows the sensitivity. Higher sensitivity indicates that the covariate has a larger impact on taxon relative abundances jointly, and lower sensitivity indicates that the covariate has a smaller impact. The y-axis shows the four environmental covariates used to fit the model. Jointly, taxon relative abundances were more sensitive to average annual temperature and precipitation seasonality, and less sensitive to total annual precipitation and soil % silt.

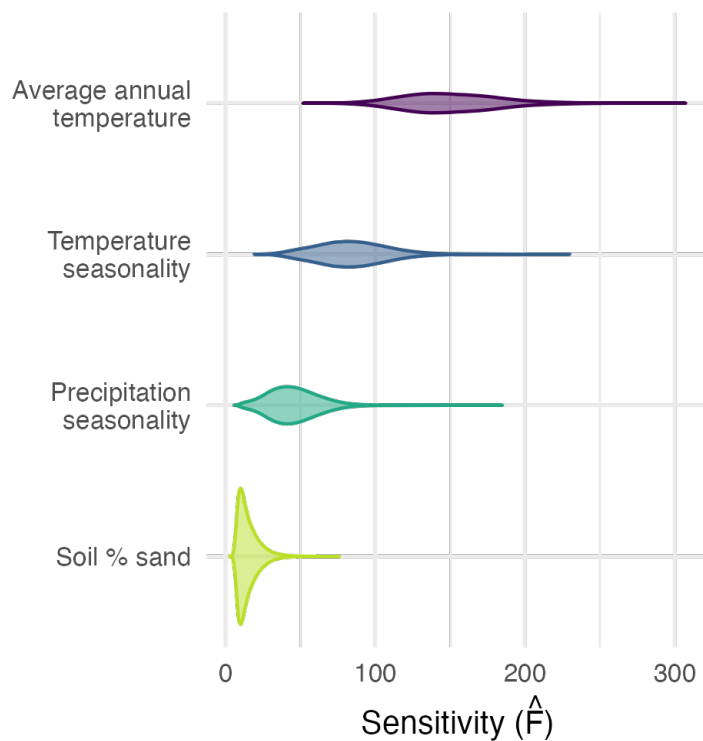


Figure D.7: Model estimated joint sensitivity of all taxon relative abundances to each environmental covariate included in the model fit with Formula 3. The x-axis shows the sensitivity. Higher sensitivity indicates that the covariate has a larger impact on taxon relative abundances jointly, and lower sensitivity indicates that the covariate has a smaller impact. The y-axis shows the four environmental covariates used to fit the model. Jointly, taxon relative abundances were more sensitive to average annual temperature, moderately sensitive to temperature seasonality, and less sensitive to precipitation seasonality and soil % sand.

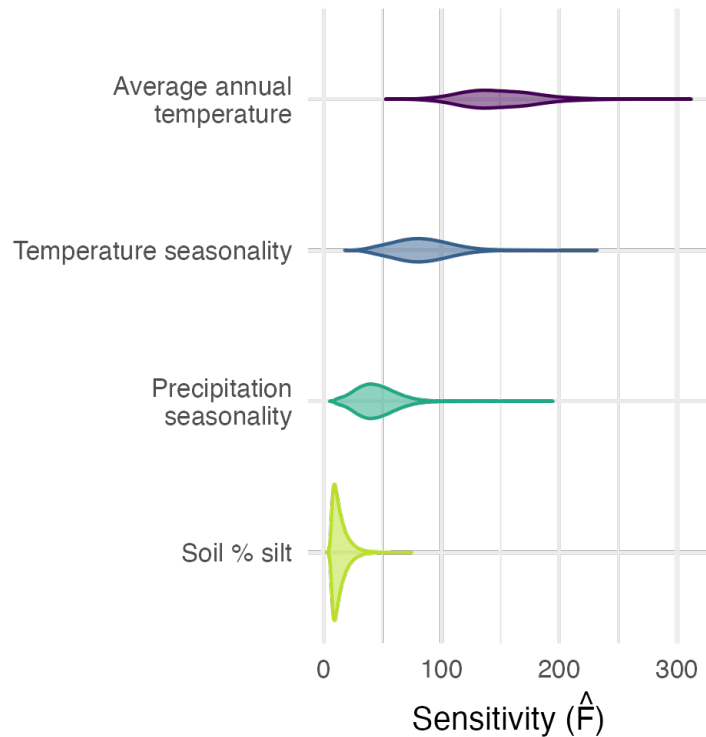


Figure D.8: Model estimated joint sensitivity of all taxon relative abundances to each environmental covariate included in the model fit with Formula 4. The x-axis shows the sensitivity. Higher sensitivity indicates that the covariate has a larger impact on taxon relative abundances jointly, and lower sensitivity indicates that the covariate has a smaller impact. The y-axis shows the four environmental covariates used to fit the model. Jointly, taxon relative abundances were more sensitive to average annual temperature, moderately sensitive to temperature seasonality, and less sensitive to precipitation seasonality and soil % silt.

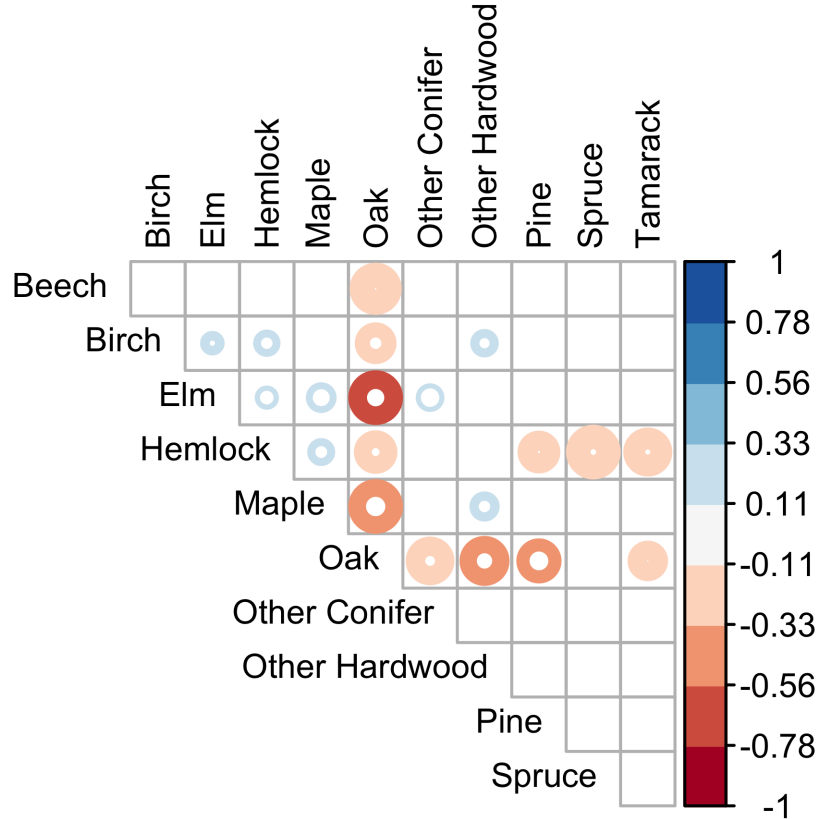


Figure D.9: Model estimated residual correlations between each taxon pair for the model fit with formula 1. Environmental covariates in this model were soil % sand, average annual temperature, total annual precipitation, and precipitation seasonality. Residual correlations quantify the relationship between taxon relative abundances after accounting for their joint dependence on the environmental covariates in the model. The size of the ring shows the magnitude of the residual correlation between the taxon pair shown to the left and top of the plot, with larger circles denoting larger residual correlations. The color of the ring shows the magnitude and direction of the correlation, with blue denoting positive correlations (taxa are more abundant together than explained by the environmental conditions) and red denoting negative correlations (taxa are less abundant together than explained by the environmental conditions). The inner and outer limits of the ring indicate the 95% credible intervals of the residual correlations from the Gibbs samples after removing burn-in and from fitting the model 100 times from 100 posterior samples of taxon relative abundances. Blank cells (with no ring) have correlations overlapping 0 at the 95% credibility level. The difference between this figure and Figure C.7 is that this figure accounts for the uncertainty in vegetation reconstructions in the coefficient estimates.

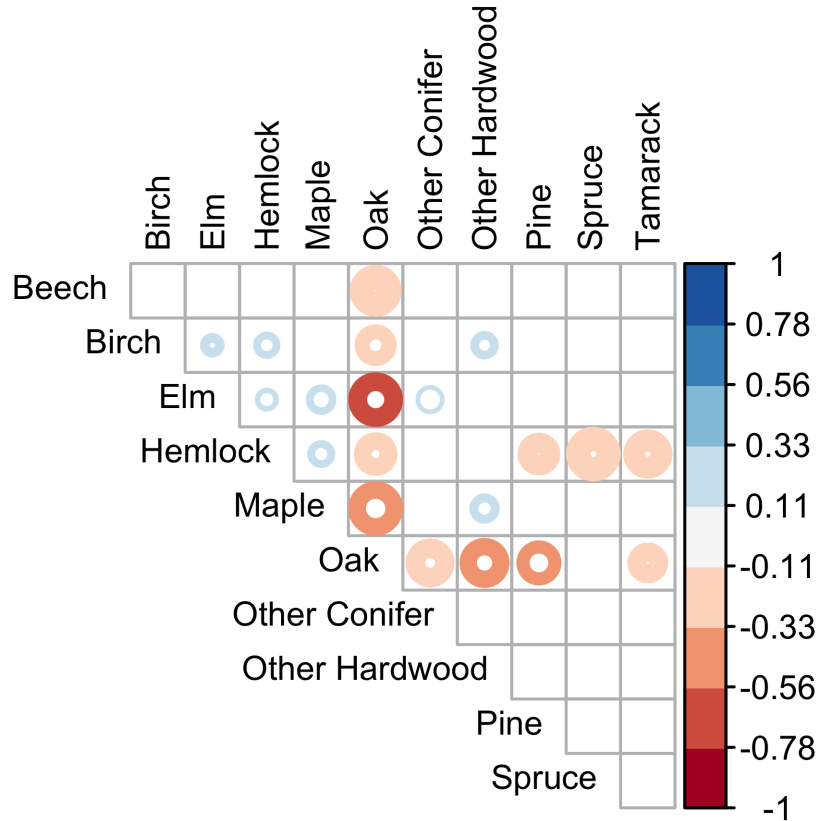


Figure D.10: Model estimated residual correlations between each taxon pair for the model fit with formula 2. Environmental covariates in this model were soil % silt, average annual temperature, total annual precipitation, and precipitation seasonality. Residual correlations quantify the relationship between taxon relative abundances after accounting for their joint dependence on the environmental covariates in the model. The size of the ring shows the magnitude of the residual correlation between the taxon pair shown to the left and top of the plot, with larger circles denoting larger residual correlations. The color of the ring shows the magnitude and direction of the correlation, with blue denoting positive correlations (taxa are more abundant together than explained by the environmental conditions) and red denoting negative correlations (taxa are less abundant together than explained by the environmental conditions). The inner and outer limits of the ring indicate the 95% credible intervals of the residual correlations from the Gibbs samples after removing burn-in and from fitting the model 100 times from 100 posterior samples of taxon relative abundances. Blank cells (with no ring) have correlations overlapping 0 at the 95% credibility level. The difference between this figure and Figure C.8 is that this figure accounts for the uncertainty in vegetation reconstructions in the coefficient estimates.

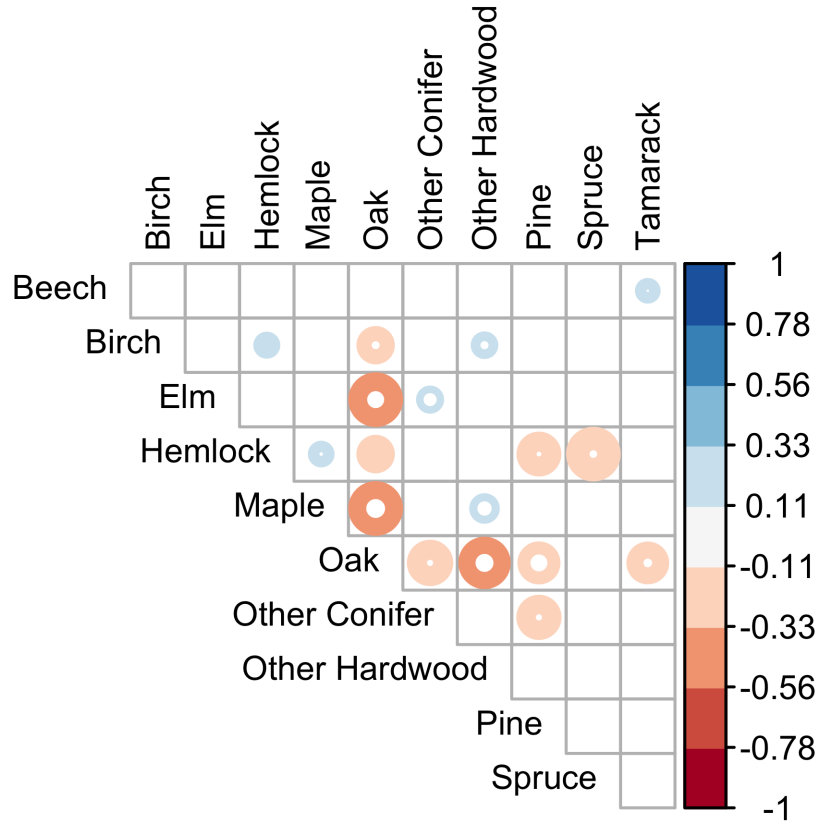


Figure D.11: Model estimated residual correlations between each taxon pair for the model fit with formula 3. Environmental covariates in this model were soil % sand, average annual temperature, temperature seasonality, and precipitation seasonality. Residual correlations quantify the relationship between taxon relative abundances after accounting for their joint dependence on the environmental covariates in the model. The size of the ring shows the magnitude of the residual correlation between the taxon pair shown to the left and top of the plot, with larger circles denoting larger residual correlations. The color of the ring shows the magnitude and direction of the correlation, with blue denoting positive correlations (taxa are more abundant together than explained by the environmental conditions) and red denoting negative correlations (taxa are less abundant together than explained by the environmental conditions). The inner and outer limits of the ring indicate the 95% credible intervals of the residual correlations from the Gibbs samples after removing burn-in and from fitting the model 100 times from 100 posterior samples of taxon relative abundances. Blank cells (with no ring) have correlations overlapping 0 at the 95% credibility level. The difference between this figure and Figure C.9 is that this figure accounts for the uncertainty in vegetation reconstructions in the coefficient estimates.

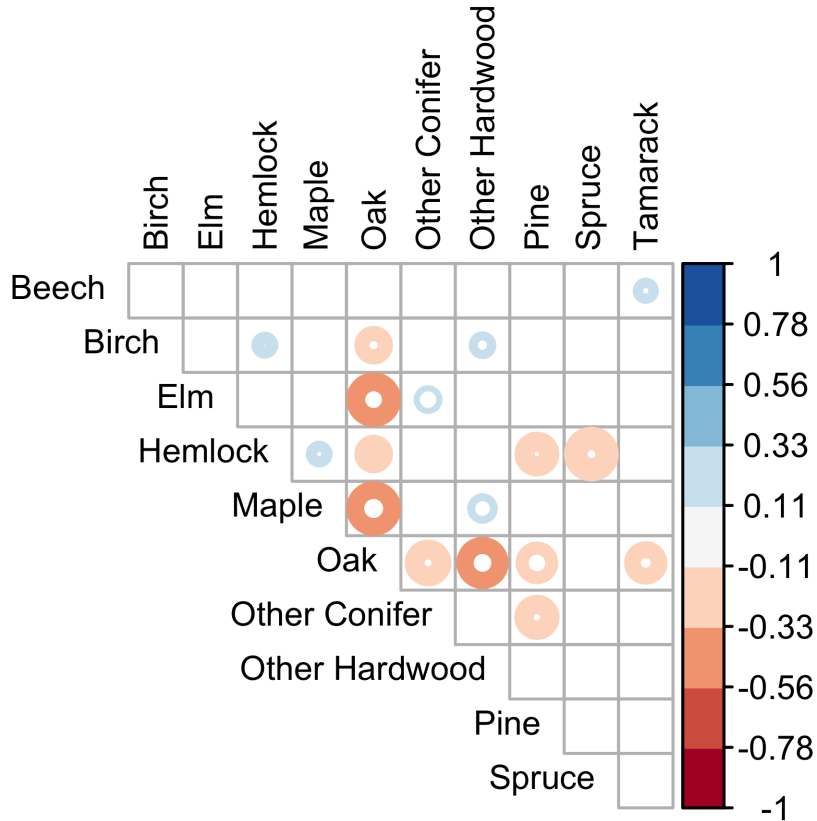


Figure D.12: Model estimated residual correlations between each taxon pair for the model fit with formula 1. Environmental covariates in this model were soil % silt, average annual temperature, temperature seasonality, and precipitation seasonality. Residual correlations quantify the relationship between taxon relative abundances after accounting for their joint dependence on the environmental covariates in the model. The size of the ring shows the magnitude of the residual correlation between the taxon pair shown to the left and top of the plot, with larger circles denoting larger residual correlations. The color of the ring shows the magnitude and direction of the correlation, with blue denoting positive correlations (taxa are more abundant together than explained by the environmental conditions) and red denoting negative correlations (taxa are less abundant together than explained by the environmental conditions). The inner and outer limits of the ring indicate the 95% credible intervals of the residual correlations from the Gibbs samples after removing burn-in and from fitting the model 100 times from 100 posterior samples of taxon relative abundances. Blank cells (with no ring) have correlations overlapping 0 at the 95% credibility level. The difference between this figure and Figure C.10 is that this figure accounts for the uncertainty in vegetation reconstructions in the coefficient estimates.

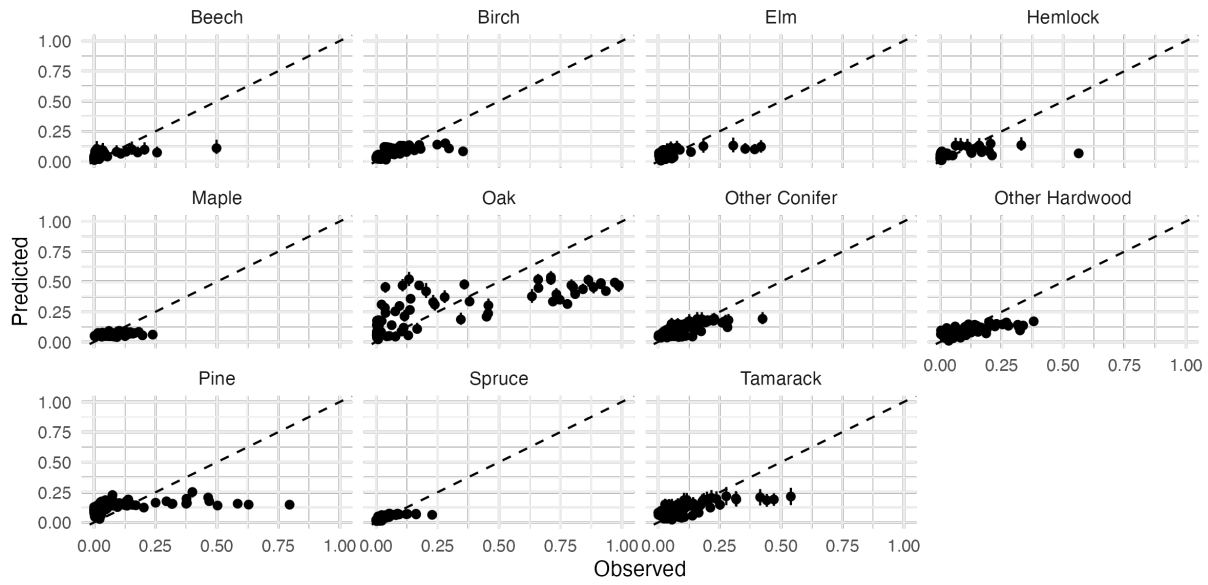


Figure D.13: Observed vs predicted relative abundance of each taxon from each grid cell for the 300 years before present (YBP) time step. Observed relative abundance (fraction of all stems) is on the x-axis; predicted relative abundance (fraction of all stems) from our GJAM conditional on environmental conditions (soil % sand, average annual temperature, total annual precipitation, precipitation seasonality). The dashed black line shows the 1:1 line indicating perfect predictions. Error bars show the 95% credibility interval of the predictions from predictions using each of the 100 model iterations fit to different posterior draws of STEPPS. Each facet shows the observed vs predicted relative abundance of one of eleven taxa. Overall, relative abundance predictions follow the correct trends but high relative abundances are highly underpredicted and oak relative abundance at intermediate observed relative abundance is overpredicted.



## Appendix E

# Final GJAM results and validation

### E.1 Methods

After analyzing the outcomes of our Validation Phase 1 (predictions of the 300 YBP time period from our GJAM fit to the posterior draws of STEPPS; Out-of-sample validation above), we refit our main model including the 300 YBP time step. Our main model included the soil % sand, average annual temperature, total annual precipitation, and precipitation seasonality environmental covariates (Formula 1), consistent with our model selection above. The parameter estimates from this model, using Formula 1 and including grid cells from the 300 YBP time step, are reported in the main text. Here, we provide tables of the coefficient (Table E.1), sensitivity (Table E.2), and correlation estimates (Table E.3), in addition to the figures provided in the main text.

After fitting our final model, we made predictions of the relative abundances of all grid cells not used to fit the model. We call this step Validation Phase 2 in the main text. The out-of-sample grid cells included the time period between the temporally subsampled time periods (i.e., 1800, 1700, 1600, 1400, 1300, 1200, 1000, 900, 800, 600, 500, and 400 YBP) and all grid cells between the spatially subsampled grid cells (see Relative abundance subsampling for grid cells used to fit the model). These spatiotemporal observations were not used in model fitting to using autocorrelated observations of taxon relative abundances; they can therefore be used as a second validation step, which allowed us to investigate spatiotemporal patterns in GJAM bias. We report the full results of the out-of-sample prediction here, including the spatiotemporal predictions of each taxon's relative abundance, spatiotemporal bias in model predictions, and observed vs. predicted plots, as shown for other validation steps above. We used the GJAM-PREDICT function in the GJAM package to make predictions. To account for the uncertainty in our relative abundance estimates, we had fit the model 100 times to each of 100 posterior draws of STEPPS. To make the corresponding predic-

tions, we used each model fit to predict the relative abundance of each taxon. We then computed the median prediction at each spatiotemporal grid cell to show the spatiotemporal distribution of model predictions (Figures E.1- E.11).

We then compared the model's predictions to the relative abundance estimate from the posterior draw used to fit the model. We compared our predictions to our estimates of relative abundance ("observations") in several ways. First, we made computed Pearson's correlation coefficients between observed and predicted relative abundance. We computed Pearson's correlation coefficients for each prediction-posterior draw pair ( $n = 100$ ), and then summarized the correlation coefficients by computing the median and 95% credible intervals across posterior draws (Table E.4). Corresponding to these Pearson's correlation coefficients, we also show observed vs predicted plots, which show the pairwise comparison between the GJAM's predictions and our estimates of relative abundance, irrespective of space or time. The observed vs predicted plots tend to emphasize where our predictions were worst, especially because many points on the plots overlap each other near zero and near the one-to-one line for most taxa. To demonstrate this, we computed the prediction bias (observed - predicted relative abundance) for each prediction at each spatiotemporal grid cell and plotted the density of prediction bias along with the observed vs. predicted plots (Figures E.12). From these prediction bias estimates, we computed the fraction of predictions with a bias greater than 10% relative abundance and report these with the Pearson correlation coefficients (Table E.4). Finally, to investigate spatiotemporal trends in relative abundance prediction bias, we plotted the median prediction bias at each spatiotemporal grid cell (Figures E.23- E.33).

## E.2 Results

### E.2.1 Trends in predictions

Our out-of-sample predictions show that, in general, our GJAM predicts each taxon to be present at relative low abundance across our entire spatiotemporal domain (Figures E.1- E.11). This highlights a limitation of our model: because all taxa are present in low abundances, the model is unable to accurately predict taxa that are at very high relative abundances (because relative abundances in a given grid cell must sum to one). Nevertheless, our model does capture trends in taxon relative abundances, particularly over space, based on spatiotemporal trends in our environmental covariates. For instance, beech relative abundance is greatest in northern Michigan, as expected from its precipitation tolerance and its post-glacial migration pattern (Figure E.1). Similarly, oak is highest in the southwest portion of our study region and other hardwood taxa in the west, reflecting their tolerance of warmer and drier environmental conditions (Figures E.6 & E.8). Finally, our model predicts pine to have its highest relative abundance in patchy areas throughout our study region, highlighting the relationship between pine relative abundance and sandy soils (Figure E.9). As with our other prediction experiments, these results suggest that our model is best

suites for inferring patterns between environmental conditions and taxon relative abundances, rather than quantifying specific magnitudes of environment-vegetation relationships or predicting specific relative abundances.

### E.2.2 Overall prediction accuracy

We additionally quantified the prediction accuracy and prediction bias of our GJAM by comparing the model's predictions to our estimates of relative abundance ("observed" relative abundance). Overall, we found fairly strong correlations between observed and predicted relative abundance across all taxa and our entire spatiotemporal region (Table E.4). Across all taxa, the median Pearson correlation coefficient between predicted and observed relative abundance was 0.58 (95% credible interval = [0.47, 0.67]). This reinforces the conclusion that our model was able to capture trends in relative abundance: as observed relative abundance increased, predicted relative abundance also increased. The taxon with the highest correlation between predicted and observed relative abundance was oak ( $r = 0.73$  [0.69, 0.78]), suggesting that the fitted relationships between oak relative abundance and environmental conditions were predictive across our broader spatiotemporal domain. On the other hand, maple had a very low correlation coefficient ( $r = 0.31$  [0.15, 0.47]). This may reflect the fact that the maple is most abundant in the center of our spatial domain, so our linear model is unable to capture the relationship between environmental conditions and maple.

The relationship between observed and predicted relative abundance is also shown in our observed vs. predicted plots (Figures E.12- E.22). The relationships shown in these plots generally reflect the trends found via our correlation coefficients (i.e., accurate prediction of trends in relative abundance). However, these plots highlight our model's inability to accurately predict high relative abundances across all taxa. For example, the relationship between observed and predicted elm relative abundance is good at low observed relative abundances, but poor at high observed relative abundance (Figure E.14). This trend was previously identified in our other prediction experiments using the 300 YBP time step as our out-of-sample validation dataset. This systematic underprediction at high relative abundance represents a systematic bias in the structure of our model and again suggests that our model should be limited to inferring trends between environmental conditions and relative abundances. This trend is related to the tendency of our model to predict that all taxa are at low abundance across our entire spatiotemporal domain: if all taxa were moderately abundant, no taxon could be highly abundant because of the sum to one constraint inherent in proportional data.

A notable exception to the general trend of good prediction except at high observed relative abundance is the oak taxon (Figure E.17). Oak is both overpredicted at low observed relative abundance and underpredicted at high observed relative abundance. We interpret these biases in our GJAM's predictions as being indicative of multiple ecosystem states in our study region. Environmental conditions were only partially responsible for changes in the relative abundance

of oak, with oak tolerant of a broader range of environmental conditions than where it was most abundant. The relative abundance of oak was additionally driven by environment-vegetation feedbacks that promoted higher disturbance in the savanna (where oak was most abundant) and lower disturbance in the forest (where oak could be present but less abundant). Therefore, our model struggled to predict where oak was highly abundant and not very abundant from environmental conditions alone. This interpretation is supported by the strong residual correlations between oak and most other tree taxa in the main text (Figure ??). Although residual correlations are used to predict relative abundances in our out-of-sample validation, when all taxa are being predicted, the correlations cannot be adequately leveraged because the model does not know whether or not oak or other tree taxa were highly abundant in a given spatiotemporal grid cell.

Plots of observed vs. predicted relative abundance tended to emphasize instances of low prediction accuracy because it was difficult to see the many overlapping points near zero and near the one-to-one line (Figures E.12- E.22). Therefore, we additionally computed the bias in model predictions (observed minus predicted relative abundance) for each model prediction at each spatiotemporal grid cell. By plotting the density of bias values (insets in Figures E.12- E.22), we were able to more clearly discern the frequency of high prediction bias in our model. We found that in general, prediction bias was very low; that is, difference between observed and predicted relative abundance was very low for most predictions for most taxa. Across taxa, there was a slight tendency to overpredict relative abundance, which is reflective of the fact that the model tends to predict all taxa to be present at low relative abundance across the entire spatiotemporal domain. Again, oak stands out, with the frequency of prediction bias being bimodal, indicating a high incidence of both slightly overpredicting relative abundance and strongly underpredicting relative abundance. This again reflects the inability of our model to predict the high abundance of oak in the savanna ecosystem and low abundance of oak outside the savanna ecosystem from environmental conditions alone.

From the density distributions of prediction bias, we computed the proportion of all predictions that differed from observed relative abundance by more than 10% relative abundance (“high bias”, Table E.4). Most taxa had very low proportion of predictions with high bias. However, oak, other conifer taxa, other hardwood taxa, pine, and tamarack had higher incidence of high prediction bias (Table E.4). Other conifer and other hardwood taxa are likely difficult to predict because they encompass many tree species, all of which have different environmental tolerances. Oak has a high proportion of high bias predictions because of the tendency to strongly underpredict oak relative abundance, as discussed above. Pine and tamarack both are highly abundant in a small number of grid cells, so our model’s inability to predict very high relative abundances may explain the high proportion of high bias predictions.

Finally, to investigate spatiotemporal patterns in prediction bias, we plotted the median prediction bias (from different posterior draws) for each taxon at each spatiotemporal grid cell (Figures E.23- E.33). These figures, again, indicate

that across most taxa at most spatiotemporal locations, our GJAM's predictions are in good agreement with observed relative abundance. Underprediction is common where the taxon is most abundant, as anticipated from above results.

However, two main exceptions exist. First, oak experienced significant underprediction within the savanna ecosystem and overprediction in both the prairie (southwest) and forest (north and east) ecosystems. In combination with other prediction results above, we interpret this as indicating that environmental conditions alone were insufficient to explain spatial trends in oak relative abundance. However, it is important to note that the prediction bias of oak remained relatively stable over time. In contrast to oak, the other significant pattern we infer from our spatiotemporal model bias plots is the increase in prediction bias for hemlock over time. Hemlock was always underpredicted in northcentral Wisconsin, but the magnitude of the underprediction increased over time. This indicates that a temporal process that was not related to our environmental drivers drove the relative abundance of hemlock. As we discuss in the main text, we suggest that this pattern could be explained by lags between previous and current relative abundance of hemlock.

Table E.1: Coefficient estimates of environment-taxon relative abundance relationships from the final model.

Taxon	Covariate	Coefficient
Beech	Soil % sand	0.14 [-0.022,0.34]
	Average annual temperature	0.37 [0.18,0.56]
	Total annual precipitation	0.069 [-0.10,0.24]
	Precipitation seasonality	-0.57 [-0.76,-0.39]
Birch	Soil % sand	-0.016 [-0.17,0.15]
	Average annual temperature	-0.80 [-1.0,-0.59]
	Total annual precipitation	0.45 [0.26,0.65]
	Precipitation seasonality	-0.37 [-0.56,-0.18]
Elm	Soil % sand	-0.15 [-0.30,0.042]
	Average annual temperature	0.78 [0.56,1.0]
	Total annual precipitation	-0.72 [-0.97,-0.49]

Table E.1: (Continued)

Taxon	Covariate	Coefficient
	Precipitation seasonality	-0.068 [-0.22,0.10]
Hemlock	Soil % sand	0.030 [-0.11,0.17]
	Average annual temperature	-0.43 [-0.60,-0.26]
	Total annual precipitation	0.65 [0.48,0.82]
	Precipitation seasonality	-0.37 [-0.54,-0.20]
Maple	Soil % sand	0.085 [-0.13,0.27]
	Average annual temperature	-0.027 [-0.31,0.26]
	Total annual precipitation	0.18 [-0.13,0.50]
	Precipitation seasonality	-0.20 [-0.45,0.0090]
Oak	Soil % sand	-0.081 [-0.23,0.063]
	Average annual temperature	0.94 [0.73,1.2]
	Total annual precipitation	-0.22 [-0.45,-0.021]
	Precipitation seasonality	0.32 [0.18,0.46]
Other conifer taxa	Soil % sand	-0.23 [-0.42,-0.055]
	Average annual temperature	-0.77 [-1.1,-0.44]
	Total annual precipitation	0.22 [-0.055,0.52]
	Precipitation seasonality	-0.35 [-0.57,-0.16]
Other hardwood taxa	Soil % sand	0.20 [0.016,0.41]
	Average annual temperature	0.38 [0.063,0.66]
	Total annual precipitation	-0.77 [-1.1,-0.48]

Table E.1: (Continued)

Taxon	Covariate	Coefficient
Pine	Precipitation seasonality	0.19 [0.017,0.36]
	Soil % sand	0.24 [0.10,0.38]
	Average annual temperature	-0.54 [-0.73,-0.36]
	Total annual precipitation	0.42 [0.26,0.58]
	Precipitation seasonality	0.16 [0.033,0.29]
Spruce	Soil % sand	-0.19 [-0.36,-0.036]
	Average annual temperature	-0.77 [-1.1,-0.48]
	Total annual precipitation	0.14 [-0.067,0.33]
	Precipitation seasonality	-0.18 [-0.37,-0.0058]
Tamarack	Soil % sand	-0.15 [-0.35,0.049]
	Average annual temperature	-0.75 [-1.0,-0.47]
	Total annual precipitation	-0.013 [-0.32,0.20]
	Precipitation seasonality	0.13 [-0.046,0.29]

Column titled “Coefficient” reports the median and 95% credible interval in brackets of each coefficient estimated in our final model.

Taxon scientific names are as follows: beech (*Fagus grandifolia*), birch (*Betula spp.*), elm (*Ulmus spp.*), hemlock (*Tsuga canadensis*), maple (*Acer spp.*), oak (*Quercus spp.*), pine (*Pinus spp.*), spruce (*Picea spp.*), and tamarack (*Larix laricina*).

Our final model includes soil % sand, average annual temperature, total annual precipitation, and precipitation seasonality covariates with no interaction terms. The final model was fit with five time steps: 1900, 1500, 1100, 700, and 300 YBP.

Table E.2: Joint sensitivity of all taxon relative abundances to each environmental covariate in our final model

Covariate	Sensitivity
Soil % sand	12.1 [6.36, 31.1]
Average annual temperature	100 [58.2, 156]
Total annual precipitation	33.3 [21.9, 63.8]
Precipitation seasonality	75.2 [46.6, 112]

Column titled “Sensitivity” reports the median and 95% credible intervals (in brackets) of the joint sensitivity of all taxa to each environmental covariate for our final model. Larger values indicate that taxa are jointly more sensitive to the given environmental covariate.

Our final model includes soil % sand, average annual temperature, total annual precipitation, and precipitation seasonality covariates with no interaction terms. The final model was fit with five time steps: 1900, 1500, 1100, 700, and 300 YBP.

Table E.3: Correlation estimates of environment-taxon relative abundance relationships from the final model.

Taxon 1	Taxon 2	Correlation
Beech	Beech	1.0 [1.0,1.0]
	Birch	-0.12 [-1.0,0.0057]
	Elm	-0.0049 [-0.44,0.057]
	Hemlock	0.0087 [-0.49,0.076]
	Maple	-0.017 [-0.73,0.083]
	Oak	-0.14 [-0.74,-0.0097]
	Other conifer taxa	-0.050 [-0.84,0.054]
	Other hardwood taxa	-0.051 [-0.53,0.033]
	Pine	-0.098 [-0.65,0.0076]
	Spruce	-0.025 [-0.74,0.043]
Birch	Tamarack	0.11 [-0.0018,0.17]
	Beech	-0.12 [-1.0,0.0057]
	Birch	1.0 [1.0,1.0]
	Elm	0.13 [0.038,0.16]
	Hemlock	0.22 [0.12,0.22]
	Maple	0.16 [-0.015,0.21]
	Oak	-0.24 [-0.55,-0.090]
	Other conifer taxa	-0.018 [-0.60,0.11]

Table E.3: (Continued)

Taxon 1	Taxon 2	Correlation
Elm	Other hardwood taxa	0.20 [0.070,0.23]
	Pine	-0.12 [-0.46,0.013]
	Spruce	-0.063 [-0.80,0.077]
	Tamarack	-0.17 [-0.74,0.014]
	Beech	-0.0049 [-0.44,0.057]
	Birch	0.13 [-0.038,0.16]
	Elm	1.0 [1.0,1.0]
	Hemlock	0.16 [0.12,0.16]
	Maple	0.22 [0.15,0.28]
	Oak	-0.56 [-1.0,-0.15]
Hemlock	Other conifer taxa	0.25 [0.19,0.23]
	Other hardwood taxa	0.071 [-0.35,0.13]
	Pine	0.0097 [-0.20,0.097]
	Spruce	0.061 [-0.18,0.098]
	Tamarack	-0.032 [-0.46,0.045]
	Beech	0.0087 [-0.49,0.076]
	Birch	0.22 [0.12,0.22]
	Elm	0.16 [0.12,0.16]
	Hemlock	1.0 [1.0,1.0]
	Maple	0.21 [0.10,0.23]
Maple	Oak	-0.21 [-0.61,-0.059]
	Other conifer taxa	-0.049 [-0.59,0.063]
	Other hardwood taxa	0.032 [-0.17,0.10]
	Pine	-0.16 [-0.59,-0.020]
	Spruce	-0.22 [-1.0,-0.034]
	Tamarack	-0.18 [-0.74,-0.029]
	Beech	-0.017 [-0.73,0.083]
	Birch	0.16 [-0.015,0.21]
	Elm	0.22 [0.15,0.28]
	Hemlock	0.21 [0.099,0.23]
Oak	Maple	1.0 [1.0,1.0]
	Oak	-0.46 [-1.0,-0.19]

Table E.3: (Continued)

Taxon 1	Taxon 2	Correlation
Other conifer taxa	Birch	-0.24 [-0.55,-0.090]
	Elm	-0.56 [-1.0,-0.15]
	Hemlock	-0.21 [-0.61,-0.059]
	Maple	-0.46 [-1.0,-0.19]
	Oak	1.0 [1.0,1.0]
	Other conifer taxa	-0.26 [-0.75,-0.067]
	Other hardwood taxa	-0.36 [-0.79,-0.13]
	Pine	-0.35 [-0.64,-0.18]
	Spruce	-0.034 [-0.35,0.062]
	Tamarack	-0.16 [-0.50,-0.013]
Other hard-wood taxa	Beech	-0.050 [-0.84,0.054]
	Birch	-0.018 [-0.60,0.11]
	Elm	0.25 [0.19,0.23]
	Hemlock	-0.049 [-0.59,0.063]
	Maple	0.16 [-0.076,0.24]
	Oak	-0.26 [-0.75,-0.067]
	Other conifer taxa	1.0 [1.0,1.0]
	Other hardwood taxa	-0.063 [-0.53,0.061]
	Pine	-0.17 [-0.60,-0.0044]
	Spruce	0.22 [-0.11,0.25]
Pine	Tamarack	-0.13 [-0.79,0.065]
	Beech	-0.051 [-0.53,0.033]
	Birch	0.20 [0.070,0.23]
	Elm	0.071 [-0.35,0.13]
	Hemlock	0.032 [-0.17,0.10]
	Maple	0.24 [0.078,0.27]
	Oak	-0.36 [-0.79,-0.13]
Other conifer taxa	Other conifer taxa	-0.063 [-0.53,0.061]
	Other hardwood taxa	1.0 [1.0,1.0]
	Pine	-0.086 [-0.36,0.033]
	Spruce	-0.069 [-0.60,0.048]
	Tamarack	-0.056 [-0.55,0.068]
	Beech	-0.098 [-0.65,0.0076]
	Birch	-0.12 [-0.46,0.013]

Table E.3: (Continued)

Taxon 1	Taxon 2	Correlation
Spruce	Other hardwood taxa	-0.086 [-0.36,0.033]
	Pine	1.0 [1.0,1.0]
	Spruce	-0.082 [-0.68,0.050]
	Tamarack	-0.20 [-0.64,0.00039]
	Beech	-0.025 [-0.74,0.043]
	Birch	-0.063 [-0.80,0.077]
	Elm	0.061 [-0.18,0.098]
	Hemlock	-0.22 [-1.0,-0.034]
	Maple	-0.077 [-0.75,0.043]
	Oak	-0.034 [-0.35,0.062]
Tamarack	Other conifer taxa	0.22 [-0.11,0.25]
	Other hardwood taxa	-0.069 [-0.60,0.048]
	Pine	-0.082 [-0.68,0.050]
	Spruce	1.0 [1.0,1.0]
	Tamarack	-0.053 [-1.0,0.75]
	Beech	0.11 [-0.0018,0.17]
	Birch	-0.17 [-0.74,0.014]
	Elm	-0.032 [-0.46,0.045]
	Hemlock	-0.18 [-0.74,-0.029]
	Maple	-0.032 [-0.41,0.089]

Residual correlations quantify the relationship between taxa after accounting for their dependence on the environmental covariates in the model. Note that correlation coefficients are reciprocal: for example, the correlation between beech and birch is the same as the correlation between birch and beech for the same formula. Column titled “Correlation” reports the median and 95% credible interval of the residual correlations in brackets.

Taxon scientific names are as follows: beech (*Fagus grandifolia*), birch (*Betula spp.*), elm (*Ulmus spp.*), hemlock (*Tsuga canadensis*), maple (*Acer spp.*), oak (*Quercus spp.*), pine (*Pinus spp.*), spruce (*Picea spp.*), and tamarack (*Larix laricina*).

Our final model includes soil % sand, average annual temperature, total annual precipitation, and precipitation seasonality covariates with no interaction terms. The final model was fit with five time steps: 1900, 1500, 1100, 700, and 300 YBP.

Table E.4: Pearson’s correlation coefficient between observed and predicted relative abundance of each taxon and proportion of grid cells with large bias from our full out-of-sample validation.

Taxon	Correlation	Fraction high bias
Beech	0.63 [0.54,0.69]	0.056
Birch	0.66 [0.61,0.71]	0.075
Elm	0.53 [0.45,0.61]	0.068
Hemlock	0.58 [0.51,0.63]	0.073
Maple	0.31 [0.15,0.47]	0.073
Oak	0.73 [0.69,0.78]	0.71
Other conifer taxa	0.59 [0.47,0.67]	0.13
Other hardwood taxa	0.56 [0.48,0.63]	0.16
Pine	0.45 [0.41,0.49]	0.45
Spruce	0.58 [0.47,0.70]	0.026
Tamarack	0.60 [0.47,0.68]	0.20

Column titled “Correlation” reports the median and 95% credible intervals (in brackets) of the Pearson correlation coefficient between predicted and observed relative abundance at all withheld spatiotemporal observations. Median and credible intervals were calculated by finding the correlation between predicted and observed relative abundance estimates from 100 posterior draws of relative abundance from STEPPS. Larger values indicate that there was better agreement between predicted and observed relative abundance and lower values indicate poorer agreement.

Column titled “Fraction high bias” reports the fraction of total spatiotemporal grid cells that had greater than 10% difference between predicted and observed relative abundance. For example, beech had 5.6% of grid cells with model bias greater than 10%.

Our final model includes soil % sand, average annual temperature, total annual precipitation, and precipitation seasonality covariates with no interaction terms. The final model was fit with five time steps: 1900, 1500, 1100, 700, and 300 YBP. All spatiotemporal observations not used to fit the model were predicted and compared with our reconstructions.

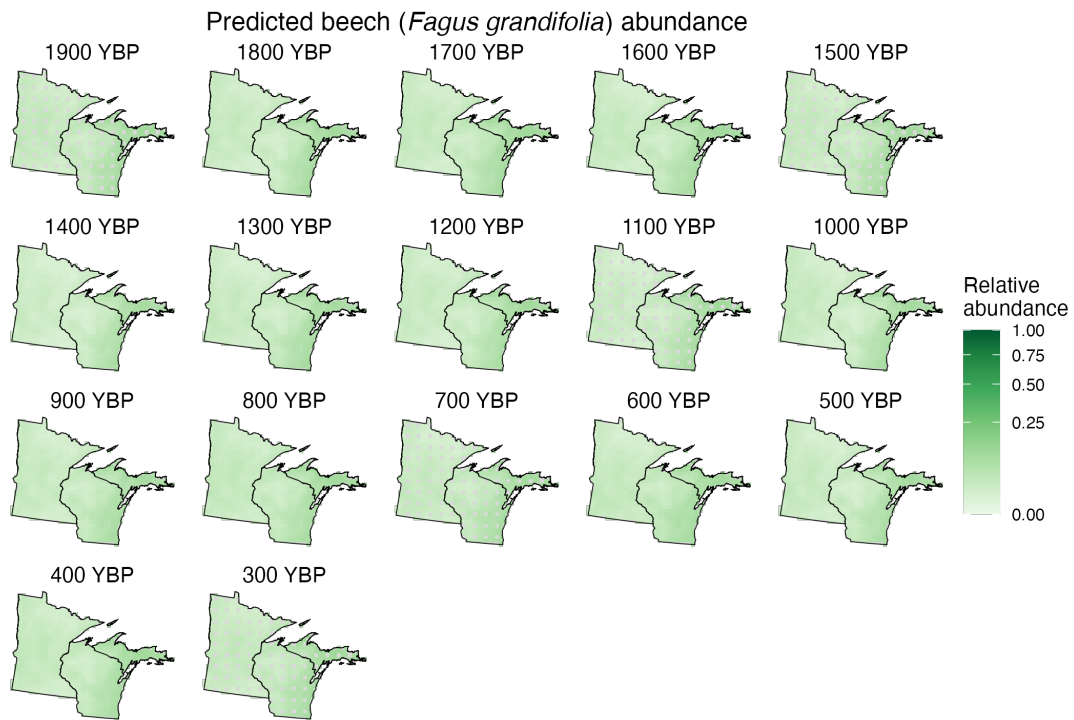


Figure E.1: Predicted relative abundance of beech (*Fagus grandifolia*) for all spatiotemporal observations not used to fit the model. Each facet shows the predicted relative abundance of beech (shades of green) across our spatial domain. Facets show predictions for each 100-year time step from 1900 to 300 YBP. Gray grid cells show locations that were not predicted in a given time step because they were used to fit the model. Note that the color scale ranges from the minimum to maximum possible prediction values and is square root transformed to emphasize lower values of relative abundance.

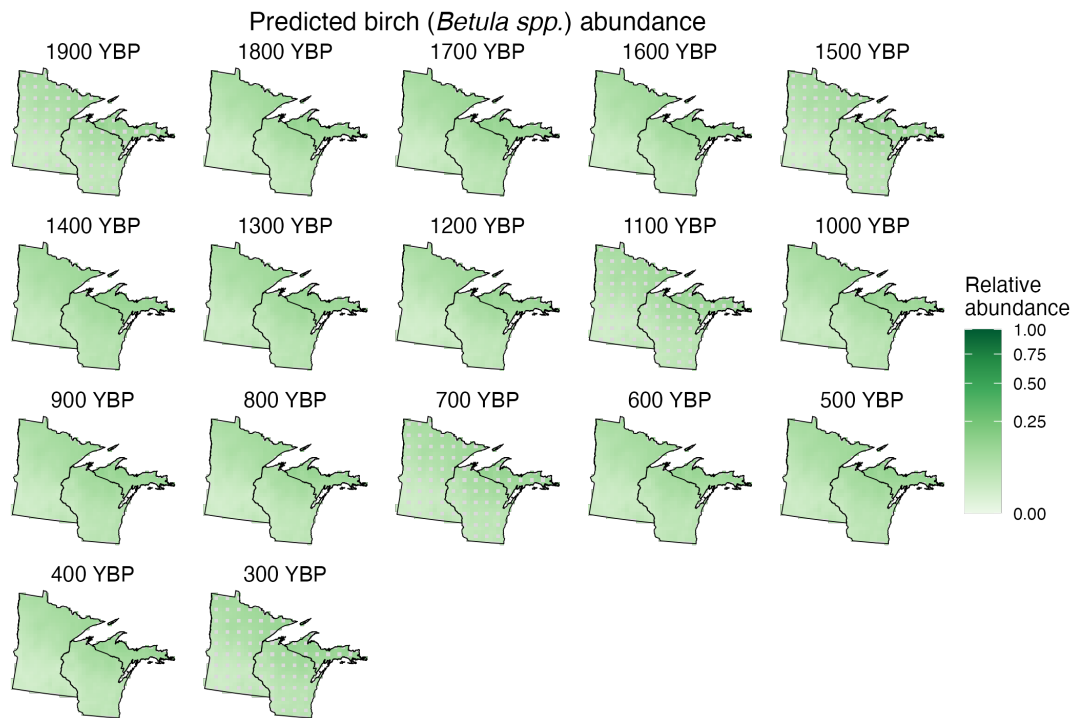


Figure E.2: Predicted relative abundance of birch (*Betula spp.*) for all spatiotemporal observations not used to fit the model. Each facet shows the predicted relative abundance of beech (shades of green) across our spatial domain. Facets show predictions for each 100-year time step from 1900 to 300 YBP. Gray grid cells show locations that were not predicted in a given time step because they were used to fit the model. Note that the color scale ranges from the minimum to maximum possible prediction values and is square root transformed to emphasize lower values of relative abundance.

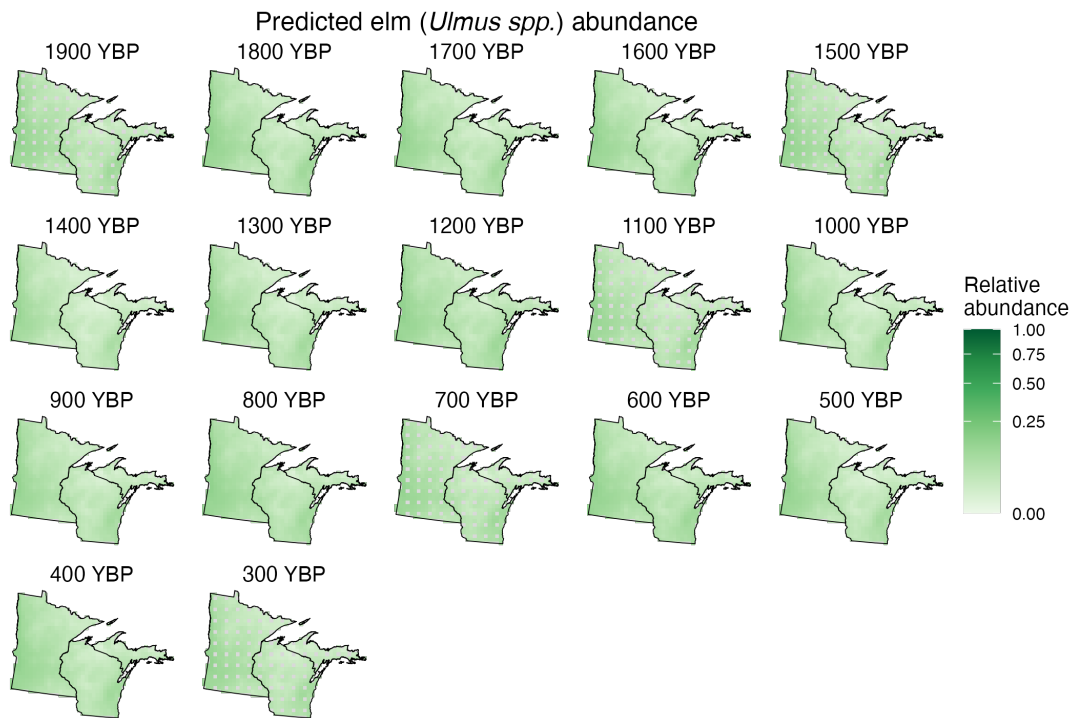


Figure E.3: Predicted relative abundance of elm (*Ulmus spp.*) for all spatiotemporal observations not used to fit the model. Each facet shows the predicted relative abundance of beech (shades of green) across our spatial domain. Facets show predictions for each 100-year time step from 1900 to 300 YBP. Gray grid cells show locations that were not predicted in a given time step because they were used to fit the model. Note that the color scale ranges from the minimum to maximum possible prediction values and is square root transformed to emphasize lower values of relative abundance.

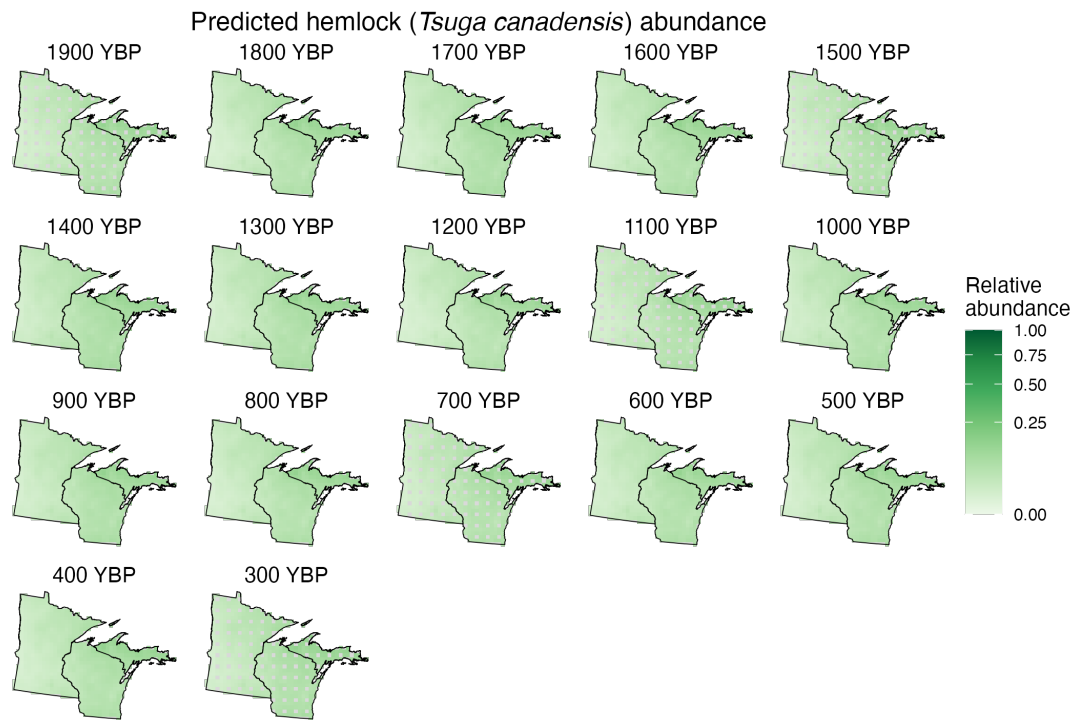


Figure E.4: Predicted relative abundance of hemlock (*Tsuga canadensis*) for all spatiotemporal observations not used to fit the model. Each facet shows the predicted relative abundance of beech (shades of green) across our spatial domain. Facets show predictions for each 100-year time step from 1900 to 300 YBP. Gray grid cells show locations that were not predicted in a given time step because they were used to fit the model. Note that the color scale ranges from the minimum to maximum possible prediction values and is square root transformed to emphasize lower values of relative abundance.

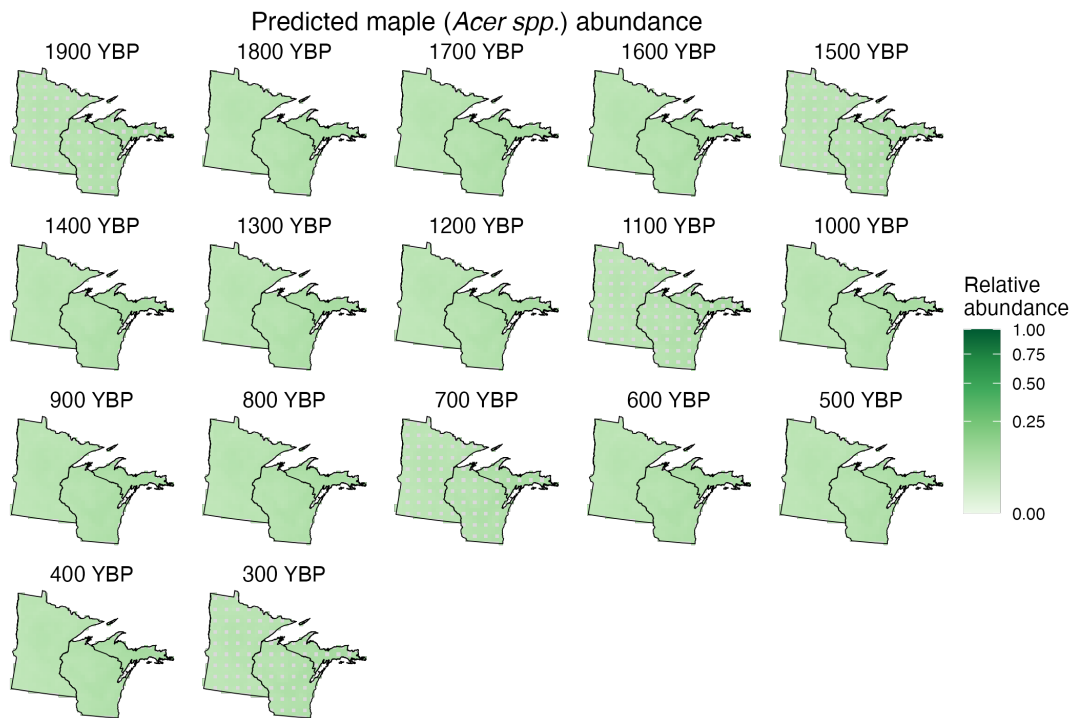


Figure E.5: Predicted relative abundance of maple (*Acer spp.*) for all spatiotemporal observations not used to fit the model. Each facet shows the predicted relative abundance of beech (shades of green) across our spatial domain. Facets show predictions for each 100-year time step from 1900 to 300 YBP. Gray grid cells show locations that were not predicted in a given time step because they were used to fit the model. Note that the color scale ranges from the minimum to maximum possible prediction values and is square root transformed to emphasize lower values of relative abundance.

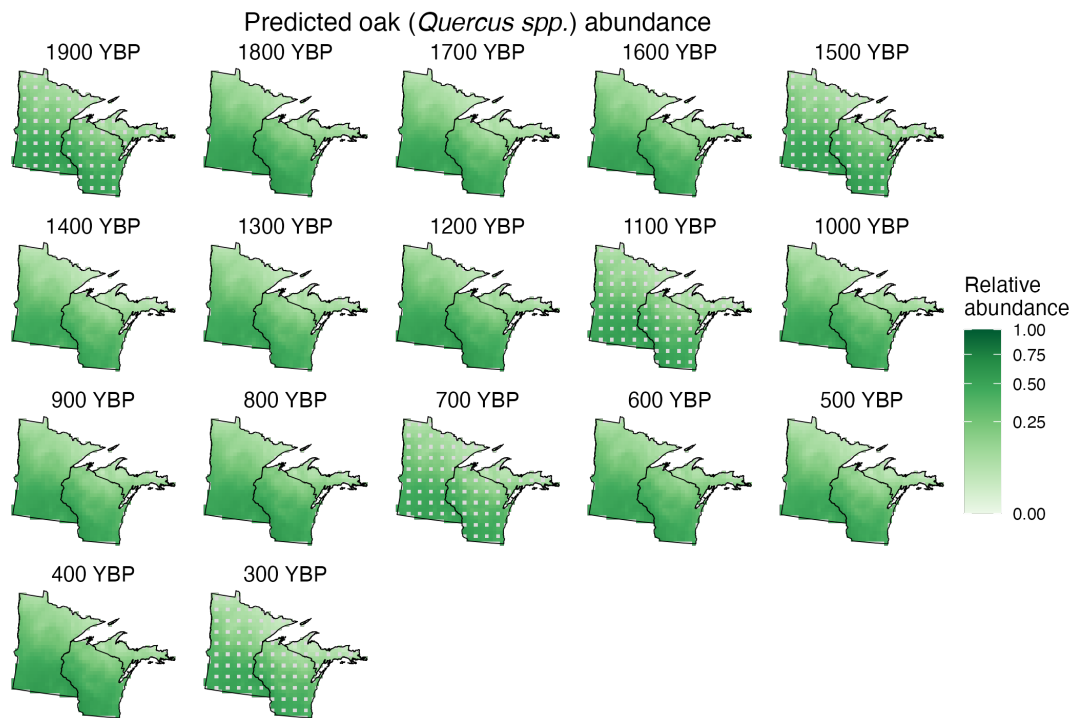


Figure E.6: Predicted relative abundance of oak (*Quercus spp.*) for all spatiotemporal observations not used to fit the model. Each facet shows the predicted relative abundance of beech (shades of green) across our spatial domain. Facets show predictions for each 100-year time step from 1900 to 300 YBP. Gray grid cells show locations that were not predicted in a given time step because they were used to fit the model. Note that the color scale ranges from the minimum to maximum possible prediction values and is square root transformed to emphasize lower values of relative abundance.

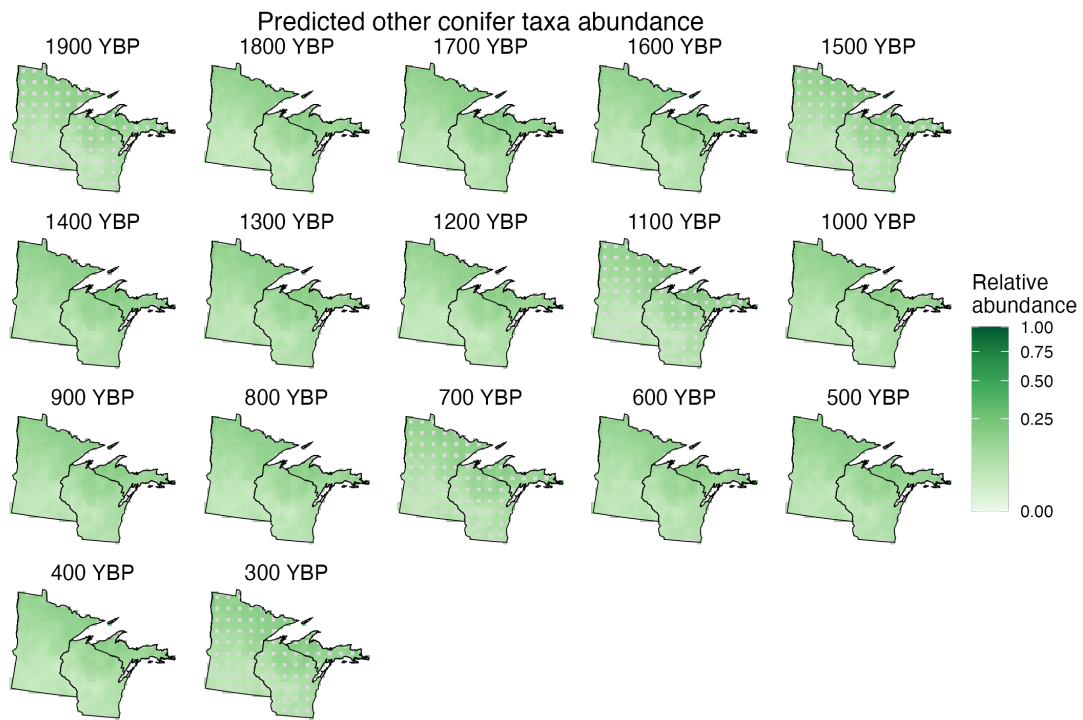


Figure E.7: Predicted relative abundance of other conifer taxa for all spatiotemporal observations not used to fit the model. Each facet shows the predicted relative abundance of beech (shades of green) across our spatial domain. Facets show predictions for each 100-year time step from 1900 to 300 YBP. Gray grid cells show locations that were not predicted in a given time step because they were used to fit the model. Note that the color scale ranges from the minimum to maximum possible prediction values and is square root transformed to emphasize lower values of relative abundance.

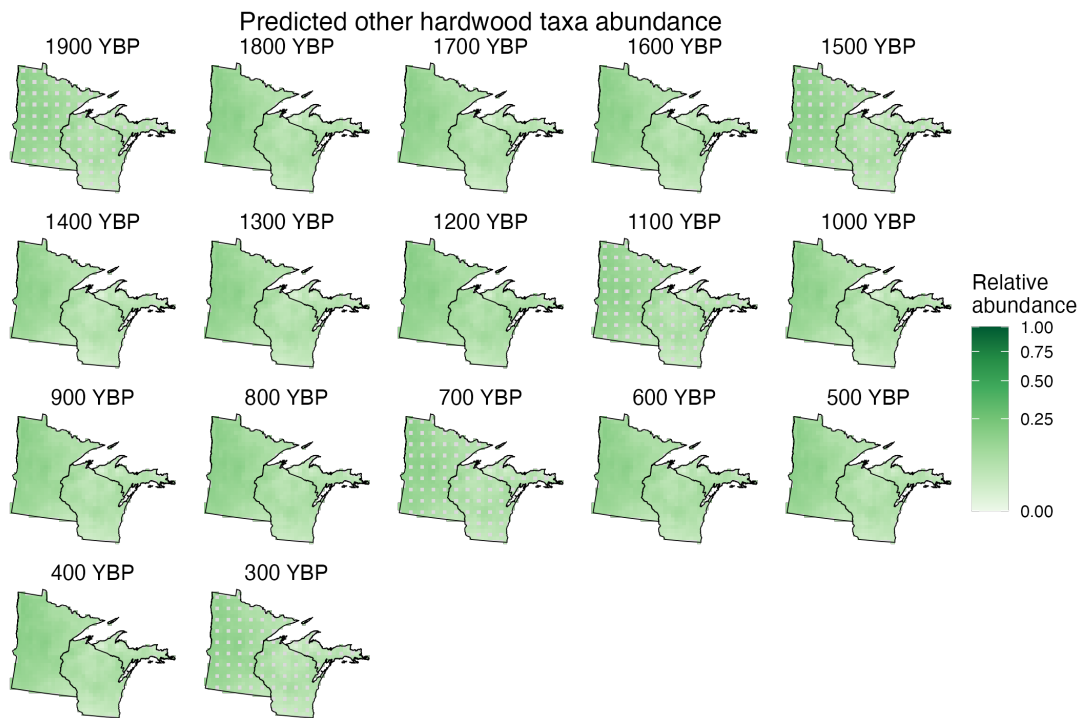


Figure E.8: Predicted relative abundance of other hardwood taxa for all spatiotemporal observations not used to fit the model. Each facet shows the predicted relative abundance of beech (shades of green) across our spatial domain. Facets show predictions for each 100-year time step from 1900 to 300 YBP. Gray grid cells show locations that were not predicted in a given time step because they were used to fit the model. Note that the color scale ranges from the minimum to maximum possible prediction values and is square root transformed to emphasize lower values of relative abundance.

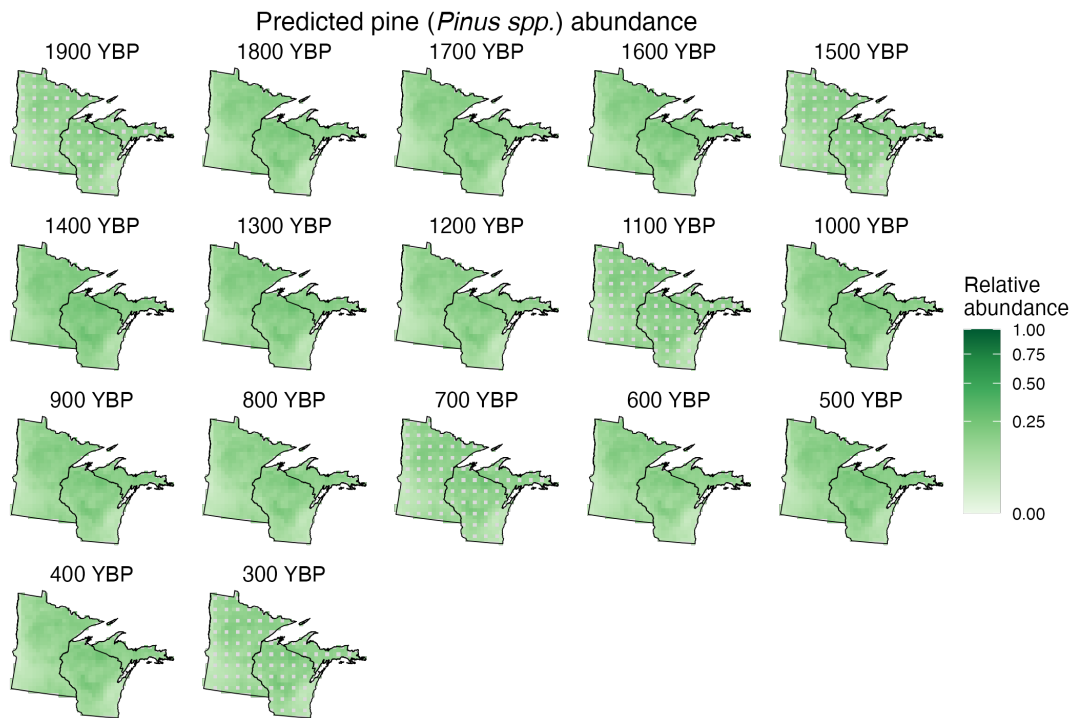


Figure E.9: Predicted relative abundance of pine (*Pinus spp.*) for all spatiotemporal observations not used to fit the model. Each facet shows the predicted relative abundance of beech (shades of green) across our spatial domain. Facets show predictions for each 100-year time step from 1900 to 300 YBP. Gray grid cells show locations that were not predicted in a given time step because they were used to fit the model. Note that the color scale ranges from the minimum to maximum possible prediction values and is square root transformed to emphasize lower values of relative abundance.

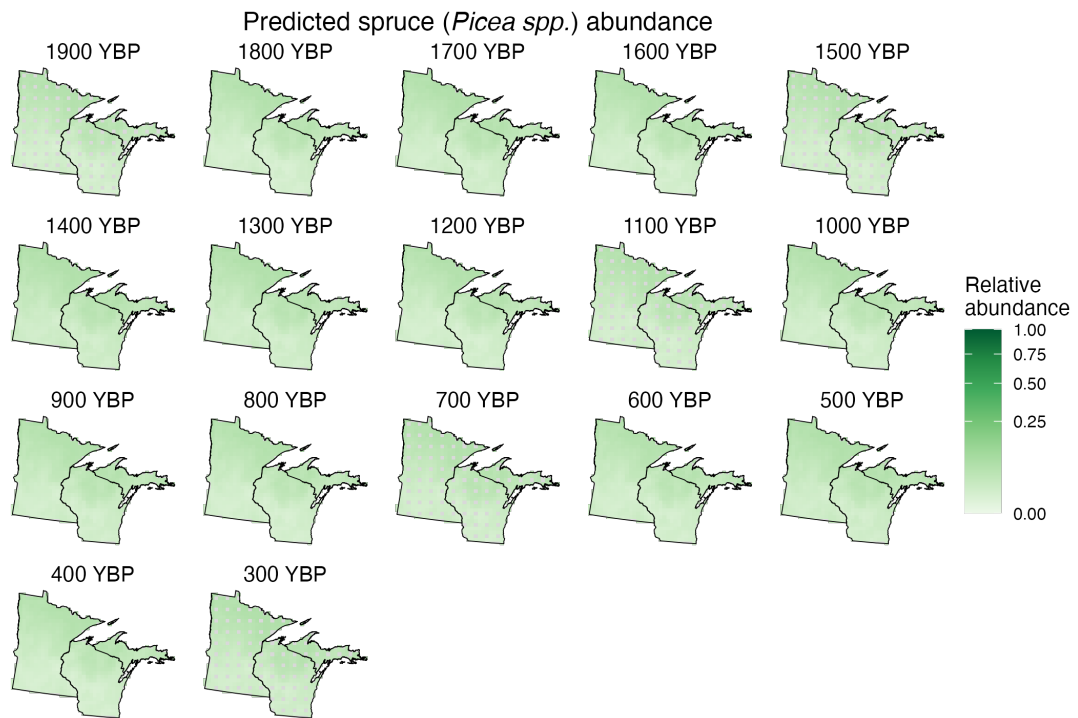


Figure E.10: Predicted relative abundance of spruce (*Picea spp.*) for all spatiotemporal observations not used to fit the model. Each facet shows the predicted relative abundance of beech (shades of green) across our spatial domain. Facets show predictions for each 100-year time step from 1900 to 300 YBP. Gray grid cells show locations that were not predicted in a given time step because they were used to fit the model. Note that the color scale ranges from the minimum to maximum possible prediction values and is square root transformed to emphasize lower values of relative abundance.

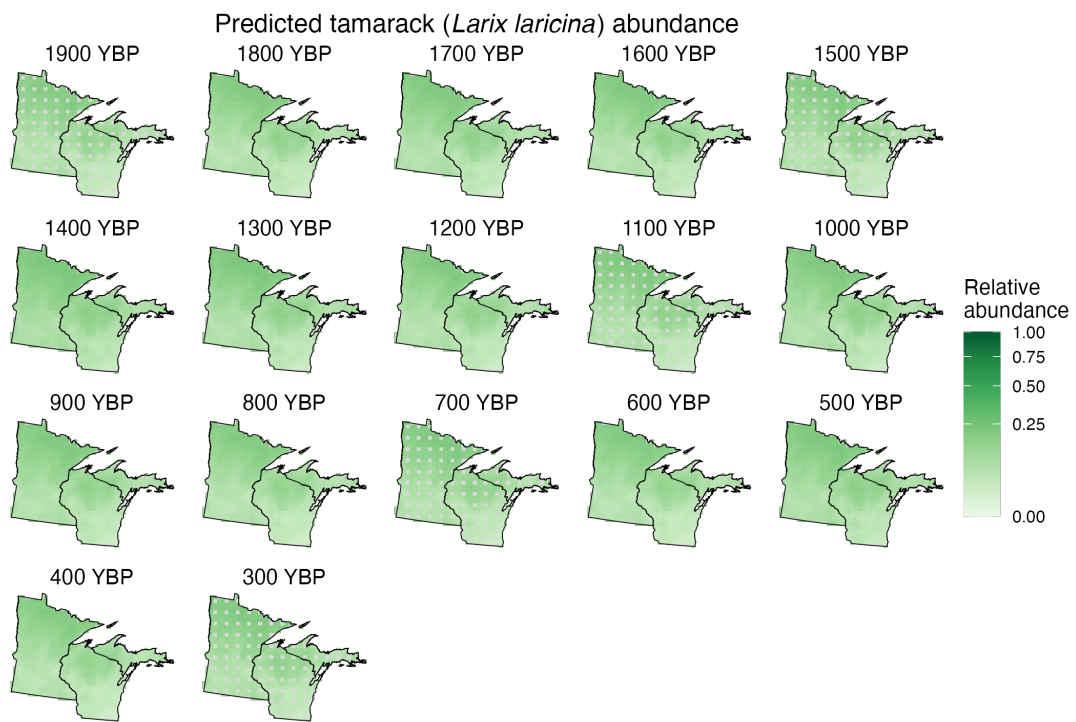


Figure E.11: Predicted relative abundance of tamarack (*Larix laricina*) for all spatiotemporal observations not used to fit the model. Each facet shows the predicted relative abundance of beech (shades of green) across our spatial domain. Facets show predictions for each 100-year time step from 1900 to 300 YBP. Gray grid cells show locations that were not predicted in a given time step because they were used to fit the model. Note that the color scale ranges from the minimum to maximum possible prediction values and is square root transformed to emphasize lower values of relative abundance.

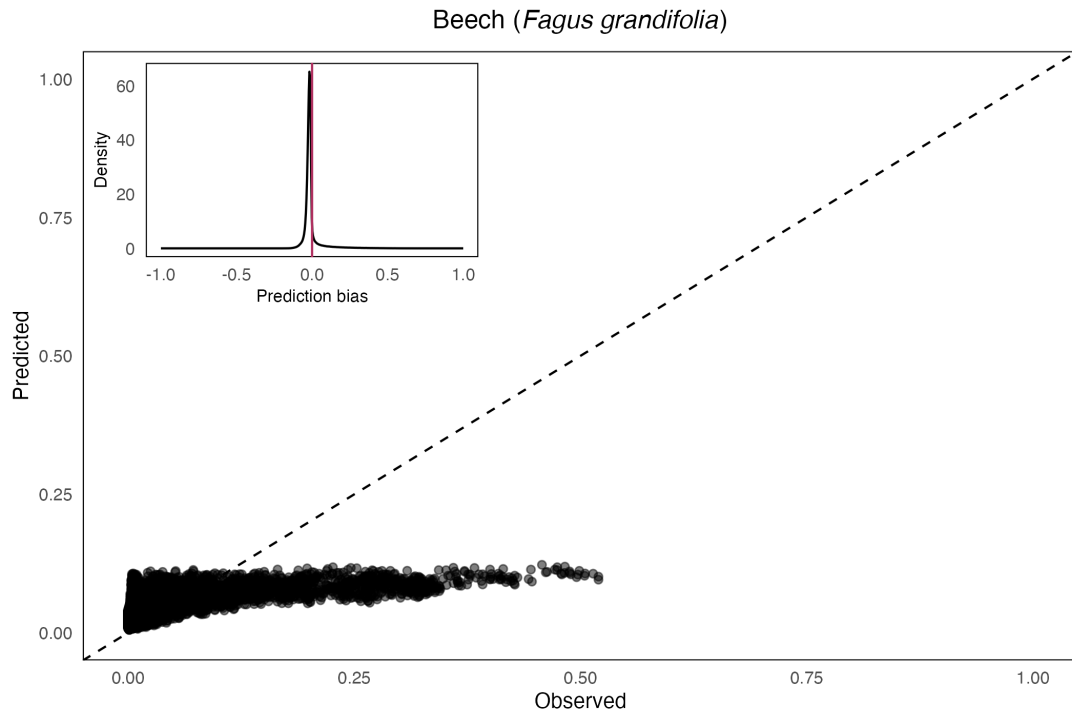


Figure E.12: Predicted vs observed relative abundance of beech (*Fagus grandifolia*) across our entire spatiotemporal domain. The x-axis is the estimated relative abundances from 100 posterior draws of STEPPS (“observed” abundance) and the y-axis is the predicted relative abundance across 100 model predictions from our GJAM. The dashed black line shows the one-to-one line indicating perfect prediction. The axes have been scaled to show the minimum to maximum possible observation and prediction scales. Inset figure: density plot of difference between observed and predicted relative abundance (“Prediction bias”) across all spatiotemporal grid cells. The red horizontal line highlights 0 (perfect prediction). The plot is scaled to show the full range of possible prediction bias values. Prediction bias of 1 = strong model underprediction. Prediction bias of -1 = strong model overprediction.

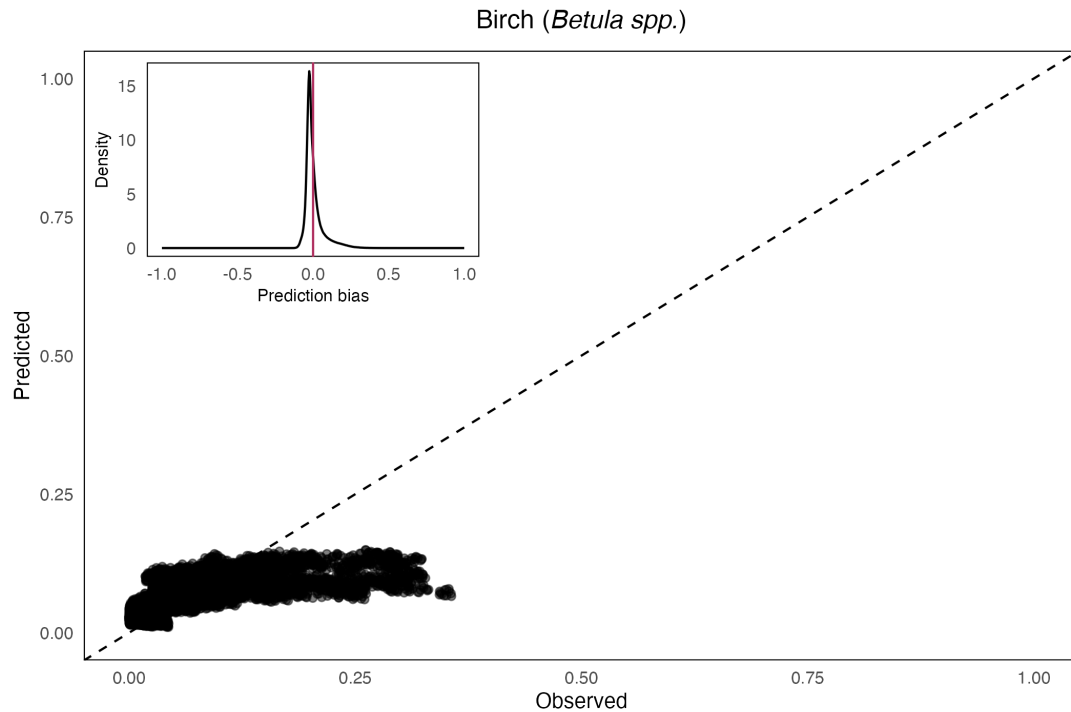


Figure E.13: Predicted vs observed relative abundance of birch (*Betula spp.*) across our entire spatiotemporal domain. The x-axis is the estimated relative abundances from 100 posterior draws of STEPPS (“observed” abundance) and the y-axis is the predicted relative abundance across 100 model predictions from our GJAM. The dashed black line shows the one-to-one line indicating perfect prediction. The axes have been scaled to show the minimum to maximum possible observation and prediction scales. Inset figure: density plot of difference between observed and predicted relative abundance (“Prediction bias”) across all spatiotemporal grid cells. The red horizontal line highlights 0 (perfect prediction). The plot is scaled to show the full range of possible prediction bias values. Prediction bias of 1 = strong model underprediction. Prediction bias of -1 = strong model overprediction.

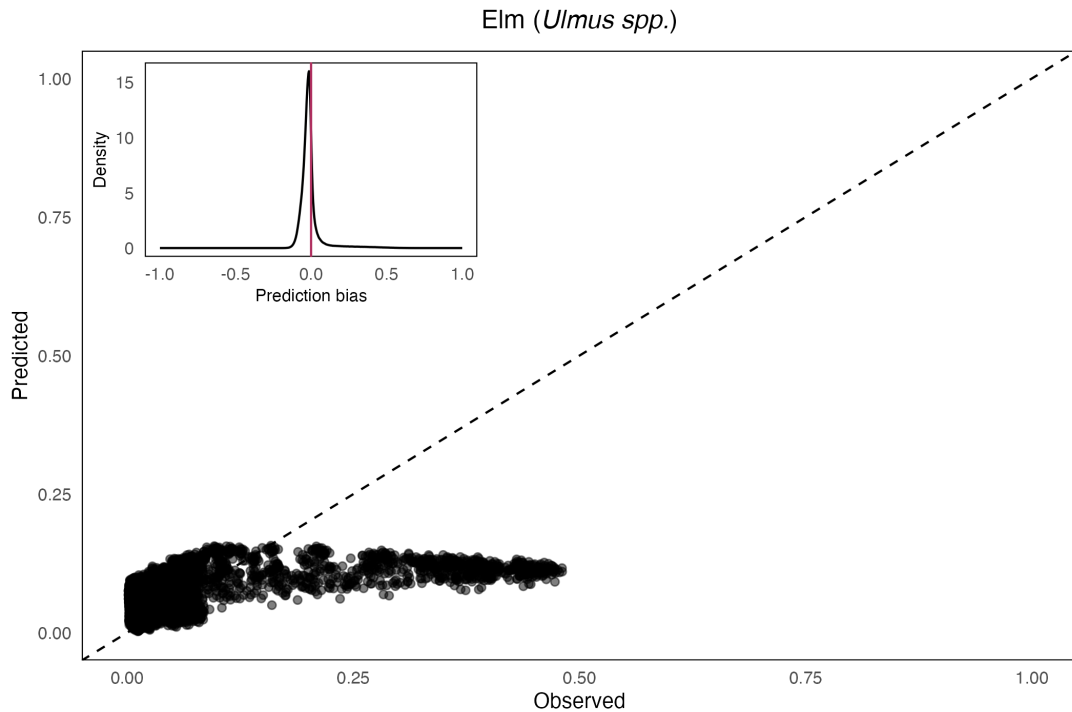


Figure E.14: Predicted vs observed relative abundance of elm (*Ulmus spp.*) across our entire spatiotemporal domain. The x-axis is the estimated relative abundances from 100 posterior draws of STEPPS (“observed” abundance) and the y-axis is the predicted relative abundance across 100 model predictions from our GJAM. The dashed black line shows the one-to-one line indicating perfect prediction. The axes have been scaled to show the minimum to maximum possible observation and prediction scales. Inset figure: density plot of difference between observed and predicted relative abundance (“Prediction bias”) across all spatiotemporal grid cells. The red horizontal line highlights 0 (perfect prediction). The plot is scaled to show the full range of possible prediction bias values. Prediction bias of 1 = strong model underprediction. Prediction bias of -1 = strong model overprediction.

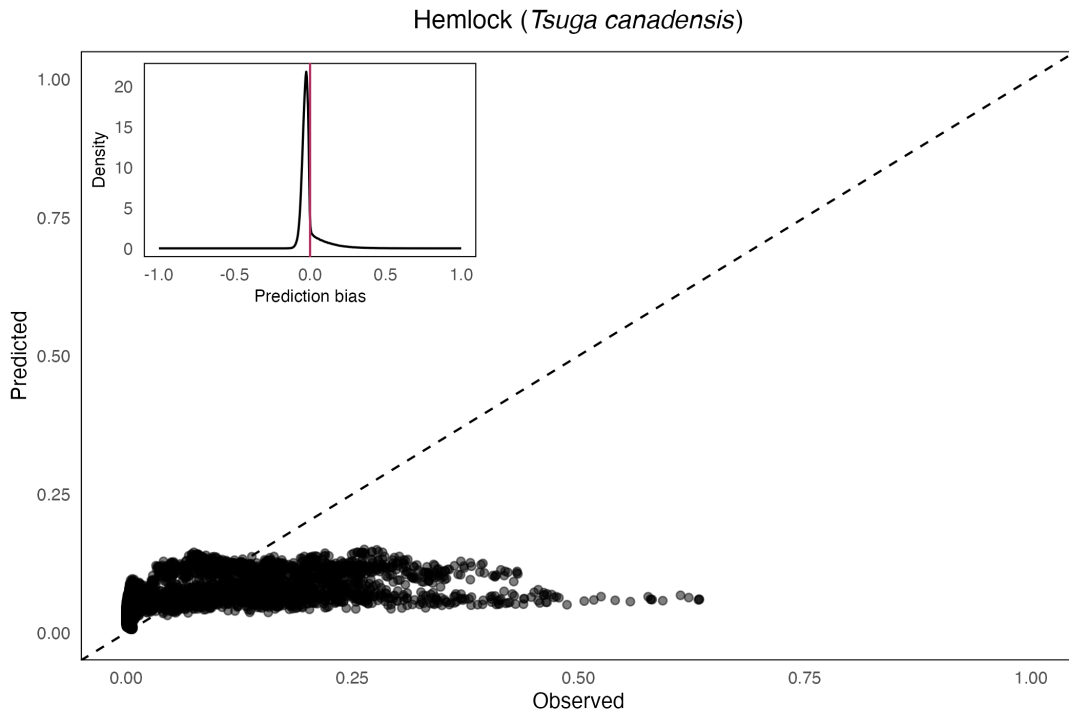


Figure E.15: Predicted vs observed relative abundance of hemlock (*Tsuga canadensis*) across our entire spatiotemporal domain. The x-axis is the estimated relative abundances from 100 posterior draws of STEPPS (“observed” abundance) and the y-axis is the predicted relative abundance across 100 model predictions from our GJAM. The dashed black line shows the one-to-one line indicating perfect prediction. The axes have been scaled to show the minimum to maximum possible observation and prediction scales. Inset figure: density plot of difference between observed and predicted relative abundance (“Prediction bias”) across all spatiotemporal grid cells. The red horizontal line highlights 0 (perfect prediction). The plot is scaled to show the full range of possible prediction bias values. Prediction bias of 1 = strong model underprediction. Prediction bias of -1 = strong model overprediction.

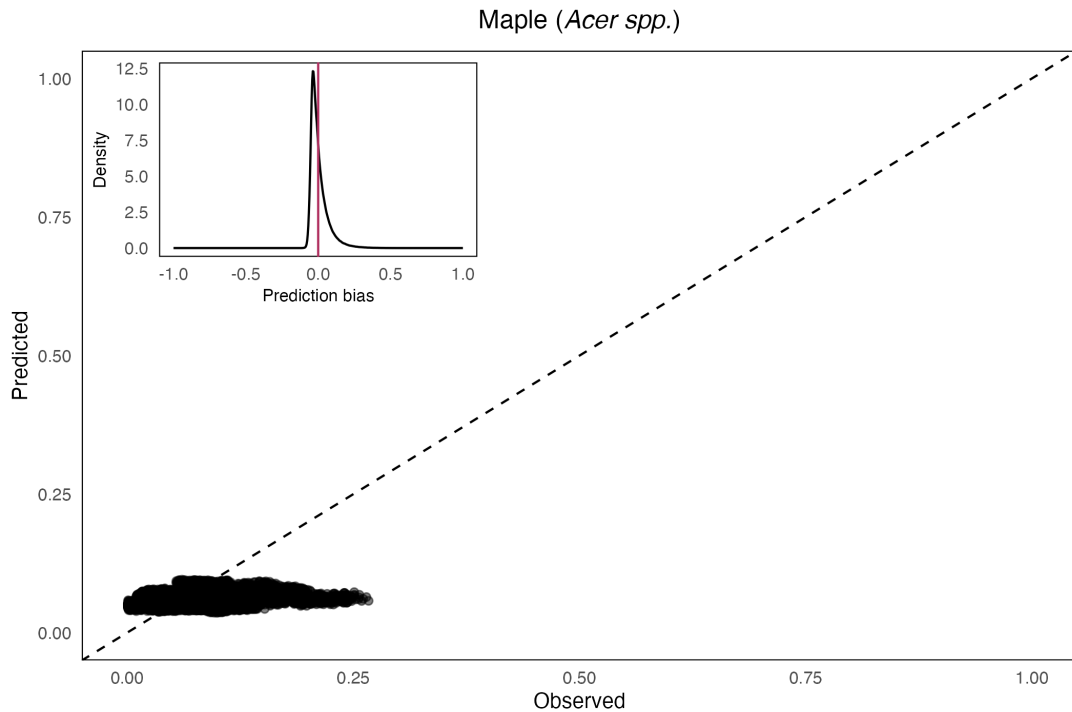


Figure E.16: Predicted vs observed relative abundance of maple (*Acer spp.*) across our entire spatiotemporal domain. The x-axis is the estimated relative abundances from 100 posterior draws of STEPPS (“observed” abundance) and the y-axis is the predicted relative abundance across 100 model predictions from our GJAM. The dashed black line shows the one-to-one line indicating perfect prediction. The axes have been scaled to show the minimum to maximum possible observation and prediction scales. Inset figure: density plot of difference between observed and predicted relative abundance (“Prediction bias”) across all spatiotemporal grid cells. The red horizontal line highlights 0 (perfect prediction). The plot is scaled to show the full range of possible prediction bias values. Prediction bias of 1 = strong model underprediction. Prediction bias of -1 = strong model overprediction.

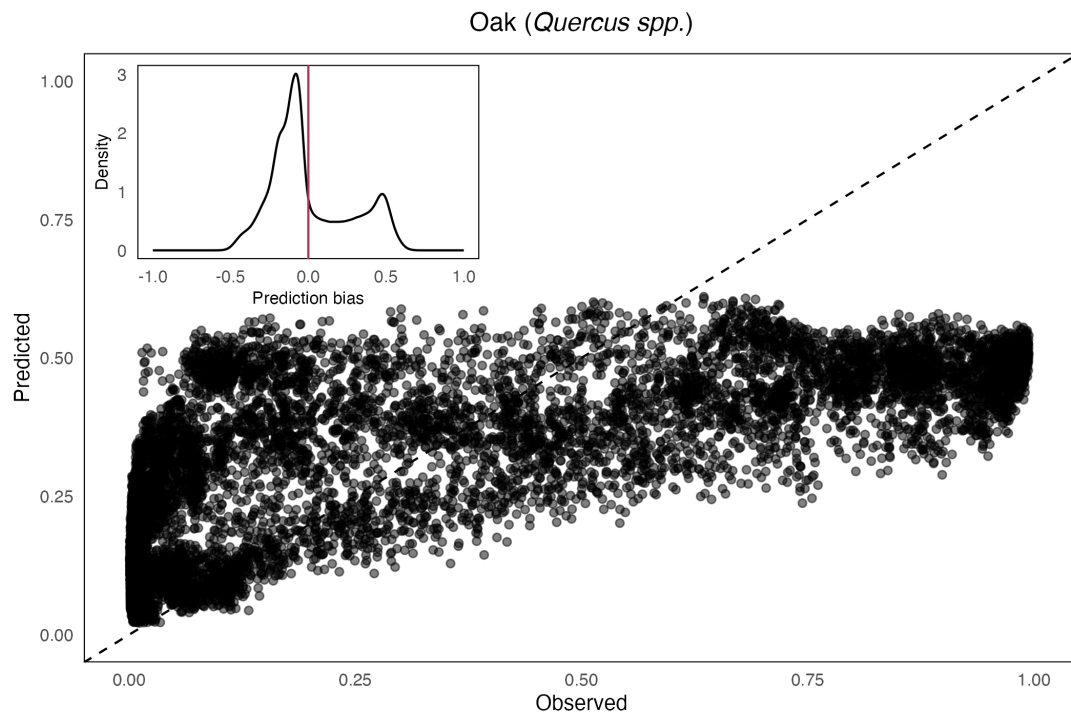


Figure E.17: Predicted vs observed relative abundance of oak (*Quercus spp.*) across our entire spatiotemporal domain. The x-axis is the estimated relative abundances from 100 posterior draws of STEPPS (“observed” abundance) and the y-axis is the predicted relative abundance across 100 model predictions from our GJAM. The dashed black line shows the one-to-one line indicating perfect prediction. The axes have been scaled to show the minimum to maximum possible observation and prediction scales. Inset figure: density plot of difference between observed and predicted relative abundance (“Prediction bias”) across all spatiotemporal grid cells. The red horizontal line highlights 0 (perfect prediction). The plot is scaled to show the full range of possible prediction bias values. Prediction bias of 1 = strong model underprediction. Prediction bias of -1 = strong model overprediction.

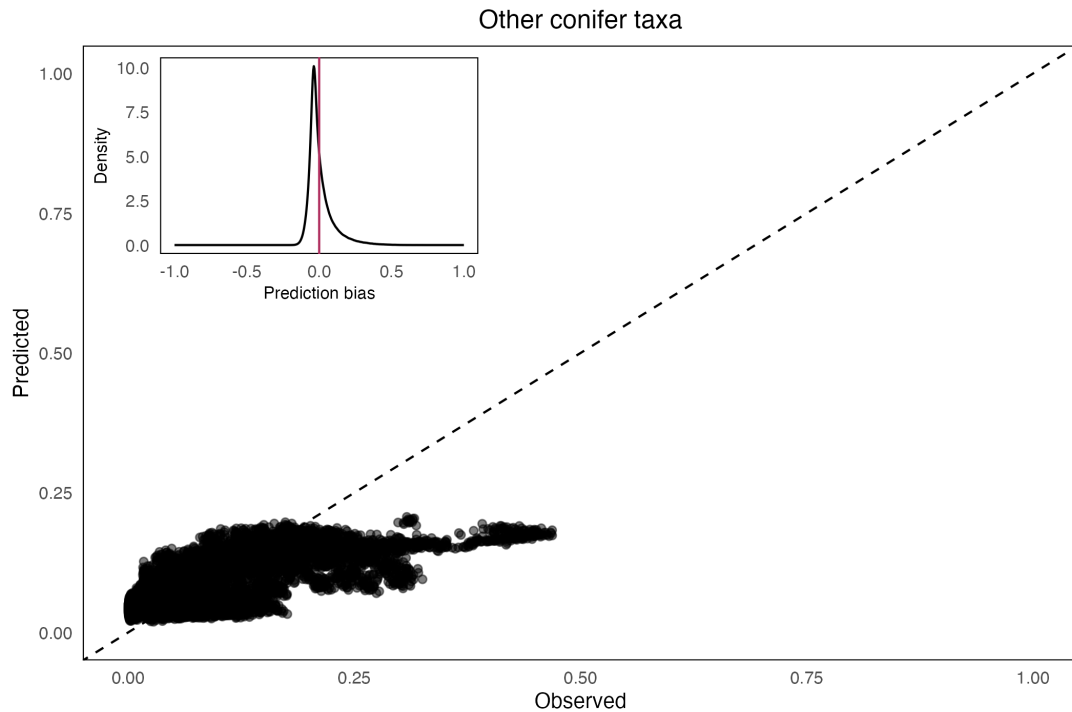


Figure E.18: Predicted vs observed relative abundance of other conifer taxa across our entire spatiotemporal domain. The x-axis is the estimated relative abundances from 100 posterior draws of STEPPS (“observed” abundance) and the y-axis is the predicted relative abundance across 100 model predictions from our GJAM. The dashed black line shows the one-to-one line indicating perfect prediction. The axes have been scaled to show the minimum to maximum possible observation and prediction scales. Inset figure: density plot of difference between observed and predicted relative abundance (“Prediction bias”) across all spatiotemporal grid cells. The red horizontal line highlights 0 (perfect prediction). The plot is scaled to show the full range of possible prediction bias values. Prediction bias of 1 = strong model underprediction. Prediction bias of -1 = strong model overprediction.

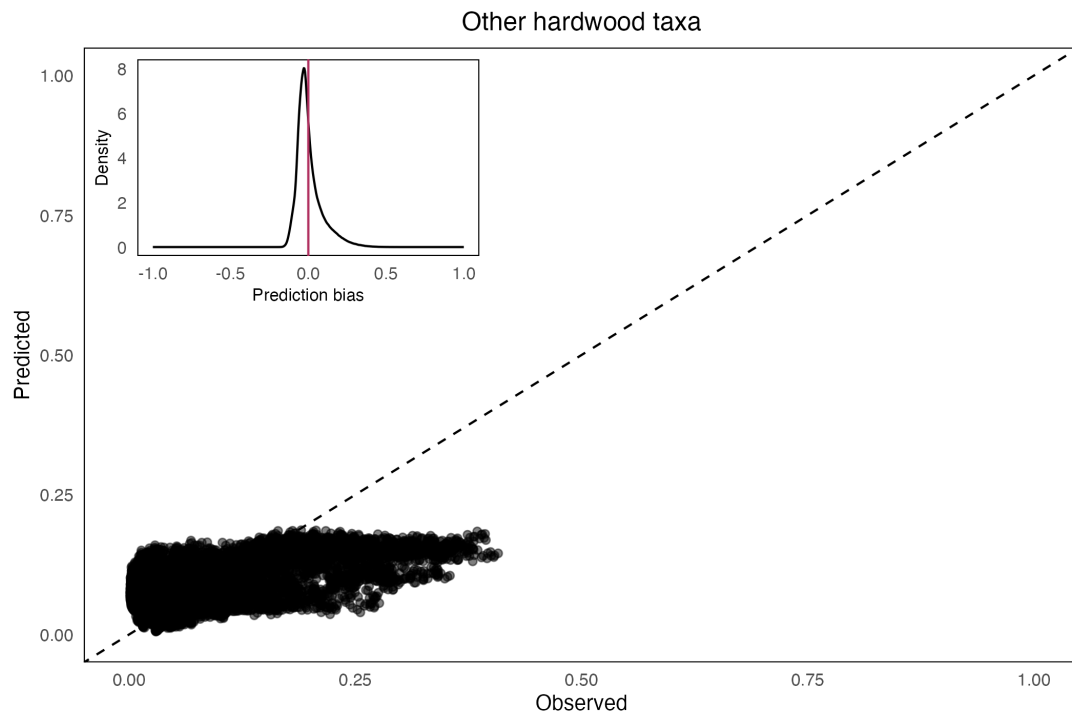


Figure E.19: Predicted vs observed relative abundance of other hardwood taxa across our entire spatiotemporal domain. The x-axis is the estimated relative abundances from 100 posterior draws of STEPPS (“observed” abundance) and the y-axis is the predicted relative abundance across 100 model predictions from our GJAM. The dashed black line shows the one-to-one line indicating perfect prediction. The axes have been scaled to show the minimum to maximum possible observation and prediction scales. Inset figure: density plot of difference between observed and predicted relative abundance (“Prediction bias”) across all spatiotemporal grid cells. The red horizontal line highlights 0 (perfect prediction). The plot is scaled to show the full range of possible prediction bias values. Prediction bias of 1 = strong model underprediction. Prediction bias of -1 = strong model overprediction.

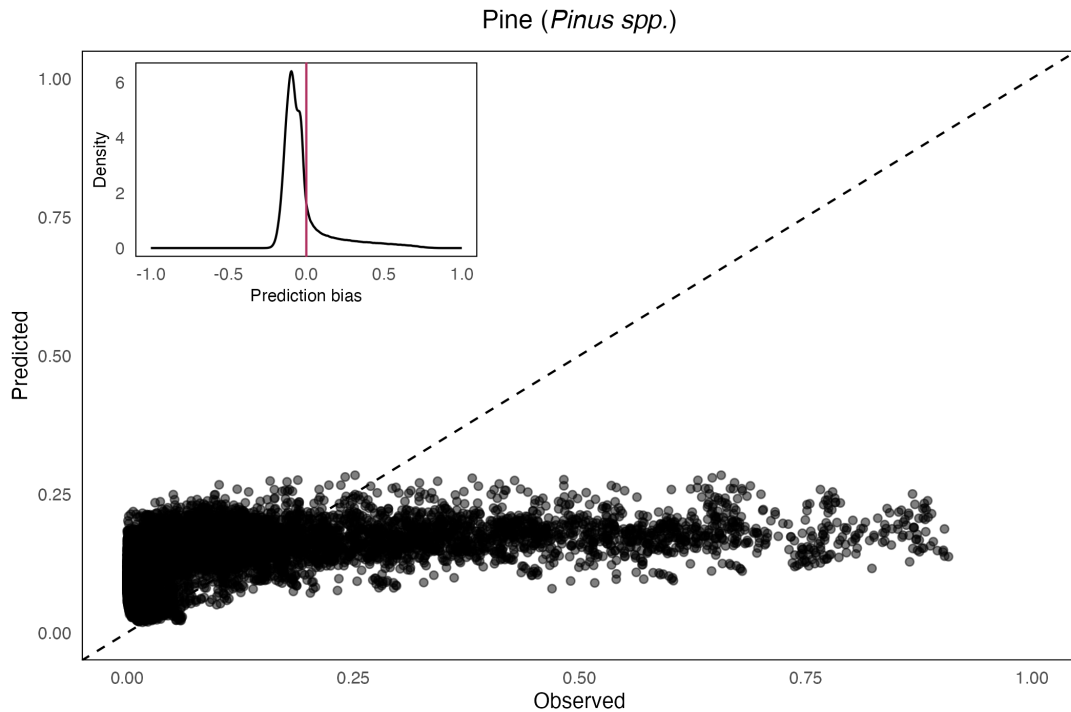


Figure E.20: Predicted vs observed relative abundance of pine (*Pinus spp.*) across our entire spatiotemporal domain. The x-axis is the estimated relative abundances from 100 posterior draws of STEPPS (“observed” abundance) and the y-axis is the predicted relative abundance across 100 model predictions from our GJAM. The dashed black line shows the one-to-one line indicating perfect prediction. The axes have been scaled to show the minimum to maximum possible observation and prediction scales. Inset figure: density plot of difference between observed and predicted relative abundance (“Prediction bias”) across all spatiotemporal grid cells. The red horizontal line highlights 0 (perfect prediction). The plot is scaled to show the full range of possible prediction bias values. Prediction bias of 1 = strong model underprediction. Prediction bias of -1 = strong model overprediction.

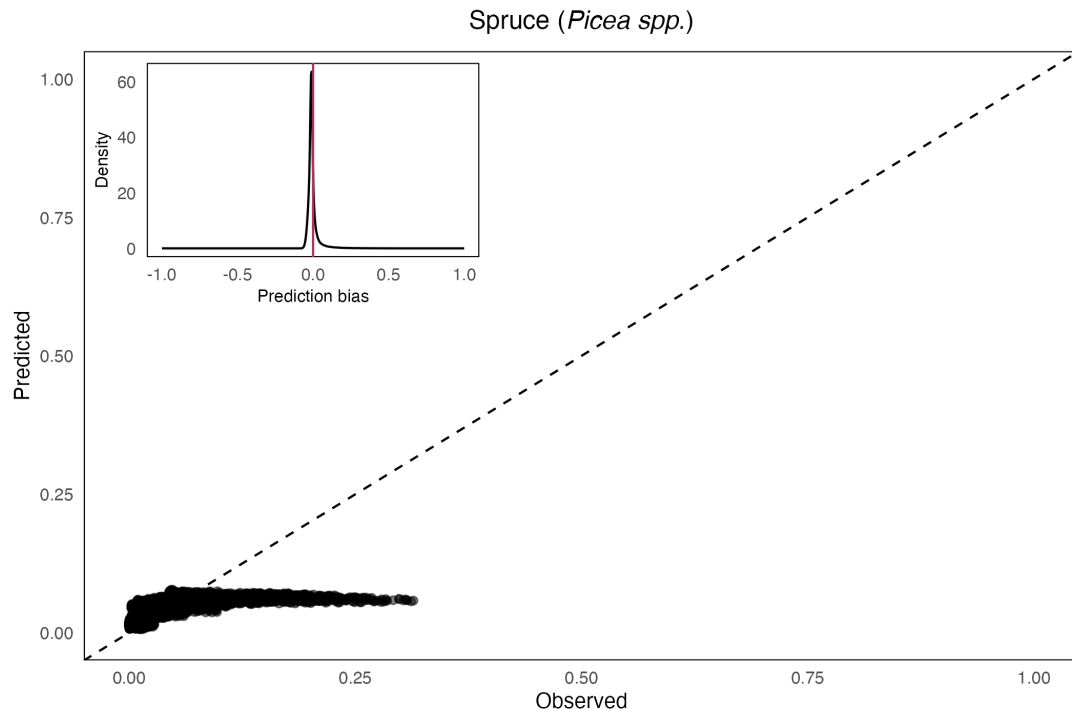


Figure E.21: Predicted vs observed relative abundance of spruce (*Picea spp.*) across our entire spatiotemporal domain. The x-axis is the estimated relative abundances from 100 posterior draws of STEPPS (“observed” abundance) and the y-axis is the predicted relative abundance across 100 model predictions from our GJAM. The dashed black line shows the one-to-one line indicating perfect prediction. The axes have been scaled to show the minimum to maximum possible observation and prediction scales. Inset figure: density plot of difference between observed and predicted relative abundance (“Prediction bias”) across all spatiotemporal grid cells. The red horizontal line highlights 0 (perfect prediction). The plot is scaled to show the full range of possible prediction bias values. Prediction bias of 1 = strong model underprediction. Prediction bias of -1 = strong model overprediction.

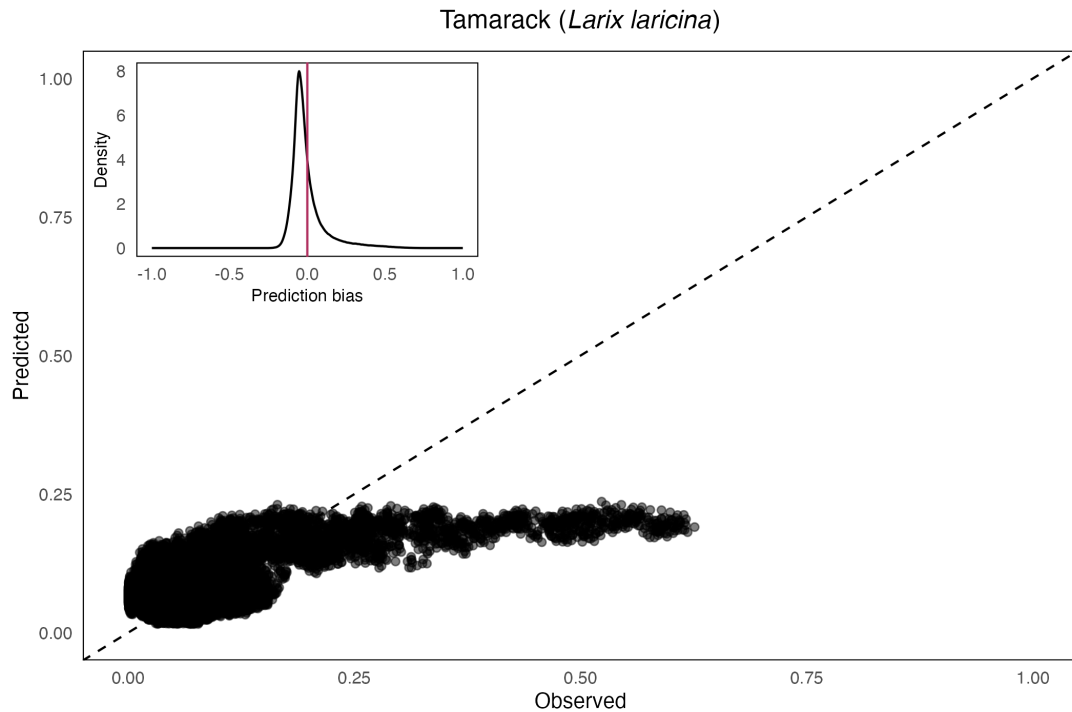


Figure E.22: Predicted vs observed relative abundance of tamarack (*Larix laricina*) across our entire spatiotemporal domain. The x-axis is the estimated relative abundances from 100 posterior draws of STEPPS (“observed” abundance) and the y-axis is the predicted relative abundance across 100 model predictions from our GJAM. The dashed black line shows the one-to-one line indicating perfect prediction. The axes have been scaled to show the minimum to maximum possible observation and prediction scales. Inset figure: density plot of difference between observed and predicted relative abundance (“Prediction bias”) across all spatiotemporal grid cells. The red horizontal line highlights 0 (perfect prediction). The plot is scaled to show the full range of possible prediction bias values. Prediction bias of 1 = strong model underprediction. Prediction bias of -1 = strong model overprediction.

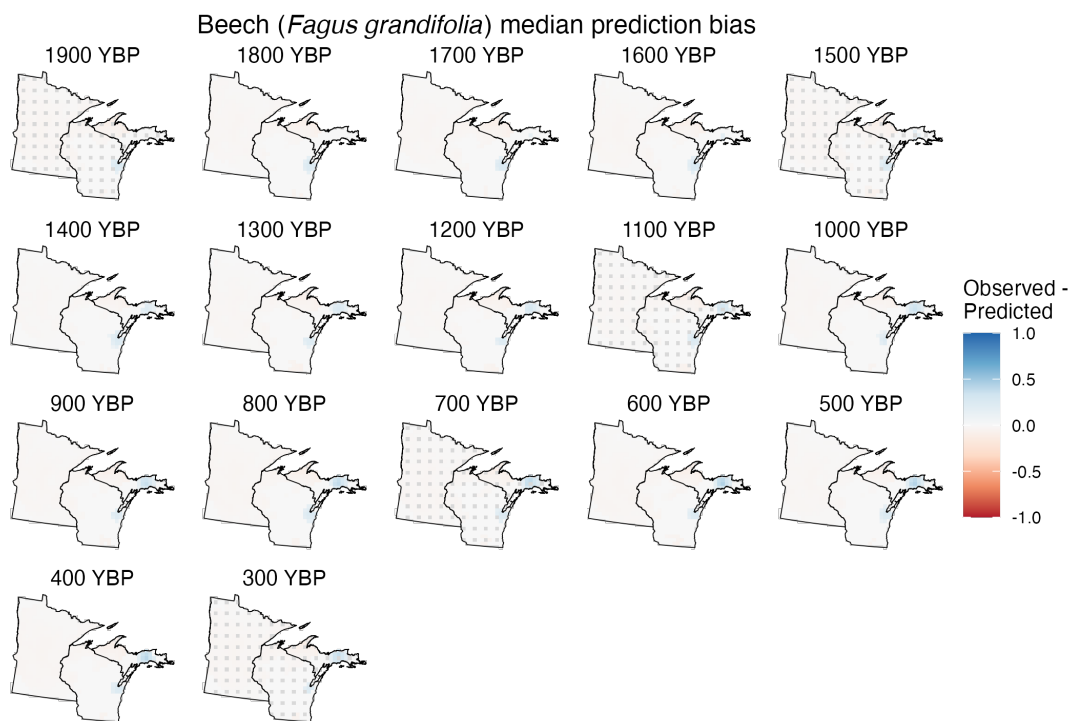


Figure E.23: GJAM prediction bias across our entire spatiotemporal domain for beech (*Fagus grandifolia*) relative abundance. Each facet shows prediction bias for all grid cells used for validation. Facets represent different 100 year intervals. Grey grid cells are those used to fit the model (not predicted). Prediction bias was calculated as the difference between observed and predicted relative abundance. The color bar shows the median bias across 100 predictions at each grid cell (one for each posterior draw of STEPPS) where the 95% credible interval showed significant bias (i.e., did not overlap 0). Prediction bias of 1 (dark blue) = strong model underprediction. Prediction bias of -1 (dark red) = strong model overprediction. Prediction bias of 0 (white) = perfect prediction.

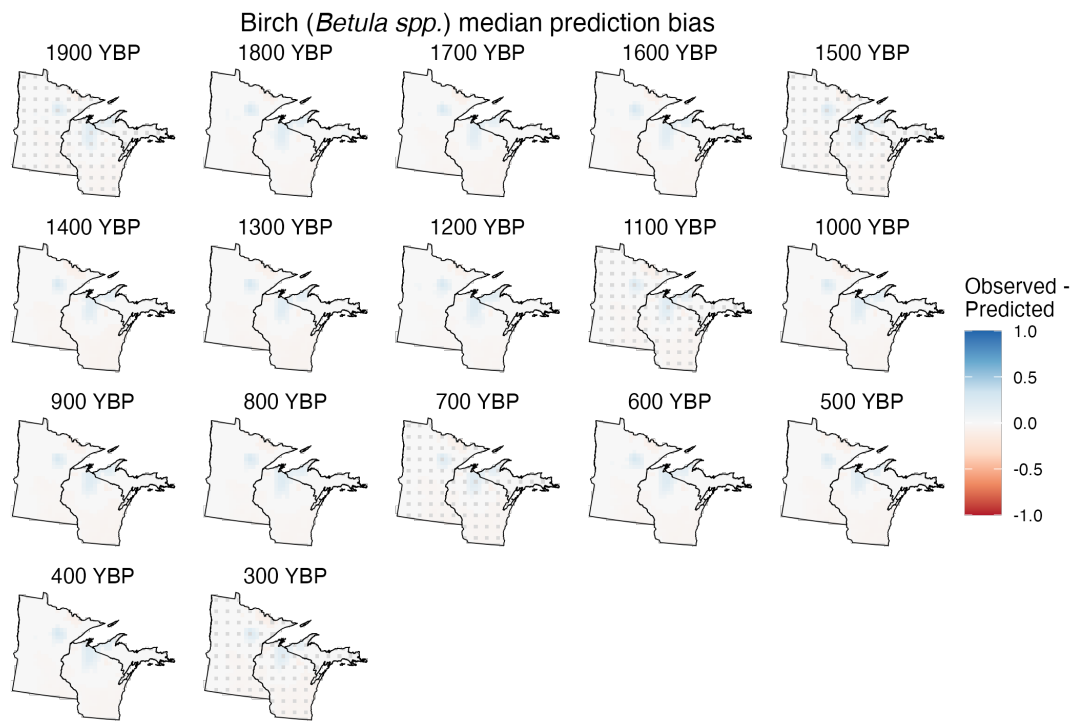


Figure E.24: GJAM prediction bias across our entire spatiotemporal domain for birch (*Betula spp.*) relative abundance. Each facet shows prediction bias for all grid cells used for validation. Facets represent different 100 year intervals. Grey grid cells are those used to fit the model (not predicted). Prediction bias was calculated as the difference between observed and predicted relative abundance. The color bar shows the median bias across 100 predictions at each grid cell (one for each posterior draw of STEPPS) where the 95% credible interval showed significant bias (i.e., did not overlap 0). Prediction bias of 1 (dark blue) = strong model underprediction. Prediction bias of -1 (dark red) = strong model overprediction. Prediction bias of 0 (white) = perfect prediction.

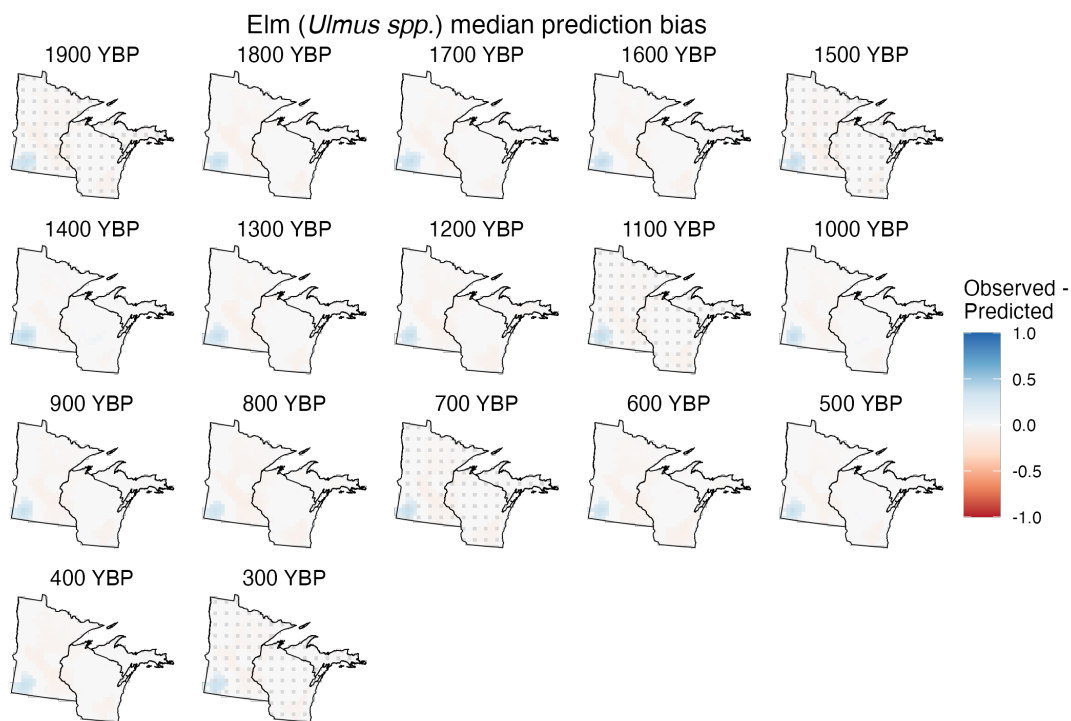


Figure E.25: GJAM prediction bias across our entire spatiotemporal domain for elm (*Ulmus spp.*) relative abundance. Each facet shows prediction bias for all grid cells used for validation. Facets represent different 100 year intervals. Grey grid cells are those used to fit the model (not predicted). Prediction bias was calculated as the difference between observed and predicted relative abundance. The color bar shows the median bias across 100 predictions at each grid cell (one for each posterior draw of STEPPS) where the 95% credible interval showed significant bias (i.e., did not overlap 0). Prediction bias of 1 (dark blue) = strong model underprediction. Prediction bias of -1 (dark red) = strong model overprediction. Prediction bias of 0 (white) = perfect prediction.

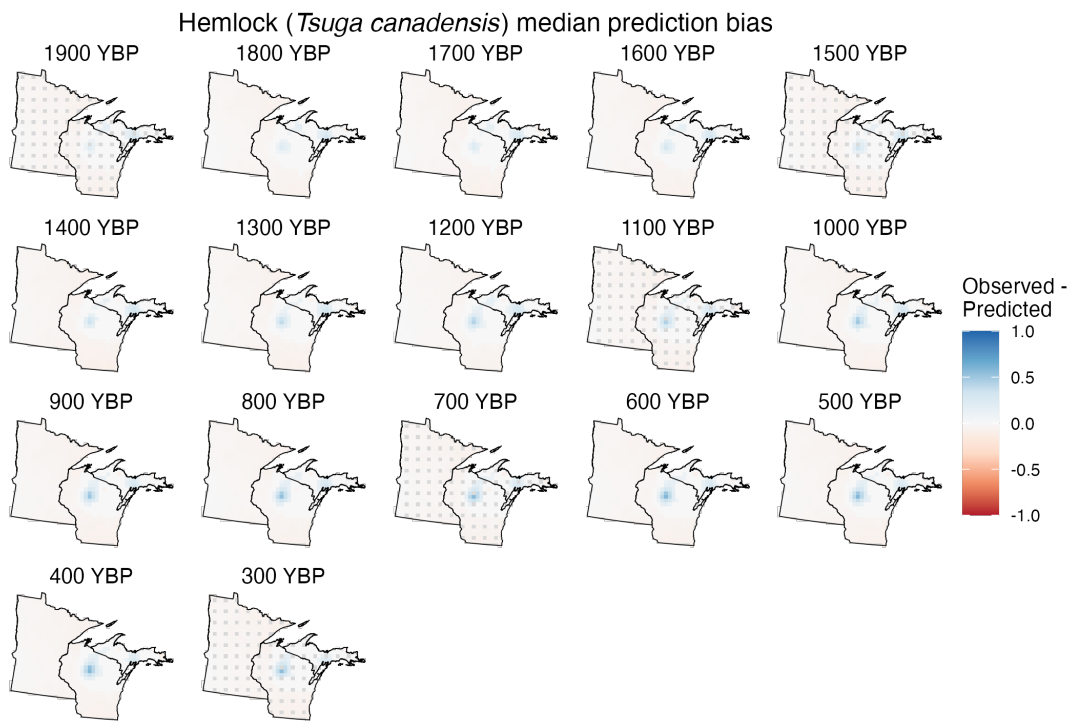


Figure E.26: GJAM prediction bias across our entire spatiotemporal domain for hemlock (*Tsuga canadensis*) relative abundance. Each facet shows prediction bias for all grid cells used for validation. Facets represent different 100 year intervals. Grey grid cells are those used to fit the model (not predicted). Prediction bias was calculated as the difference between observed and predicted relative abundance. The color bar shows the median bias across 100 predictions at each grid cell (one for each posterior draw of STEPPS) where the 95% credible interval showed significant bias (i.e., did not overlap 0). Prediction bias of 1 (dark blue) = strong model underprediction. Prediction bias of -1 (dark red) = strong model overprediction. Prediction bias of 0 (white) = perfect prediction.

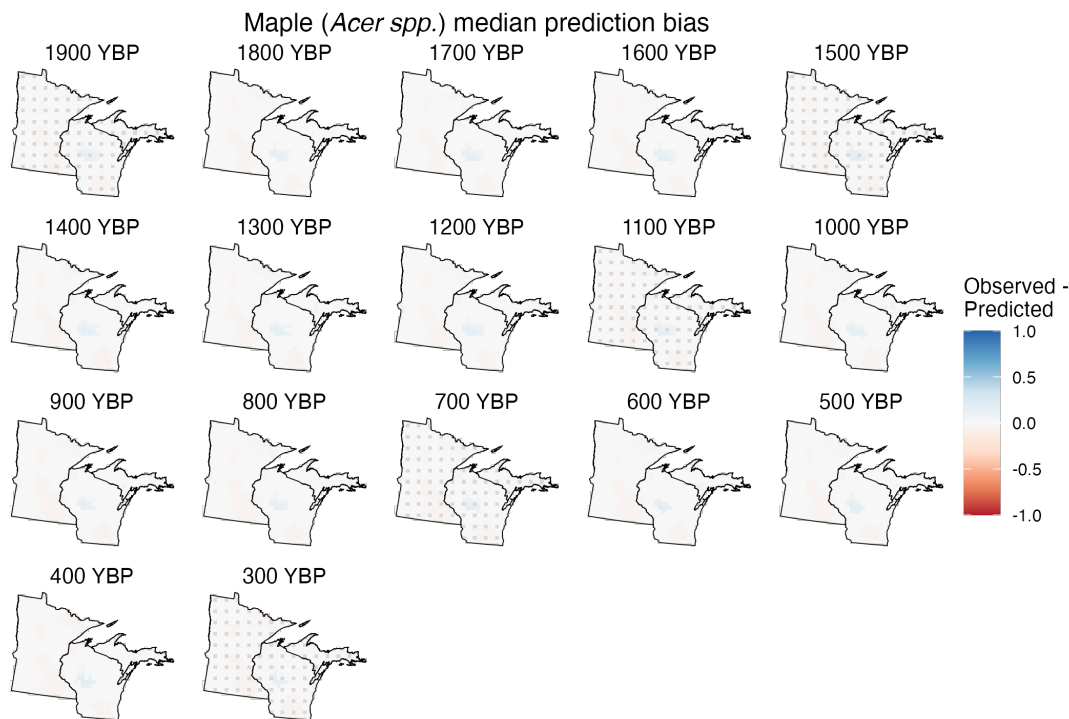


Figure E.27: GJAM prediction bias across our entire spatiotemporal domain for maple (*Acer spp.*) relative abundance. Each facet shows prediction bias for all grid cells used for validation. Facets represent different 100 year intervals. Grey grid cells are those used to fit the model (not predicted). Prediction bias was calculated as the difference between observed and predicted relative abundance. The color bar shows the median bias across 100 predictions at each grid cell (one for each posterior draw of STEPPS) where the 95% credible interval showed significant bias (i.e., did not overlap 0). Prediction bias of 1 (dark blue) = strong model underprediction. Prediction bias of -1 (dark red) = strong model overprediction. Prediction bias of 0 (white) = perfect prediction.

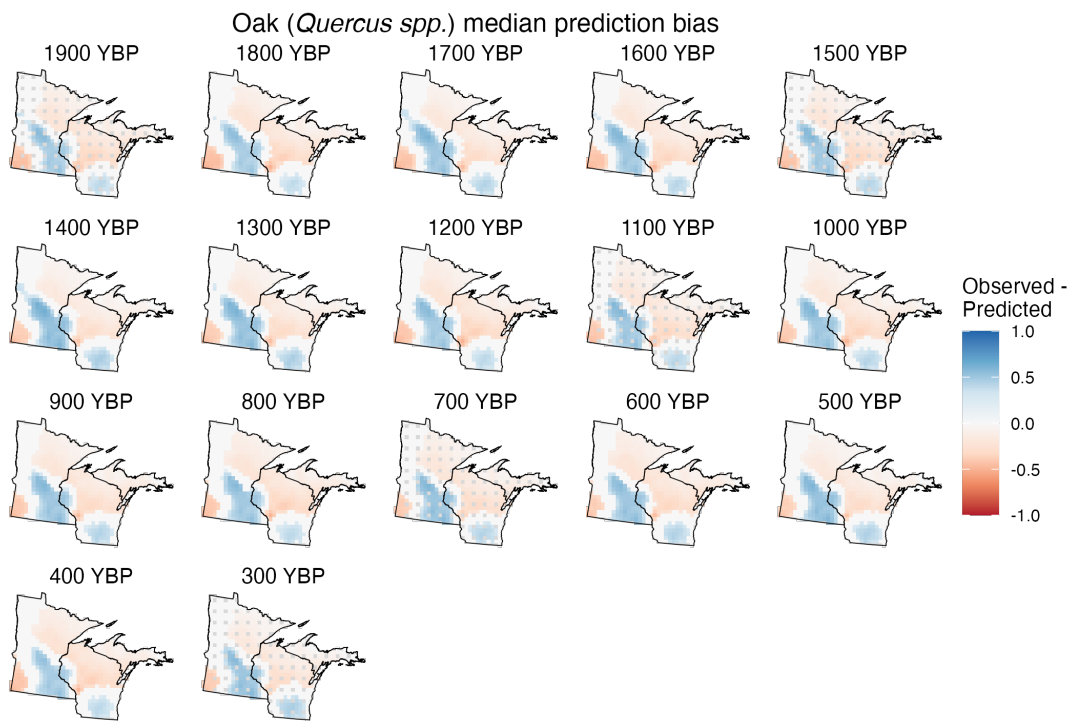


Figure E.28: GJAM prediction bias across our entire spatiotemporal domain for oak (*Quercus spp.*) relative abundance. Each facet shows prediction bias for all grid cells used for validation. Facets represent different 100 year intervals. Grey grid cells are those used to fit the model (not predicted). Prediction bias was calculated as the difference between observed and predicted relative abundance. The color bar shows the median bias across 100 predictions at each grid cell (one for each posterior draw of STEPPS) where the 95% credible interval showed significant bias (i.e., did not overlap 0). Prediction bias of 1 (dark blue) = strong model underprediction. Prediction bias of -1 (dark red) = strong model overprediction. Prediction bias of 0 (white) = perfect prediction.

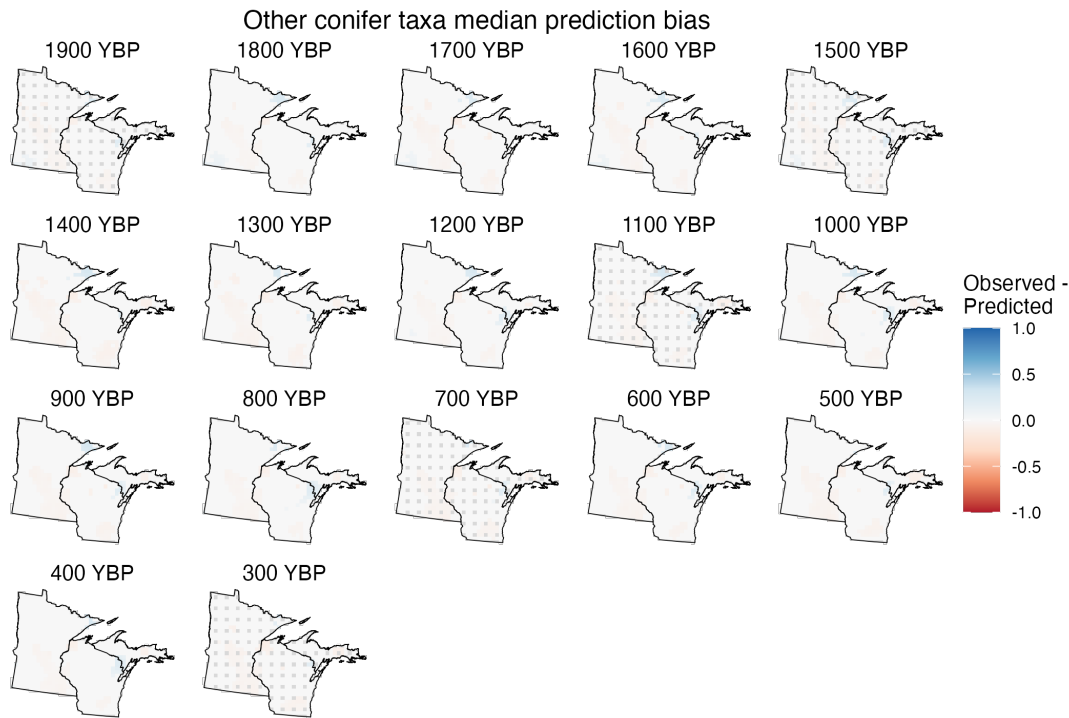


Figure E.29: GJAM prediction bias across our entire spatiotemporal domain for other conifer taxa relative abundance. Each facet shows prediction bias for all grid cells used for validation. Facets represent different 100 year intervals. Grey grid cells are those used to fit the model (not predicted). Prediction bias was calculated as the difference between observed and predicted relative abundance. The color bar shows the median bias across 100 predictions at each grid cell (one for each posterior draw of STEPPS) where the 95% credible interval showed significant bias (i.e., did not overlap 0). Prediction bias of 1 (dark blue) = strong model underprediction. Prediction bias of -1 (dark red) = strong model overprediction. Prediction bias of 0 (white) = perfect prediction.

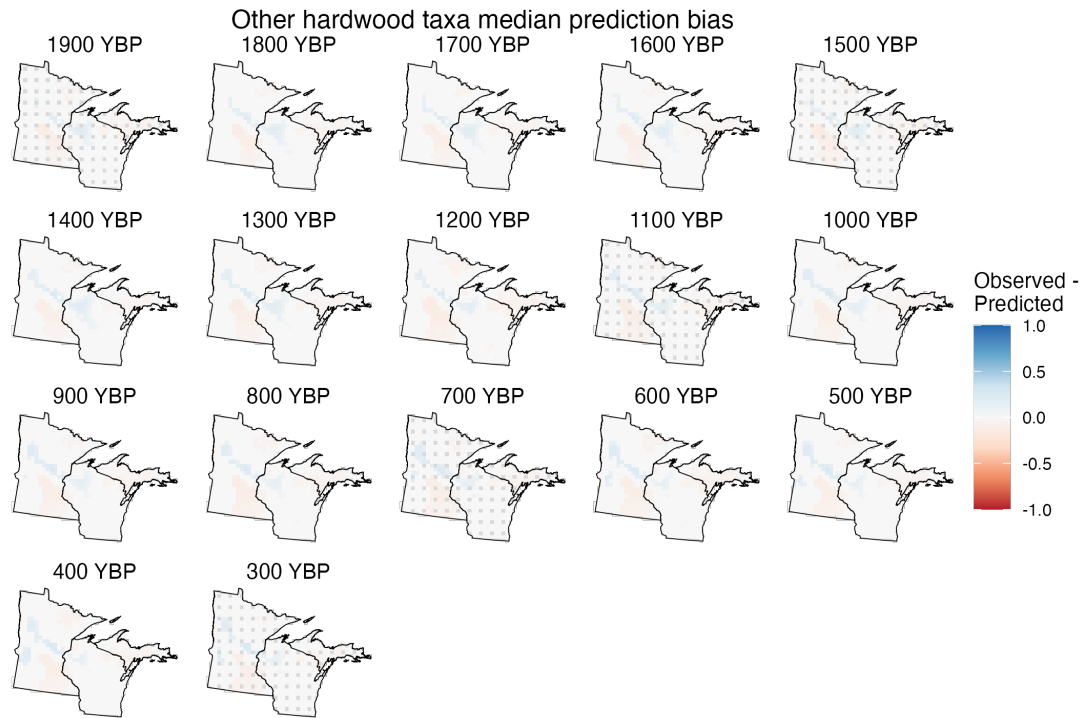


Figure E.30: GJAM prediction bias across our entire spatiotemporal domain for other hardwood taxa relative abundance. Each facet shows prediction bias for all grid cells used for validation. Facets represent different 100 year intervals. Grey grid cells are those used to fit the model (not predicted). Prediction bias was calculated as the difference between observed and predicted relative abundance. The color bar shows the median bias across 100 predictions at each grid cell (one for each posterior draw of STEPPS) where the 95% credible interval showed significant bias (i.e., did not overlap 0). Prediction bias of 1 (dark blue) = strong model underprediction. Prediction bias of -1 (dark red) = strong model overprediction. Prediction bias of 0 (white) = perfect prediction.

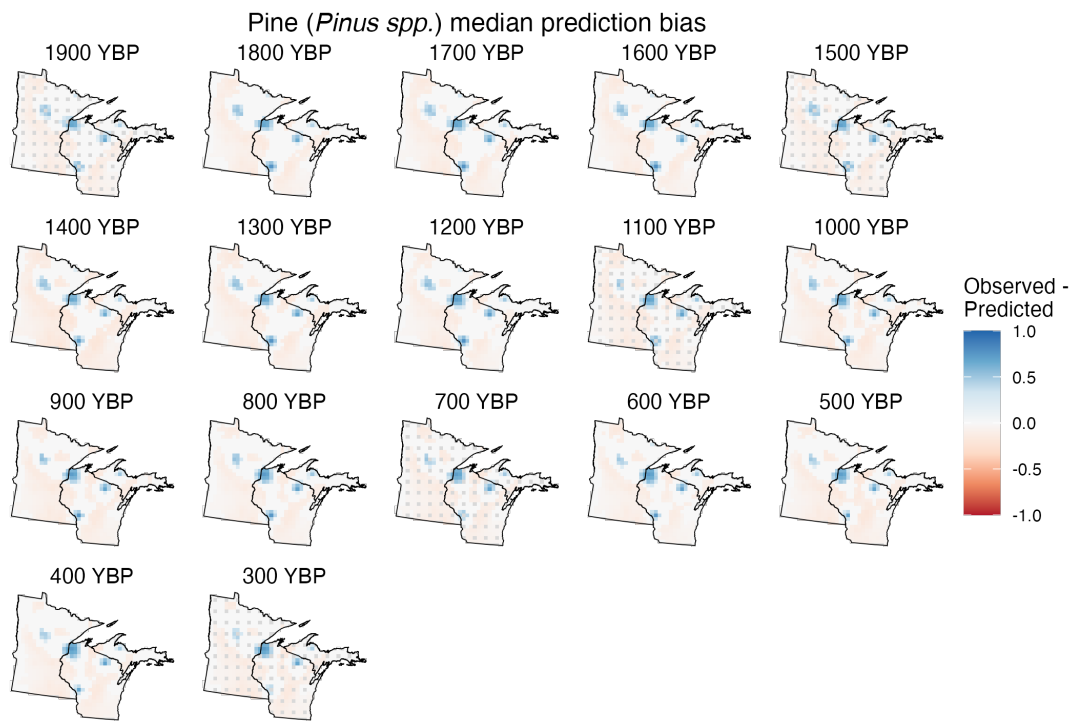


Figure E.31: GJAM prediction bias across our entire spatiotemporal domain for pine (*Pinus spp.*) relative abundance. Each facet shows prediction bias for all grid cells used for validation. Facets represent different 100 year intervals. Grey grid cells are those used to fit the model (not predicted). Prediction bias was calculated as the difference between observed and predicted relative abundance. The color bar shows the median bias across 100 predictions at each grid cell (one for each posterior draw of STEPPS) where the 95% credible interval showed significant bias (i.e., did not overlap 0). Prediction bias of 1 (dark blue) = strong model underprediction. Prediction bias of -1 (dark red) = strong model overprediction. Prediction bias of 0 (white) = perfect prediction.

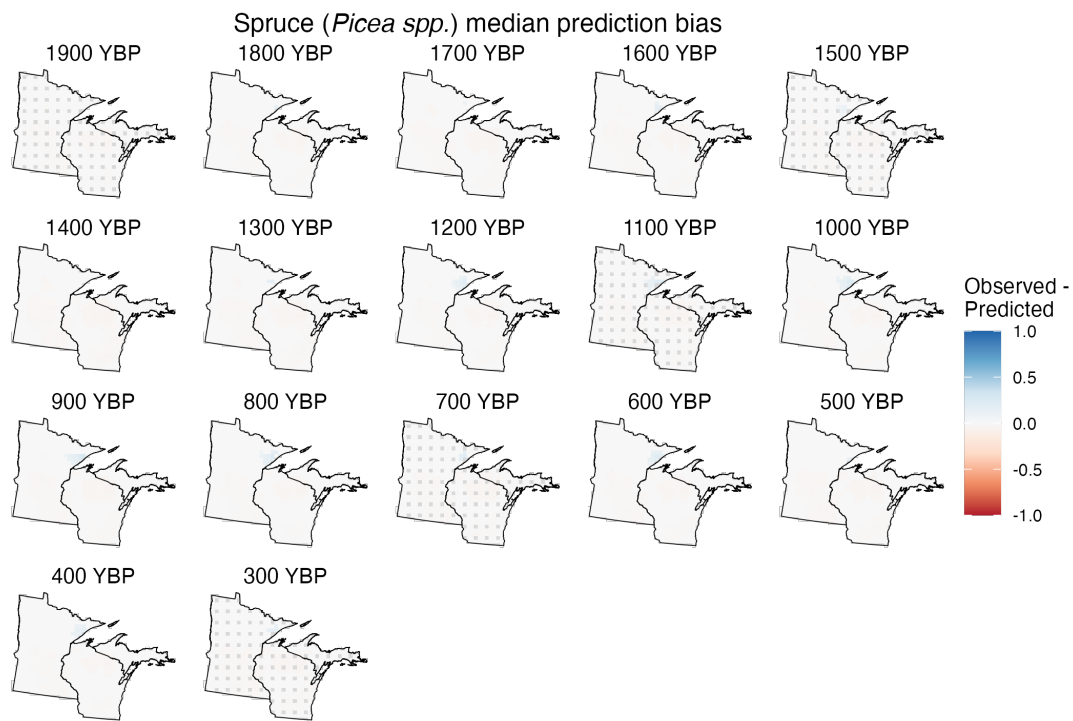


Figure E.32: GJAM prediction bias across our entire spatiotemporal domain for spruce (*Picea spp.*) relative abundance. Each facet shows prediction bias for all grid cells used for validation. Facets represent different 100 year intervals. Grey grid cells are those used to fit the model (not predicted). Prediction bias was calculated as the difference between observed and predicted relative abundance. The color bar shows the median bias across 100 predictions at each grid cell (one for each posterior draw of STEPPS) where the 95% credible interval showed significant bias (i.e., did not overlap 0). Prediction bias of 1 (dark blue) = strong model underprediction. Prediction bias of -1 (dark red) = strong model overprediction. Prediction bias of 0 (white) = perfect prediction.

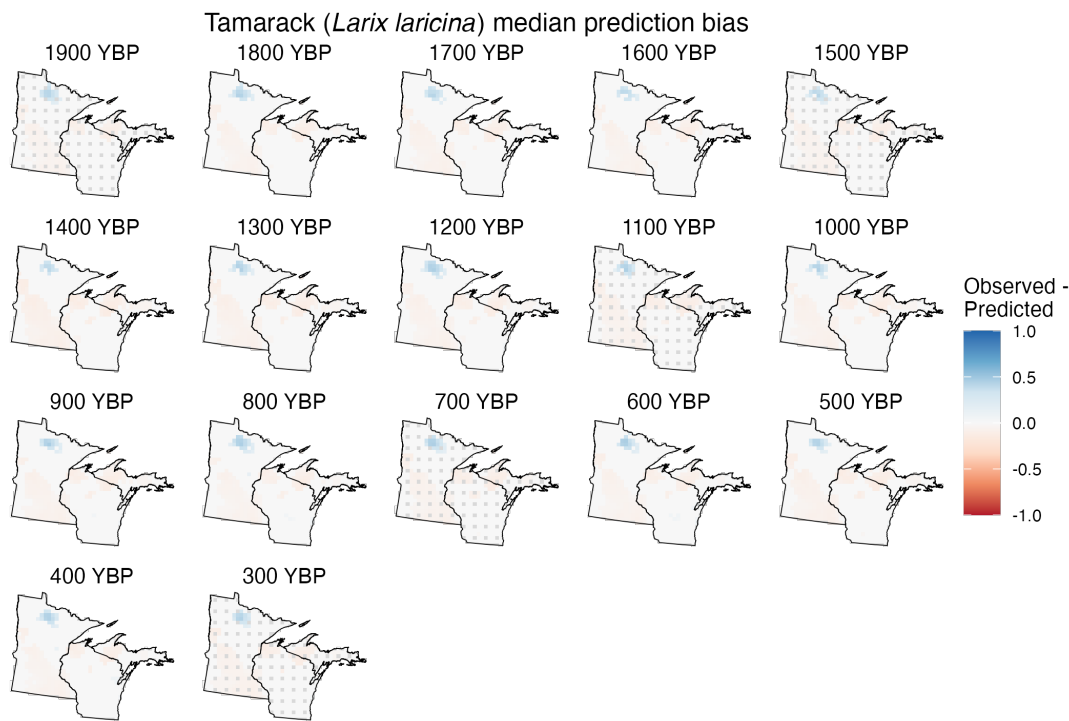


Figure E.33: GJAM prediction bias across our entire spatiotemporal domain for tamarack (*Larix laricina*) relative abundance. Each facet shows prediction bias for all grid cells used for validation. Facets represent different 100 year intervals. Grey grid cells are those used to fit the model (not predicted). Prediction bias was calculated as the difference between observed and predicted relative abundance. The color bar shows the median bias across 100 predictions at each grid cell (one for each posterior draw of STEPPS) where the 95% credible interval showed significant bias (i.e., did not overlap 0). Prediction bias of 1 (dark blue) = strong model underprediction. Prediction bias of -1 (dark red) = strong model overprediction. Prediction bias of 0 (white) = perfect prediction.